ETH
Eidgenössische Technische Hochschule Zürich
Swiss Federal Institute of Technology Zurich

Seminar for Applied Mathematics SAM

Exponential Convergence of hp-FEM for Elliptic Problems in Polyhedra: Mixed Boundary Conditions and Anisotropic Polynomial Degrees

D. Schötzau and Ch. Schwab

Research Report No. 2016-05
January 2016

Seminar für Angewandte Mathematik
Eidgenössische Technische Hochschule
CH-8092 Zürich
Switzerland

Funding: Natural Sciences and Engineering Research Council of Canada (NSERC) and the Swiss National Science Foundation (SNF)

EXPONENTIAL CONVERGENCE OF *hp*-FEM FOR ELLIPTIC PROBLEMS IN POLYHEDRA: MIXED BOUNDARY CONDITIONS AND ANISOTROPIC POLYNOMIAL DEGREES

DOMINIK SCHÖTZAU AND CHRISTOPH SCHWAB

Abstract. We prove exponential rates of convergence of *hp*-version finite element methods on geometric meshes consisting of hexahedral elements for linear, second-order elliptic boundary-value problems in axiparallel polyhedral domains. We extend and generalize our earlier work for homogeneous Dirichlet boundary conditions and uniform isotropic polynomial degrees to mixed Dirichlet-Neumann boundary conditions and to anisotropic, linearly increasing polynomial degree distributions. In particular, we construct H^1-conforming quasi-interpolation projectors with exponential consistency bounds on countably normed classes of piecewise analytic functions with singularities at edges, vertices and interfaces of boundary conditions, based on scales of weighted Sobolev norms with non-homogeneous weights in the vicinity of Neumann edges.

1. Introduction

We prove exponential converge estimates for conforming *hp*-version finite element methods (FEMs) for the following elliptic boundary-value problem in an open and bounded polyhedron $\Omega \subset \mathbb{R}^3$ with mixed boundary conditions:

$$-\nabla \cdot (\boldsymbol{A}\nabla)u = f \qquad \text{in } \Omega \subset \mathbb{R}^3, \tag{1.1}$$

$$\gamma_0(u) = 0 \qquad \text{on } \Gamma_{\boldsymbol{\iota}} \subset \partial\Omega, \quad \boldsymbol{\iota} \in \mathcal{J}_D, \tag{1.2}$$

$$\gamma_1(u) = 0 \qquad \text{on } \Gamma_{\boldsymbol{\iota}} \subset \partial\Omega, \quad \boldsymbol{\iota} \in \mathcal{J}_N. \tag{1.3}$$

The Lipschitz boundary $\Gamma = \partial\Omega$ is assumed to consist of a finite union of plane *axiparallel* faces $\Gamma_{\boldsymbol{\iota}}$ indexed by $\boldsymbol{\iota} \in \mathcal{J}$. The faces $\Gamma_{\boldsymbol{\iota}}$ are bounded, plane polygons whose sides form the (open) edges of Ω. The set $\{\Gamma_{\boldsymbol{\iota}}\}_{\boldsymbol{\iota}\in\mathcal{J}}$ is partitioned into a subset of Dirichlet faces $\{\Gamma_{\boldsymbol{\iota}}\}_{\boldsymbol{\iota}\in\mathcal{J}_D}$ and a subset of Neumann faces $\{\Gamma_{\boldsymbol{\iota}}\}_{\boldsymbol{\iota}\in\mathcal{J}_N}$, with corresponding (disjoint) index sets $\mathcal{J}_D$ and $\mathcal{J}_N$, respectively (i.e., $\mathcal{J} = \mathcal{J}_D \,\dot\cup\, \mathcal{J}_N$). The diffusion coefficient matrix $\boldsymbol{A}$ is assumed to be constant and and symmetric, positive definite. The function f is a given forcing term, and the operators γ_0 and γ_1 denote the trace and (co)normal derivative operators, respectively.

Upon introducing the Sobolev space $V := \{v \in H^1(\Omega) : v|_{\Gamma_{\boldsymbol{\iota}}} = 0,\ \boldsymbol{\iota} \in \mathcal{J}_D\}$, the weak formulation of problem (1.1)–(1.3) is to find $u \in V$ such that

$$a(u,v) := \int_\Omega \boldsymbol{A}\nabla u \cdot \nabla v \,\mathrm{d}\boldsymbol{x} = \int_\Omega f v \,\mathrm{d}\boldsymbol{x} \qquad \forall v \in V, \tag{1.4}$$

2010 *Mathematics Subject Classification.* 65N30.

Key words and phrases. *hp*-FEM, second-order elliptic problems in polyhedra, mixed boundary conditions, anisotropic polynomial degrees, exponential convergence.

This work was supported in part by the Natural Sciences and Engineering Research Council of Canada (NSERC) and the Swiss National Science Foundation (SNF).

where we understand the integral on the right-hand side in (1.4) as the duality pairing in $V^\star \times V$, with $V^\star$ denoting the dual space of V. For every $f \in V^\star$, problem (1.4) admits a weak solution $u \in V$. The solution is unique if $\mathcal{J}_D \neq \emptyset$, and unique in the factor space $V/\mathbb{R}$ if $\mathcal{J}_D = \emptyset$ (in which case we also require the compatibility condition $\int_\Omega f \, \mathrm{d}\boldsymbol{x} = 0$).

The *hp*-version of the finite element method for elliptic problems was proposed by Babuška and his coworkers, inspired by exponential convergence results in free-knot, variable order spline interpolation. We refer to [6, 17] and the references therein for these approximation theoretic estimates. The *hp*-version FEM unified the hitherto largely separate developments of fixed-order "*h*-version FEM", which achieve convergence through reduction of the mesh size h, and the so-called "*spectral* (or *p*-version) FEM", which achieve convergence through increasing the polynomial order p on a fixed mesh. Apart from unifying the existing approaches, *hp*-FEMs were shown to achieve *exponential convergence rates for solutions with singularities* in terms of the number N of degrees of freedom, in function spaces where the differential equation is well-posed.

In [9], the exponential convergence rate $C\exp(-b\sqrt{N})$ was shown for univariate *hp*-FEM for the model singular solution solution $u(x) = x^\alpha - x \in H^1_0(\Omega)$ in $\Omega = (0,1)$, with $\alpha > 1/2$ not an integer, with constants $b, C > 0$ independent of N. This result required σ-geometric mesh refinement towards $x = 0$ with *a fixed subdivision ratio* $\sigma \in (0,1)$ (in particular, $\sigma = 1/2$ yields geometric bisection meshes). The constant b in the convergence estimate strongly depends on the singularity exponent α as well as on σ: among all $\sigma \in (0,1)$, the optimal value for σ was proved in [9, Theorem 3.2] to be $\sigma_{\mathrm{opt}} = (\sqrt{2}-1)^2 \approx 0.17$, *provided that geometric mesh refinement be combined with nonuniform polynomial degrees* $p_i \geq 1$ *in element* Ω_i *which are* $\mathfrak{s}$-linearly *increasing away from* $x = 0$, *i.e.,* $p_i \simeq \mathfrak{s} i$, *with the optimal slope* $\mathfrak{s}$ *being* $\mathfrak{s}_{\mathrm{opt}} = 2(\alpha - 1/2)$. In this case, $b = 1.76\ldots \times \sqrt{(\alpha - 1/2)}$.

In two dimensions, exponential convergence bounds of the form $C\exp(-b\sqrt[3]{N})$ for the errors of the *hp*-version FEM in polygons Ω were proved by Babuška and Guo in [1, 2, 11, 12] and the references therein. Key ingredients in their proof were again *geometric mesh refinement* towards the singular support $\mathcal{S}$ (being a finite set of vertices of the polygon Ω) of the solution and *nonuniform elemental polynomial degrees* which increase $\mathfrak{s}$-linearly with the elements' distance from $\mathcal{S}$. In addition to the approximation results, their papers also provide *elliptic regularity results in countably normed weighted spaces of the solutions.* This constituted an essential advance with respect to the earlier works in [6, 9, 17], where only particular singular solutions had been considered.

Steps to extend the analytic regularity and the *hp*-convergence analysis in [1, 2, 11, 12] to three dimensions were undertaken in [3, 10, 13, 15] and the references therein. In [5], Costabel, Dauge and Nicaise established an analytic regularity shift in scales of anisotropically and non-homogeneously weighted spaces for variational solutions for a class of of second-order elliptic boundary-value problems with constant coefficients. Their regularity result will be the basis of our exponential convergence proof.

The present paper builds on and extends our recent work [18] on exponential convergence for *hp*-version finite element methods in polyhedral domains. It also builds on our earlier work [22, 23, 24] on *hp*-version discontinuous Galerkin (DG) methods for second-order elliptic boundary-value problems in polyhedra. Specifically, in [18],

we considered the boundary-value problem (1.1) with the homogeneous Dirichlet boundary conditions in (1.2) imposed on the entire boundary $\partial\Omega$. For axiparallel configurations, we then used the non-conforming hp-version interpolation operators constructed in [23] in conjunction with suitable polynomial jump liftings to prove exponential rates of convergence in terms of the number of degrees of freedom for conforming hp-FEM discretizations on appropriate combinations of geometrically and anisotropically refined meshes and for the *uniform and isotropic polynomial degree* $p \geq 1$.

The principal contribution of the present work is the construction of exponentially convergent conforming hp-FE quasi-interpolation projectors on axiparallel, σ-geometric mesh patches with *variable and anisotropic polynomial degree distributions* for the *mixed* second-order problem (1.1)–(1.3) (and generalizations thereof). Our main result shows the H^1-norm convergence rate estimate $C\exp(-b\sqrt[5]{N})$, where N is the number of degrees of freedom of the conforming hp-FE space, and where $b, C > 0$ are independent of N. While asymptotically of the same form as the rate in [18], the univariate hp-approximation results [9, 17] suggest that the use of subdivision ratios $\sigma < 1/2$ and of variable and, in particular, *anisotropic polynomial degree distributions* will significantly reduce the number of degrees of freedom required to reach a prescribed accuracy of approximation. This is corroborated in preliminary numerical results in three space dimensions. Loosely speaking, our construction and convergence proof combine the arguments in [22, 23, 24] to define *non-conforming base projectors with exponential convergence in broken norms* with the constructions of *polynomially stable polynomial trace jump liftings* in [18]. However, the lower regularity of the solutions and the more general hp-finite element spaces under consideration entail several new technical difficulties addressed in this work. We discuss them in detail.

First, the mixed boundary conditions in (1.2), (1.3) are considerably more involved than the pure Dirichlet conditions analyzed in [18]. Indeed, with the regularity theory from [5], solutions of problem (1.1)–(1.3) with piecewise analytic data belong to countably normed Sobolev spaces $N^m_{\boldsymbol{\beta}}(\Omega)$ with *non-homogeneous weights*. In [24], the non-homogeneous structure of the weights was dealt with by splitting the errors in edge-perpendicular and edge-parallel contributions and by bounding these two contributions separately. The crucial stability with respect to element anisotropy of the error splitting was ensured in [24] by the use of L^2-projections in edge-parallel directions, up to algebraic losses in the polynomial degrees. While this was sufficient for proving exponential convergence of discontinuous Galerkin discretizations, finding stable liftings of the polynomial jumps introduced by the L^2-projections in edge-parallel direction over edge-perpendicular faces between *highly anisotropic* elements along the same edge seems an open problem.

To overcome this difficulty, the first principal contribution of the paper is a novel construction of non-conforming hp-version base projectors. It employs L^2-projections in edge-perpendicular directions and nodally exact H^1-projections in edge-parallel direction along anisotropic elements appearing in edge- and in corner-edge neighborhoods. The nodal exactness property in parallel direction then removes the need for liftings over the critical faces mentioned above, while still allowing to split the errors in edge-perpendicular and edge-parallel contributions in the spirit of [24]. The non-conforming hp-base projectors constructed in the present paper are well-defined on $H^1(\Omega)$, in contrast to those used in [18]. As the proof

of exponential convergence in broken norms for the base projectors thus obtained follows along the lines of [24], with only a few modifications, we outline it for completeness in Appendix A. In addition, we provide an analogous exponential L^2-norm consistency bound for L^2-projections under the weak $N^1_{\boldsymbol{\beta}}(\Omega)$-regularity. This may be of independent interest for approximations of the pressure in mixed *hp*-version discretizations of the (Navier-)Stokes equations in polyhedra as considered in [20, 21, 27].

Second, we consider in this paper the $\mathfrak{s}$-linear polynomial degree distributions introduced [22], which increase *linearly and anisotropically* away from edges and corners with a *slope parameter* $\mathfrak{s} > 0$. While such degree distributions can be relatively easily accommodated by the discontinuous Galerkin approaches in [22, 23, 24], enforcing conformity for variable polynomial degrees and irregular mesh refinement is not straightforward. To deal with this, we propose a *minimum rule* approach for edge and face polynomial degrees in the spirit of [7], by introducing suitable *hp*-version elemental basis functions with respect to nodal, edge, faces and interior degrees of freedom. The second principal contribution of this paper then is the construction of conforming approximations in the presence of $\mathfrak{s}$-linear polynomial degree distributions and irregular meshes. Starting from the non-conforming *hp* base projectors, we adopt an *averaging approach* from [28] to assign unique nodal, edge and face values while keeping exponential convergence. This yields intermediate approximations which are continuous across all regularly matching faces and which satisfy homogeneous boundary conditions on Dirichlet boundary faces, while retaining the exponential convergence estimates. Finally, we introduce polynomial edge and face jump liftings along the lines of our previous work [18] to remove discontinuities over all irregular faces. Our liftings admit bounds with are independent of element aspect ratios, with algebraic growth in the elemental polynomial degree, thereby preserving the exponential convergence estimates of the *hp*-version base projectors. We note that the present analysis is in particular applicable to the pure Dirichlet problem, i.e., when $\mathcal{J}_N = \emptyset$. Hence, the analysis here extends and generalizes the results in [18] to $\mathfrak{s}$-linear and anisotropic polynomial degree distributions. Our exponential convergence proofs apply directly to *hp*-FEMs for more general and vector-valued second-order elliptic boundary-value problems which admit analytic regularity shifts in the function classes of [5].

The outline of the remainder of the article is as follows: In Section 2, we recapitulate analytic regularity results for solutions to (1.1)–(1.3) from [5]. In Section 3, we introduce *hp*-version finite element spaces on σ-geometric meshes of hexahedral axiparallel elements with $\mathfrak{s}$-linear polynomial degree distributions, specify the continuous Galerkin methods to be analyzed, and state and discuss our main exponential exponential convergence result (Theorem 3.4), with an outline of the proof provided in Section 3.4. Base projectors with partial conformity and exponential convergence estimates are introduced in Section 4. Details of the convergence estimates can be found in Appendix A. Finally, in Sections 5 and 6, we complete the constructions of conforming approximations by averaging and lifting operators, respectively, which are of independent interest.

Our notation employed throughout the paper is kept consistent with [22, 23, 24]. We shall use the notations "$\lesssim$" or "$\simeq$" to denote an inequality or an equivalence containing generic positive multiplicative constants which are independent of the

discretization and regularity parameters, as well as of the geometric refinement level, but which may depend on the parameters σ and $\mathfrak{s}$.

2. Regularity

In this section, we review the regularity for weak solutions of (1.1)–(1.3). The weighted spaces and the analytic regularity shifts are due to [5].

2.1. **Subdomains and weights.** We denote by $\mathcal{C}$ the finite set of corners $\boldsymbol{c}$, and by $\mathcal{E}$ the finite set of (open) edges $\boldsymbol{e}$ of Ω. The singular set of Ω is then given by

$$\mathcal{S} := \mathcal{C} \cup \mathcal{E} = \Big(\bigcup_{\boldsymbol{c}\in\mathcal{C}} \boldsymbol{c} \Big) \cup \Big(\bigcup_{\boldsymbol{e}\in\mathcal{E}} \boldsymbol{e} \Big) \subset \Gamma\,. \tag{2.1}$$

For $\boldsymbol{c} \in \mathcal{C}$, $\boldsymbol{e} \in \mathcal{E}$, and $\boldsymbol{x} \in \Omega$, we define the following distance functions:

$$r_{\boldsymbol{c}}(\boldsymbol{x}) = |\boldsymbol{x}-\boldsymbol{c}|, \qquad r_{\boldsymbol{e}}(\boldsymbol{x}) = \inf_{\boldsymbol{y}\in\boldsymbol{e}} |\boldsymbol{x}-\boldsymbol{y}|, \qquad \rho_{\boldsymbol{ce}}(\boldsymbol{x}) = r_{\boldsymbol{e}}(\boldsymbol{x})/r_{\boldsymbol{c}}(\boldsymbol{x}). \tag{2.2}$$

For each corner $\boldsymbol{c} \in \mathcal{C}$, we denote by $\mathcal{E}_{\boldsymbol{c}} := \{\, \boldsymbol{e} \in \mathcal{E} \,:\, \boldsymbol{c} \cap \overline{\boldsymbol{e}} \neq \emptyset \,\}$ the set of all edges of Ω which meet at $\boldsymbol{c}$. Similarly, for any $\boldsymbol{e} \in \mathcal{E}$, the set of corners of $\boldsymbol{e}$ is given by $\mathcal{C}_{\boldsymbol{e}} := \{\, \boldsymbol{c} \in \mathcal{C} \,:\, \boldsymbol{c} \cap \overline{\boldsymbol{e}} \neq \emptyset \,\}$. Then, for $\varepsilon > 0$, $\boldsymbol{c} \in \mathcal{C}$, $\boldsymbol{e} \in \mathcal{E}$ respectively $\boldsymbol{e} \in \mathcal{E}_{\boldsymbol{c}}$, we define the neighborhoods

$$\begin{aligned}
\omega_{\boldsymbol{c}} &= \{\, \boldsymbol{x} \in \Omega \,:\, r_{\boldsymbol{c}}(\boldsymbol{x}) < \varepsilon \;\wedge\; \rho_{\boldsymbol{ce}}(\boldsymbol{x}) > \varepsilon \quad \forall\, \boldsymbol{e} \in \mathcal{E}_{\boldsymbol{c}} \,\},\\
\omega_{\boldsymbol{e}} &= \{\, \boldsymbol{x} \in \Omega \,:\, r_{\boldsymbol{e}}(\boldsymbol{x}) < \varepsilon \;\wedge\; r_{\boldsymbol{c}}(\boldsymbol{x}) > \varepsilon \quad \forall\, \boldsymbol{c} \in \mathcal{C}_{\boldsymbol{e}} \,\},\\
\omega_{\boldsymbol{ce}} &= \{\, \boldsymbol{x} \in \Omega \,:\, r_{\boldsymbol{c}}(\boldsymbol{x}) < \varepsilon \;\wedge\; \rho_{\boldsymbol{ce}}(\boldsymbol{x}) < \varepsilon \,\}.
\end{aligned} \tag{2.3}$$

Without loss of generality as in [22], the domain Ω can be partitioned into four *disjoint* subdomains, $\overline{\Omega} = \overline{\Omega_{\mathcal{C}} \,\dot\cup\, \Omega_{\mathcal{E}} \,\dot\cup\, \Omega_{\mathcal{CE}} \,\dot\cup\, \Omega_0}$, referred to as *corner*, *edge* and *corner-edge* and *interior* neighborhoods of Ω, respectively, where $\Omega_0 := \Omega \setminus \overline{\Omega_{\mathcal{C}} \cup \Omega_{\mathcal{E}} \cup \Omega_{\mathcal{CE}}}$ and

$$\Omega_{\mathcal{C}} = \bigcup_{\boldsymbol{c}\in\mathcal{C}} \omega_{\boldsymbol{c}}, \qquad \Omega_{\mathcal{E}} = \bigcup_{\boldsymbol{e}\in\mathcal{E}} \omega_{\boldsymbol{e}}, \qquad \Omega_{\mathcal{CE}} = \bigcup_{\boldsymbol{c}\in\mathcal{C}} \bigcup_{\boldsymbol{e}\in\mathcal{E}_{\boldsymbol{c}}} \omega_{\boldsymbol{ce}}\,. \tag{2.4}$$

We distinguish Dirichlet and Neumann edges by setting

$$\mathcal{E}_D := \big\{\, \boldsymbol{e} \in \mathcal{E} \,:\, \exists \boldsymbol{\iota} \in \mathcal{J}_D \text{ with } \boldsymbol{e} \cap \overline{\Gamma}_{\boldsymbol{\iota}} \neq \emptyset \,\big\}, \qquad \mathcal{E}_N := \mathcal{E} \setminus \mathcal{E}_D. \tag{2.5}$$

Edges in $\mathcal{E}_D$ abut at at least one Dirichlet face $\Gamma_{\boldsymbol{\iota}}$ for $\boldsymbol{\iota} \in \mathcal{J}_D$. Note that we possibly have $\mathcal{E}_N = \emptyset$.

2.2. **Weighted Sobolev spaces.** To each $\boldsymbol{c} \in \mathcal{C}$ and $\boldsymbol{e} \in \mathcal{E}$ we associate a corner and an edge exponent $\beta_{\boldsymbol{c}}, \beta_{\boldsymbol{e}} \in \mathbb{R}$, respectively. We collect these quantities in the weight exponent vector $\boldsymbol{\beta} = \{\beta_{\boldsymbol{c}} \,:\, \boldsymbol{c} \in \mathcal{C}\} \cup \{\beta_{\boldsymbol{e}} \,:\, \boldsymbol{e} \in \mathcal{E}\} \in \mathbb{R}^{|\mathcal{C}|+|\mathcal{E}|}$. Inequalities of the form $\boldsymbol{\beta} < 1$ and expressions like $\boldsymbol{\beta} \pm s$, where $s \in \mathbb{R}$, are to be understood componentwise. We shall often use the notation

$$b_{\boldsymbol{c}} := -1 - \beta_{\boldsymbol{c}}, \quad \boldsymbol{c} \in \mathcal{C}\,, \qquad b_{\boldsymbol{e}} := -1 - \beta_{\boldsymbol{e}}, \quad \boldsymbol{e} \in \mathcal{E}\,. \tag{2.6}$$

To review the analytic regularity results of [5], we choose local coordinate systems in $\omega_{\boldsymbol{e}}$ and $\omega_{\boldsymbol{ce}}$, for $\boldsymbol{c} \in \mathcal{C}$ and $\boldsymbol{e} \in \mathcal{E}_{\boldsymbol{c}}$, such that the edge $\boldsymbol{e}$ corresponds to the direction $(0,0,1)$. Then, we indicate quantities transversal to $\boldsymbol{e}$ by $(\cdot)^{\perp}$, and quantities parallel to $\boldsymbol{e}$ by $(\cdot)^{\parallel}$. In particular, if $\boldsymbol{\alpha} = (\alpha_1, \alpha_2, \alpha_3) \in \mathbb{N}_0^3$ is a multi-index of order $|\boldsymbol{\alpha}| = \alpha_1 + \alpha_2 + \alpha_3$, then we write $\boldsymbol{\alpha} = (\boldsymbol{\alpha}^{\perp}, \alpha^{\parallel})$ with $\boldsymbol{\alpha}^{\perp} = (\alpha_1, \alpha_2)$ and $\alpha^{\parallel} = \alpha_3$, and denote the partial derivative operator $\mathsf{D}^{\boldsymbol{\alpha}}$ by $\mathsf{D}^{\boldsymbol{\alpha}} = \mathsf{D}_{\perp}^{\boldsymbol{\alpha}^{\perp}} \mathsf{D}_{\parallel}^{\alpha^{\parallel}}$, where $\mathsf{D}_{\perp}^{\boldsymbol{\alpha}^{\perp}}$ and $\mathsf{D}_{\parallel}^{\alpha^{\parallel}}$ signify derivatives in edge-perpendicular and edge-parallel

directions, respectively. We further denote by $\mathsf{D}_\perp$ the gradient operator in edge-perpendicular direction, and set $\mathsf{D}_\parallel = \mathsf{D}_\parallel^1$.

The solution u of problem (1.1)–(1.3) belongs to a scale of countably normed spaces; cf. [5]. For sets $\emptyset \subseteq \mathcal{C}' \subseteq \mathcal{C}$ and $\emptyset \subseteq \mathcal{E}' \subseteq \mathcal{E}$, we introduce the following semi-norm of order $k \geq 0$:

$$
\begin{aligned}
|u|^2_{N^k_{\boldsymbol{\beta}}(\Omega;\mathcal{C}',\mathcal{E}')} := \sum_{|\boldsymbol{\alpha}|=k} \Bigg\{ & \|\mathsf{D}^{\boldsymbol{\alpha}} u\|^2_{L^2(\Omega_0)} \\
& + \sum_{\boldsymbol{c}\in\mathcal{C}'} \big\| r_{\boldsymbol{c}}^{\beta_{\boldsymbol{c}}+|\boldsymbol{\alpha}|} \mathsf{D}^{\boldsymbol{\alpha}} u \big\|^2_{L^2(\omega_{\boldsymbol{c}})} + \sum_{\boldsymbol{c}\in\mathcal{C}\setminus\mathcal{C}'} \big\| r_{\boldsymbol{c}}^{\max\{\beta_{\boldsymbol{c}}+|\boldsymbol{\alpha}|,0\}} \mathsf{D}^{\boldsymbol{\alpha}} u \big\|^2_{L^2(\omega_{\boldsymbol{c}})} \\
& + \sum_{\boldsymbol{e}\in\mathcal{E}'} \big\| r_{\boldsymbol{e}}^{\beta_{\boldsymbol{e}}+|\boldsymbol{\alpha}^\perp|} \mathsf{D}^{\boldsymbol{\alpha}} u \big\|^2_{L^2(\omega_{\boldsymbol{e}})} + \sum_{\boldsymbol{e}\in\mathcal{E}\setminus\mathcal{E}'} \big\| r_{\boldsymbol{e}}^{\max\{\beta_{\boldsymbol{e}}+|\boldsymbol{\alpha}^\perp|,0\}} \mathsf{D}^{\boldsymbol{\alpha}} u \big\|^2_{L^2(\omega_{\boldsymbol{e}})} \\
& + \sum_{\boldsymbol{c}\in\mathcal{C}'} \sum_{\boldsymbol{e}\in\mathcal{E}_{\boldsymbol{c}}\cap\mathcal{E}'} \big\| r_{\boldsymbol{c}}^{\beta_{\boldsymbol{c}}+|\boldsymbol{\alpha}|} \rho_{\boldsymbol{ce}}^{\beta_{\boldsymbol{e}}+|\boldsymbol{\alpha}^\perp|} \mathsf{D}^{\boldsymbol{\alpha}} u \big\|^2_{L^2(\omega_{\boldsymbol{ce}})} \\
& + \sum_{\boldsymbol{c}\in\mathcal{C}'} \sum_{\boldsymbol{e}\in\mathcal{E}_{\boldsymbol{c}}\cap(\mathcal{E}\setminus\mathcal{E}')} \big\| r_{\boldsymbol{c}}^{\beta_{\boldsymbol{c}}+|\boldsymbol{\alpha}|} \rho_{\boldsymbol{ce}}^{\max\{\beta_{\boldsymbol{e}}+|\boldsymbol{\alpha}^\perp|,0\}} \mathsf{D}^{\boldsymbol{\alpha}} u \big\|^2_{L^2(\omega_{\boldsymbol{ce}})} \\
& + \sum_{\boldsymbol{c}\in\mathcal{C}\setminus\mathcal{C}'} \sum_{\boldsymbol{e}\in\mathcal{E}_{\boldsymbol{c}}\cap\mathcal{E}'} \big\| r_{\boldsymbol{c}}^{\max\{\beta_{\boldsymbol{c}}+|\boldsymbol{\alpha}|,0\}} \rho_{\boldsymbol{ce}}^{\beta_{\boldsymbol{e}}+|\boldsymbol{\alpha}^\perp|} \mathsf{D}^{\boldsymbol{\alpha}} u \big\|^2_{L^2(\omega_{\boldsymbol{ce}})} \\
& + \sum_{\boldsymbol{c}\in\mathcal{C}\setminus\mathcal{C}'} \sum_{\boldsymbol{e}\in\mathcal{E}_{\boldsymbol{c}}\cap(\mathcal{E}\setminus\mathcal{E}')} \big\| r_{\boldsymbol{c}}^{\max\{\beta_{\boldsymbol{c}}+|\boldsymbol{\alpha}|,0\}} \rho_{\boldsymbol{ce}}^{\max\{\beta_{\boldsymbol{e}}+|\boldsymbol{\alpha}^\perp|,0\}} \mathsf{D}^{\boldsymbol{\alpha}} u \big\|^2_{L^2(\omega_{\boldsymbol{ce}})} \Bigg\} .
\end{aligned}
\tag{2.7}
$$

For $m > k_{\boldsymbol{\beta}}$, with

$$
k_{\boldsymbol{\beta}} := -\min\{\min_{\boldsymbol{c}\in\mathcal{C}} \beta_{\boldsymbol{c}}, \min_{\boldsymbol{e}\in\mathcal{E}} \beta_{\boldsymbol{e}}\},
\tag{2.8}
$$

we write $N^m_{\boldsymbol{\beta}}(\Omega;\mathcal{C}',\mathcal{E}')$ for the space of functions u such that $\|u\|_{N^m_{\boldsymbol{\beta}}(\Omega;\mathcal{C}',\mathcal{E}')} < \infty$, with the norm $\|u\|^2_{N^m_{\boldsymbol{\beta}}(\Omega;\mathcal{C}',\mathcal{E}')} := \sum_{k=0}^m |u|^2_{N^k_{\boldsymbol{\beta}}(\Omega;\mathcal{C}',\mathcal{E}')}$. For subdomains $K \subseteq \Omega$ we shall denote by $|\cdot|_{N^k_{\boldsymbol{\beta}}(K;C',\mathcal{E}')}$ the semi-norm (2.7) with all domains of integration replaced by their intersections with $K \subseteq \Omega$, and likewise we shall use the norm $\|\cdot\|_{N^m_{\boldsymbol{\beta}}(K;\mathcal{C}',\mathcal{E}')}$. We note that we have $M^m_{\boldsymbol{\beta}}(\Omega) := N^m_{\boldsymbol{\beta}}(\Omega;\mathcal{C},\mathcal{E})$, where $M^m_{\boldsymbol{\beta}}(\Omega)$ is the weighted Sobolev space considered in [18] for the pure Dirichlet problem.

2.3. **Analytic regularity.** We adopt the analytic function classes of [5].

Definition 2.1. The class $B_{\boldsymbol{\beta}}(\Omega';\mathcal{C}',\mathcal{E}')$ consists of all functions u such that $u \in N^m_{\boldsymbol{\beta}}(\Omega';\mathcal{C}',\mathcal{E}')$ for $m > k_{\boldsymbol{\beta}}$, with $k_{\boldsymbol{\beta}}$ as in (2.8), and such that there exists a constant $C_u > 0$ such that $|u|_{N^k_{\boldsymbol{\beta}}(\Omega';\mathcal{C}',\mathcal{E}')} \leq C_u^{k+1}\Gamma(k+1)$ for all $k > k_{\boldsymbol{\beta}}$.

We have the following regularity result from [5, Theorem 7.3] for variational solutions of problem (1.1)–(1.3) (with constant coefficients).

Proposition 2.2. *Let $\emptyset \subset \mathcal{E}_D \subset \mathcal{E}$. Then there are bounds $b_{\mathcal{E}}, b_{\mathcal{C}} > 0$ (depending on Ω, the coefficient matrix $\boldsymbol{A}$ and the set $\mathcal{E}_D$) such that for weight exponent vectors $\boldsymbol{b}$ with*

$$
0 < b_{\boldsymbol{c}} < b_{\mathcal{C}}, \quad 0 < b_{\boldsymbol{e}} < b_{\mathcal{E}}, \qquad \boldsymbol{c} \in \mathcal{C},\ \boldsymbol{e} \in \mathcal{E},
\tag{2.9}
$$

the weak solution $u \in V$ *defined* (1.4) *of problem* (1.1)–(1.3) *satisfies:*

$$f \in B_{1-\boldsymbol{b}}(\Omega;\mathcal{C},\mathcal{E}_D) \implies u \in B_{-1-\boldsymbol{b}}(\Omega;\mathcal{C},\mathcal{E}_D)\,. \tag{2.10}$$

Remark 2.3. For pure Dirichlet and Neumann problems, we have corresponding analytic regularity shifts:

$$\mathcal{E}_D = \mathcal{E}: \quad f \in B_{1-\boldsymbol{b}}(\Omega;\mathcal{C},\mathcal{E}) \implies u \in B_{-1-\boldsymbol{b}}(\Omega;\mathcal{C},\mathcal{E})\,, \tag{2.11}$$

$$\mathcal{E}_D = \emptyset: \quad f \in B_{1-\boldsymbol{b}}(\Omega;\emptyset,\emptyset) \implies u \in B_{-1-\boldsymbol{b}}(\Omega;\emptyset,\emptyset)\,; \tag{2.12}$$

cf. [5, Corollary 7.1 and Theorem 7.4]. Due to the inclusions $B_{-1-\boldsymbol{b}}(\Omega;\mathcal{C},\mathcal{E}) \subset B_{-1-\boldsymbol{b}}(\Omega;\mathcal{C},\mathcal{E}_D) \subset B_{-1-\boldsymbol{b}}(\Omega;\emptyset,\emptyset)$, we shall focus on proving exponential approximation properties for the maximal space $B_{-1-\boldsymbol{b}}(\Omega;\emptyset,\emptyset)$.

Remark 2.4. As in [24, Remark 2.5], we assume that in (2.9) there holds

$$0 < b_{\boldsymbol{c}} < 1, \quad 0 < b_{\boldsymbol{e}} < 1, \qquad \boldsymbol{c} \in \mathcal{C},\ \boldsymbol{e} \in \mathcal{E}. \tag{2.13}$$

With (2.6), we then have $\kappa_\beta \in (1,2)$ in (2.8). Hence, the regularity property in Definition 2.1 holds for $k \geq 2$. In addition, we shall assume that, for any polyhedron Ω and right-hand side f in the class of problems considered here, there exists *some* $\theta \in (0,1)$ such that the weak solution $u \in V$ belongs to $H^{1+\theta}(\Omega)$. For weight exponents $b_{\boldsymbol{c}} \in (1/2,1)$, $b_{\boldsymbol{e}} \in (0,1)$, this follows from [5, Remark 6.2(ii)] and [14, Theorem 3.5]. We also refer to the discussion in [24, Remark 2.5].

3. Finite Element Discretization and Exponential Convergence

3.1. **Geometric meshes.** We review geometric mesh constructions from [22, 23].

3.1.1. *Geometric mesh patches.* We partition the domain Ω into a finite number $\mathfrak{P}$ of open, axiparallel and hexahedral *patches* $\{Q_{\mathfrak{p}}\}_{\mathfrak{p}=1}^{\mathfrak{P}}$ which constitute the patch mesh $\mathcal{M}^0$. In the axiparallel setting, each $Q_{\mathfrak{p}} \in \mathcal{M}^0$ is an affine-orthogonal image $Q_{\mathfrak{p}} = G_{\mathfrak{p}}(\widetilde{Q})$ of the *reference patch* $\widetilde{Q} = (-1,1)^3$. We assume $\mathcal{M}^0$ to be regular, i.e., the intersection $\overline{Q}_{\mathfrak{p}} \cap \overline{Q}_{\mathfrak{p}'}$ of any two patches $Q_{\mathfrak{p}}, Q_{\mathfrak{p}'} \in \mathcal{M}^0$, $\mathfrak{p} \neq \mathfrak{p}'$, is either empty or a vertex, an entire edge, or an entire face of both patches. Without loss of generality we assume that (the closure of) each patch intersects either with at most one corner $\boldsymbol{c} \in \mathcal{C}$, and with either none, one or several edges $\boldsymbol{e} \in \mathcal{E}_{\boldsymbol{c}}$ meeting in $\boldsymbol{c}$. In addition, we shall always assume that boundary faces on the patch $Q_{\mathfrak{p}}$ belong to exactly one boundary plane $\Gamma_{\boldsymbol{\iota}}$.

With each patch $Q_{\mathfrak{p}} \in \mathcal{M}^0$, we associate a *geometric reference mesh patch* $\widetilde{\mathcal{M}}_{\mathfrak{p}}$ *on* $\widetilde{Q}$. We recall from [22, Section 3.3] that the geometric patch meshes are generated recursively by iterating *four basic geometric refinement operations*, the so-called *hp-extensions* (Ex1)–(Ex4) on the initial mesh $\mathcal{M}^0$, resulting in *four geometric mesh patch types* $\mathfrak{t} \in \{\boldsymbol{c},\boldsymbol{e},\boldsymbol{ce},\mathrm{int}\}$ on $\widetilde{Q}$. That is, we take

$$\widetilde{\mathcal{M}}_{\mathfrak{p}} \in \widetilde{\mathcal{RP}} := \{\widetilde{\mathcal{M}}_\sigma^{\ell,\boldsymbol{c}}, \widetilde{\mathcal{M}}_\sigma^{\ell,\boldsymbol{e}}, \widetilde{\mathcal{M}}_\sigma^{\ell,\boldsymbol{ce}}, \widetilde{\mathcal{M}}_\sigma^{\ell,\mathrm{int}}\} = \{\widetilde{\mathcal{M}}_\sigma^{\ell,\mathfrak{t}}\}_{\mathfrak{t}\in\{\boldsymbol{c},\boldsymbol{e},\boldsymbol{ce},\mathrm{int}\}}. \tag{3.1}$$

Whenever $Q_{\mathfrak{p}}$ abuts at the singular set $\mathcal{S}$, we assign to $\widetilde{\mathcal{M}}_{\mathfrak{p}}$ (a suitably rotated and oriented version) of the geometrically refined reference mesh patches shown in Figure 1 and denoted by $\widetilde{\mathcal{M}}_\sigma^{\ell,\boldsymbol{c}}$ (corner patch), $\widetilde{\mathcal{M}}_\sigma^{\ell,\boldsymbol{e}}$ (edge patch), and $\widetilde{\mathcal{M}}_\sigma^{\ell,\boldsymbol{ce}}$ (corner-edge patch), respectively. We implicitly allow for simultaneous geometric refinements towards several edges in the corner-edge patch $\widetilde{\mathcal{M}}_\sigma^{\ell,\boldsymbol{ce}}$, which corresponds to an overlap of at most three rotated versions of the basic corner-edge patch; see Figure 3 below. The geometric refinements in these reference patches

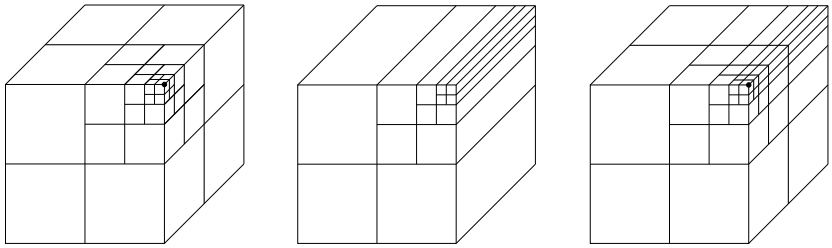

FIGURE 1. Three geometric reference mesh patches on $\widetilde{Q}$ with $\sigma = 0.5$: corner patch $\widetilde{\mathcal{M}}_\sigma^{\ell,\boldsymbol{c}}$ (left), edge patch $\widetilde{\mathcal{M}}_\sigma^{\ell,\boldsymbol{e}}$ (center), and corner-edge patch $\widetilde{\mathcal{M}}_\sigma^{\ell,\boldsymbol{ce}}$ (right).

are characterized by (i) a fixed parameter $\sigma \in (0,1)$ defining the subdivision ratio of the geometric refinements and (ii) the index ℓ defining the number of refinements. For interior patches $Q_{\mathfrak{p}} \in \mathcal{M}^0$, which have empty intersection with $\mathcal{S}$, we assign to $\widetilde{\mathcal{M}}_{\mathfrak{p}}$ a geometric reference mesh patch $\widetilde{\mathcal{M}}_\sigma^{\ell,\mathrm{int}}$ on $\widetilde{Q}$, which comprises only *finitely many regular refinements* and does not introduce irregular faces in $\widetilde{Q}$. In the refinement process, the reference mesh $\widetilde{\mathcal{M}}_\sigma^{\ell,\mathrm{int}}$ is kept unchanged and is independent of the refinement level ℓ. As different interior patches can be refined differently, without loss of generality the notation $\widetilde{\mathcal{M}}_\sigma^{\ell,\mathrm{int}}$ is to be understood in a generic fashion.

The geometric reference mesh patch $\widetilde{\mathcal{M}}_{\mathfrak{p}} \in \widetilde{\mathcal{RP}}$ introduces the corresponding patch partition $\mathcal{M}_{\mathfrak{p}} = G_{\mathfrak{p}}(\widetilde{\mathcal{M}}_{\mathfrak{p}}) := \{K : K = G_{\mathfrak{p}}(\widetilde{K}),\, \widetilde{K} \in \widetilde{\mathcal{M}}_{\mathfrak{p}}\}$ on $Q_{\mathfrak{p}}$. *Inter-patch continuity* of *hp*-approximations will be ensured by the following hypothesis; cf. [18, Assumption 3.1]. Here and in the sequel, we denote by $m_d(\cdot)$ the d-dimensional Lebesgue measure.

Assumption 3.1. For $\mathfrak{p} \neq \mathfrak{p}'$, let $Q_{\mathfrak{p}}, Q_{\mathfrak{p}'} \in \mathcal{M}^0$ be two distinct patches with $\Gamma_{\mathfrak{p}\mathfrak{p}'} := \overline{Q}_{\mathfrak{p}} \cap \overline{Q}_{\mathfrak{p}'} \neq \emptyset$ and either $m_2(\Gamma_{\mathfrak{p}\mathfrak{p}'}) > 0$ or $m_2(\Gamma_{\mathfrak{p}\mathfrak{p}'}) = 0$, $m_1(\Gamma_{\mathfrak{p}\mathfrak{p}'}) > 0$. Then the parametrizations induced by the patch maps on the patch interfaces $\Gamma_{\mathfrak{p}\mathfrak{p}'}$ are assumed to coincide "from either side": $G_{\mathfrak{p}} \circ \big(G_{\mathfrak{p}'}^{-1} \,|_{\Gamma_{\mathfrak{p}\mathfrak{p}'}}\big) = G_{\mathfrak{p}'} \circ \big(G_{\mathfrak{p}}^{-1} \,|_{\Gamma_{\mathfrak{p}\mathfrak{p}'}}\big)$. In addition, the mesh patches $\mathcal{M}_{\mathfrak{p}}, \mathcal{M}_{\mathfrak{p}'}$ are assumed to coincide on $\Gamma_{\mathfrak{p}\mathfrak{p}'}$.

3.1.2. *Geometric meshes.* For fixed parameters $\sigma \in (0,1)$ and $\ell \in \mathbb{N}$, a σ-geometric mesh on Ω is now given by the disjoint union

$$\mathcal{M} = \mathcal{M}_\sigma^\ell := \cup_{\mathfrak{p}=1}^{\mathfrak{P}} \mathcal{M}_{\mathfrak{p}}\,. \tag{3.2}$$

If we denote by $\widehat{K} := (-1,1)^3$ the reference cube, then each $K \in \mathcal{M}$ is the image of $\widehat{K}$ under an element mapping $\Phi_K : \widehat{K} \to K$, given as *the composition of the corresponding patch map $G_{\mathfrak{p}}$ with an anisotropic dilation-translation.* To achieve a proper geometric refinement towards corners and edges of Ω without violating Assumption 3.1, the geometric refinements $\mathcal{M}_{\mathfrak{p}}$ in the patches $Q_{\mathfrak{p}}$ have to be suitably selected and oriented. For a fixed subdivision ratio $\sigma \in (0,1)$, we call the sequence $\mathfrak{M}_\sigma = \{\mathcal{M}_\sigma^\ell\}_{\ell \geq 1}$ of geometric meshes a *σ-geometric mesh family*; see [22, Definition 3.4]. As before, we shall refer to the index ℓ as *refinement level.*

Without loss of generality as in [23, Section 5.1.4], every element $K \in \mathcal{M}$ can be assumed to be a Cartesian product of the form

$$K = K^\perp \times K^\parallel = (0, h_K^\perp)^2 \times (0, h_K^\parallel), \tag{3.3}$$

with $h_K^\perp \lesssim h_K^\parallel$. We call K *isotropic* if $h_K^\perp \simeq h_K^\parallel \simeq h_K$ uniformly in ℓ; otherwise, element K is *anisotropic*. Elements in corner and interior patches are isotropic, whereas elements in edge and corner-edge patches may be anisotropic. We also note that the elemental diameters $h_K^\perp$ and $h_K^\parallel$ are related to the relative distances to the edge $\boldsymbol{e}$ and corner $\boldsymbol{c}$ located nearest to K; cf. [23, Proposition 3.2].

3.1.3. *Vertices, edges and faces.* Let $\mathcal{M} = \mathcal{M}_\sigma^\ell$ be a geometric mesh. For an axiparallel hexahedral element $K \in \mathcal{M}$, we denote by $\mathcal{N}(K)$, $\mathcal{E}(K)$ and $\mathcal{F}(K)$ the sets of its elemental vertices, its elemental edges and its elemental faces, respectively. If $E \in \mathcal{E}(K)$ and $\mathcal{F} \in \mathcal{F}(K)$, we write $\mathcal{N}(E) \subset \mathcal{N}(K)$ for the two end points of E and $\mathcal{E}(F) \subset \mathcal{F}(K)$ for the four elemental edges of F.

The set of all vertex nodes is defined by

$$\mathcal{N}(\mathcal{M}) := \bigcup_{K \in \mathcal{M}} \mathcal{N}(K)\,. \tag{3.4}$$

The subset $\mathcal{N}_D(\mathcal{M})$ of all Dirichlet nodes consists of all $\boldsymbol{N} \in \mathcal{N}(\mathcal{M})$ with $\boldsymbol{N} \in \overline{\Gamma}_{\boldsymbol{\iota}}$ for some index $\boldsymbol{\iota} \in \mathcal{J}_D$. The node $\boldsymbol{N}$ is called regular if $\boldsymbol{N} \in \mathcal{N}(K)$ for all $K \in \mathcal{M}$ with $\boldsymbol{N} \cap \overline{K} \neq \emptyset$; otherwise it is called irregular.

The non-trivial one-dimensional intersection $E = E_{K,K'}$ of the elemental edges of two neighboring elements $K, K' \in \mathcal{M}$ is called an *edge of* $\mathcal{M}$. The edge $E_{K,K'}$ is called regular if $E \in \mathcal{E}(K)$ and $E \in \mathcal{E}(K')$; otherwise we call it irregular. Note that $E_{K,K'}$ can be located on a Dirichlet plane $\overline{\Gamma}_{\boldsymbol{\iota}}$ for $\boldsymbol{\iota} \in \mathcal{J}_D$, in which case we call it a *Dirichlet boundary edge of* $\mathcal{M}$. Moreover, the non-trivial one-dimensional intersection $E = E_{K,\boldsymbol{e}} \in \mathcal{E}(K)$ of an elemental edge of K with $\boldsymbol{e} \in \mathcal{E}_D$ is also called a *Dirichlet boundary edge*. The set of all edges is denoted by $\mathcal{E}(\mathcal{M})$ and the set of all Dirichlet boundary edges by $\mathcal{E}_D(\mathcal{M})$.

Similarly, the non-trivial two-dimensional intersection $F = F_{K,K'}$ of the elemental faces of two neighboring elements $K, K' \in \mathcal{M}$ is called an *interior face of* $\mathcal{M}$. For our class of geometric meshes, one can always assume that $F = F_{K,K'}$ is an elemental face of at least one element and a non-vanishing subset of an elemental face of the other element. For example,

$$F \in \mathcal{F}(K) \quad \text{and} \quad F \subseteq F' \text{ for } F' \in \mathcal{F}(K') \text{ with } m_2(F \cap F') > 0. \tag{3.5}$$

The face F is called regular if $F \in \mathcal{F}(K)$ and $F \in \mathcal{F}(K')$; otherwise it is said to be irregular. Furthermore, the non-empty and two-dimensional intersection $F = F_{K,\Gamma_{\boldsymbol{\iota}}}$ of an elemental face of $K \in \mathcal{M}$ with a Dirichlet plane $\Gamma_{\boldsymbol{\iota}}$ for $\boldsymbol{\iota} \in \mathcal{J}_D$ is a *Dirichlet boundary face of* $\mathcal{M}$. We always have $F_{K,\Gamma_{\boldsymbol{\iota}}} \in \mathcal{F}(K)$. *Neumann boundary faces* are defined correspondingly. However, as Neumann boundary conditions are enforced naturally, they will only play a minor role in our analysis. We write $\mathcal{F}_I(\mathcal{M})$, $\mathcal{F}_D(\mathcal{M})$ and $\mathcal{F}_N(\mathcal{M})$ for the sets of interior, Dirichlet and Neumann boundary faces of $\mathcal{M}$, respectively, and set $\mathcal{F}_{ID}(\mathcal{M}) := F_I(\mathcal{M}) \cup \mathcal{F}_D(\mathcal{M})$.

Remark 3.2. As in [18, Assumption 3.2] and under Assumption 3.1, for any distinct axiparallel elements $K, K' \in \mathcal{M}$ which share a common edge $E_{K,K'}$ or an interior face $F_{K,K'}$, the traces of the elemental polynomial spaces on $E_{K,K'}$ and $F_{K,K'}$ in local coordinates induced by the corresponding elemental maps coincide.

For a piecewise smooth function v, we define the jump of v over $F_{K,K'} \in \mathcal{F}_I(\mathcal{M})$ respectively over $F_{K,\Gamma_{\boldsymbol{\iota}}} \in \mathcal{F}_D(\mathcal{M})$ by

$$[\![v]\!]_{F_{K,K'}} := v|_K - v|_{K'} \quad \text{respectively by} \quad [\![v]\!]_{F_{K,\Gamma_{\boldsymbol{\iota}}}} := v|_K. \tag{3.6}$$

For $F \in \mathcal{F}(K)$, we denote by $h^{\perp}_{K,F}$ the height of K in direction perpendicular to F. We then introduce the *trace mesh size function* by

$$\mathtt{h}_F := \begin{cases} \min\{h^{\perp}_{K,F}, h^{\perp}_{K',F'}\}, & F = F_{K,K'} \in \mathcal{F}_I(\mathcal{M}), \\ h^{\perp}_{K,F}, & F = F_{K,\Gamma_\iota} \in \mathcal{F}_D(\mathcal{M}), \end{cases} \tag{3.7}$$

with $F' \in \mathcal{F}(K')$ as in (3.5). The bounded variation property in [22, Section 3.3.2] implies $\mathtt{h}_F \simeq h^{\perp}_{K,F} \simeq h^{\perp}_{K',F'}$ for interior faces $F_{K,K'} \in \mathcal{F}_I(\mathcal{M})$.

3.2. **Finite element spaces.** We next introduce discontinuous and continuous finite element spaces with anisotropic and $\mathfrak{s}$-linear degree distributions.

3.2.1. *Local finite element spaces.* Let $\mathcal{M} = \mathcal{M}^{\ell}_{\sigma}$ be a geometric mesh. With each $K \in \mathcal{M}$ and in accordance with (3.3), we assign an *anisotropic* polynomial degree vector $\boldsymbol{p}_K := (p^{\perp}_K, p^{\parallel}_K)$, with degrees $p^{\perp}_K \geq 1$ and $p^{\parallel}_K \geq 1$ in edge-perpendicular and edge-parallel directions, respectively. We always will assume that $p^{\perp}_K \leq p^{\parallel}_K$; cf. [23, Section 3]. For $K \in \mathcal{M}$, the elemental tensor-product polynomial space is defined by

$$\mathbb{Q}_{\boldsymbol{p}_K}(K) := \{\, v \in L^2(K) \,:\, v|_K \circ \Phi_K \in \mathbb{Q}_{\boldsymbol{p}_K}(\widehat{K}) \,\}, \tag{3.8}$$

where $\Phi_K : \widehat{K} \to K$ is the element mapping and $\mathbb{Q}_{\boldsymbol{p}_K}(\widehat{K})$ the anisotropic tensor-product polynomial space on $\widehat{K} = \widehat{I}^3$ with $\widehat{I} = (-1, 1)$:

$$\mathbb{Q}_{\boldsymbol{p}_K}(\widehat{K}) := \mathbb{Q}_{p^{\perp}_K}(\widehat{I}^2) \otimes \mathbb{P}_{p^{\perp}_K}(\widehat{I}) = \mathbb{P}_{p_K}(\widehat{I}) \otimes \mathbb{P}_{p^{\perp}_K}(\widehat{I}) \otimes \mathbb{P}_{p^{\parallel}_K}(\widehat{I}), \tag{3.9}$$

with $\mathbb{P}_p(I)$ denoting the univariate polynomials of degree less than or equal to p on an interval I. The polynomial degree vector $\boldsymbol{p}_K$ is called *isotropic* if $p^{\perp}_K = p^{\parallel}_K = p_K$. In this case, we write $\mathbb{Q}_{p_K}(K)$ in place of $\mathbb{Q}_{\boldsymbol{p}_K}(K)$.

The elemental polynomial degree vectors $\boldsymbol{p}_K$ are combined into the *polynomial degree distribution* $\boldsymbol{p} := \{\, \boldsymbol{p}_K : K \in \mathcal{M} \,\}$ on $\mathcal{M}$. We set $|\boldsymbol{p}| := \max_{K\in\mathcal{M}} |\boldsymbol{p}_K|$, with $|\boldsymbol{p}_K| := \max\{p^{\perp}_K, p^{\parallel}_K\}$. We then introduce the generic discontinuous space

$$V^0(\mathcal{M}, \boldsymbol{p}) := \big\{\, v \in L^2(\Omega) \,:\, v|_K \in \mathbb{Q}_{\boldsymbol{p}_K}(K),\ K \in \mathcal{M} \,\big\}. \tag{3.10}$$

The *hp*-extensions (Ex1)–(Ex4) introduced in [22] provide $\mathfrak{s}$-*linear polynomial degree distributions* $\boldsymbol{p}_{\mathfrak{s}}(\widetilde{\mathcal{M}}^{\ell,\mathtt{t}}_{\sigma})$ on the geometric reference mesh patches $\widetilde{\mathcal{M}}^{\ell,\mathtt{t}}_{\sigma}$ for $\mathtt{t} \in \{\boldsymbol{c}, \boldsymbol{e}, \boldsymbol{ce}, \mathrm{int}\}$, which increase $\mathfrak{s}$-linearly and possibly anisotropically away from singularities for a *slope parameter* $\mathfrak{s} > 0$; see [22, Section 3] for more details. By construction, the patchwise distributions $\boldsymbol{p}_{\mathfrak{s}}(\widetilde{\mathcal{M}}^{\ell,\mathtt{t}}_{\sigma})$ induce a $\mathfrak{s}$-linear polynomial degree distribution on a geometric mesh $\mathcal{M}^{\ell}_{\sigma}$, which we denote by $\boldsymbol{p}_{\mathfrak{s}}(\mathcal{M}^{\ell}_{\sigma})$.

3.2.2. *Face and edge polynomial degrees.* Let $\mathcal{M} = \mathcal{M}^{\ell}_{\sigma}$ be a geometric mesh and $\boldsymbol{p}$ a polynomial degree distribution on $\mathcal{M}$. To define conforming spaces, we introduce edge and face polynomial degrees in conjunction with a suitable *minimum rule* over neighoring edges and faces; cf. [7].

Let $K \in \mathcal{M}$ and $\boldsymbol{p}_K = (p^{\perp}_K, p^{\parallel}_K)$ the elemental degree vector. For $E \in \mathcal{E}(K)$ and $F \in \mathcal{F}(K)$, we denote by $p_{K,E} \in \mathbb{N}$ and $\boldsymbol{p}_{K,F} = (p^1_{K,F}, p^2_{K,F}) \in \mathbb{N}^2$ the polynomial degrees induced by $\boldsymbol{p}_K$ on E and F in local coordinates, respectively. We further introduce the sets

$$\delta_{K,E} := \{\, K' \in \mathcal{M} \,:\, E \subseteq E' \in \mathcal{E}(K') \text{ with } m_1(E \cap \partial F') > 0 \,\}, \tag{3.11}$$

$$\delta_{K,F} := \{\, K' \in \mathcal{M} \,:\, F \subseteq F' \text{ for } F' \in \mathcal{F}(K') \text{ with } m_2(F \cap F') > 0 \,\}. \tag{3.12}$$

Notice that $K \in \delta_{K,E}$ and $K \in \delta_{K,F}$ and that the cardinalities of $\delta_{K,E}$ and $\delta_{K,F}$ are uniformly bounded. For $E \in \mathcal{E}(K)$ and $F \in \mathcal{F}(K)$, the *minimum edge and face degrees* are then defined by

$$\overline{p}_{K,E} := \min_{K' \in \delta_{K,E}} p_{K',E'} \in \mathbb{N}, \tag{3.13}$$

$$\overline{\boldsymbol{p}}_{K,F} := \min_{K' \in \delta_{K,F}} \boldsymbol{p}_{K',F'} \in \mathbb{N}^2, \tag{3.14}$$

where the sets E' and F' are as in (3.11) and (3.12), respectively, and where the minimun in (3.14) is understood componentwise. With Remark 3.2, we may denote by $\mathbb{P}_{\overline{p}_{K,E}}(E)$ and $\mathbb{Q}_{\overline{\boldsymbol{p}}_{K,F}}(F)$ the corresponding polynomial spaces on $E \in \mathcal{E}(K)$ and $F \in \mathcal{F}(K)$, respectively.

3.2.3. *Finite element spaces.* On an axiparallel element $K \in \mathcal{M}$, we consider polynomial functions $v|_K \in \mathbb{Q}_{\boldsymbol{p}_K}(K)$ which can be expanded into basis functions as

$$v|_K := v|_K^{\mathrm{nod}} + v|_K^{\mathrm{edge}} + v|_K^{\mathrm{face}} + v|_K^{\mathrm{int}}, \tag{3.15}$$

where, with the minimum degrees $\overline{p}_{K,E}$ in (3.13) and $\overline{\boldsymbol{p}}_{K,F}$ in (3.14),

$$\begin{aligned} v|_K^{\mathrm{nod}} &= \sum_{\boldsymbol{N} \in \mathcal{N}(K)} c_K^{\boldsymbol{N}} \Phi_K^{\boldsymbol{N}}, \\ v|_K^{\mathrm{edge}} &= \sum_{E \in \mathcal{E}(K)} \sum_{i=1}^{\overline{p}_{K,E}-1} c_K^{E,i} \Phi_K^{E,i}, \\ v|_K^{\mathrm{face}} &= \sum_{F \in \mathcal{F}(K)} \sum_{i=1}^{\overline{p}^1_{K,F}-1} \sum_{j=1}^{\overline{p}^2_{K,F}-1} c_K^{F,i,j} \Phi_K^{F,i,j}, \end{aligned} \tag{3.16}$$

with coefficients $c_K^{\boldsymbol{N}}$, $c_K^{E,i}$ and $c_K^{F,i,j}$. Here, the function $\Phi_K^{\boldsymbol{N}} \in \mathbb{Q}_1(K)$ denotes the trilinear nodal shape function on K with the property that $\Phi_K^{\boldsymbol{N}}(\boldsymbol{N}') = \delta_{\boldsymbol{N},\boldsymbol{N}'}$ for $\boldsymbol{N}' \in \mathcal{N}(K)$. For $E \in \mathcal{E}(K)$ the edge shape functions $\{\Phi_K^{E,i}\}_{i=1}^{\overline{p}_{K,E}-1}$ on K are polynomials of degree $\overline{p}_{K,E}$ along the edge E tensorized with linear blending functions in the two directions perpendicular to F. Restricted to E, they span the space $\mathbb{P}\overline{p}_{K,E}(E) \cap H_0^1(E)$. They vanish on the other elemental edges $E' \neq E$, as well as on faces $F \in \mathcal{F}(K)$ with $E \notin \mathcal{E}(F)$. Similarly, for $F \in \mathcal{F}(K)$ the face shape functions $\{\Phi_K^{F,i,j}\}_{i,j}$ are anisotropic polynomials of vector degree $\overline{\boldsymbol{p}}_{K,F}$ on the face F tensorized with linear blending functions in the direction perpendicular to F. Restricted to F, they span the space $\mathbb{Q}\overline{\boldsymbol{p}}_{K,F}(F) \cap H_0^1(F)$, and vanish on the remaining elemental faces $F' \neq F$. Finally, the interior part $v|_K^{\mathrm{int}}$ in (3.15) is a polynomial bubble function in $\mathbb{Q}_{\boldsymbol{p}_K}(K) \cap H_0^1(K)$; as it will be left unchanged in the subsequent analysis, we will not further specify it. For empty ranges of the indices in (3.16), the corresponding sums are understood as zero. We refer the reader to [7, Section 2.3] for an explicit construction of shape functions as in (3.15), (3.16).

For $K \in \mathcal{M}$, we collect the edge and face degrees in (3.13), (3.14) in the vector $\overline{\boldsymbol{p}}_K$, and define the elemental polynomial space

$$\mathbb{S}_{\overline{\boldsymbol{p}}_K}(K) := \big\{\, v|_K \in \mathbb{Q}_{\boldsymbol{p}_K}(K) \,:\, v|_K \text{ is of the form (3.15), (3.16)} \,\big\}, \tag{3.17}$$

Thus, a polynomial $v \in \mathbb{S}_{\overline{\boldsymbol{p}}_K}(K)$ satisfies

$$\big(v|_K\big)|_E \in \mathbb{P}_{\overline{p}_{K,E}}(E), \qquad E \in \mathcal{E}(K), \tag{3.18}$$

$$\big(v|_K\big)|_F \in \mathbb{Q}_{\overline{\boldsymbol{p}}_{K,F}}(F), \qquad F \in \mathcal{F}(K). \tag{3.19}$$

We then introduce the *minimum rule hp-finite element spaces*

$$\overline{V}^0(\mathcal{M},\boldsymbol{p}) := \big\{\, v \in L^2(\Omega) \,:\, v|_K \in \mathbb{S}_{\overline{\boldsymbol{p}}_K}(K),\ K \in \mathcal{M} \big\}, \tag{3.20}$$

$$V^1(\mathcal{M},\boldsymbol{p}) := \big\{\, v \in V \,:\, v|_K \in \mathbb{S}_{\overline{\boldsymbol{p}}_K}(K),\ K \in \mathcal{M} \,\big\}; \tag{3.21}$$

cf. [7]. By construction, we have $\overline{V}^0(\mathcal{M},\boldsymbol{p}) \subseteq V^0(\mathcal{M},\boldsymbol{p})$.

3.3. **Conforming *hp*-FEM and exponential convergence.** For parameters $\sigma \in (0,1)$ and $\mathfrak{s} > 0$, let $\mathfrak{M}_\sigma = \{\mathcal{M}_\sigma^\ell\}_{\ell\geq 1}$ be a σ-geometric mesh family on Ω and $\{\boldsymbol{p}_\mathfrak{s}(\mathcal{M}_\sigma^\ell)\}_{\ell\geq 1}$ the corresponding $\mathfrak{s}$-linear polynomial degree distributions. We consider the sequence of conforming *hp*-version finite element spaces

$$V_{\sigma,\mathfrak{s}}^{\ell,1} := V^1(\mathcal{M}_\sigma^\ell, \boldsymbol{p}_\mathfrak{s}(\mathcal{M}_\sigma^\ell)), \qquad \ell \geq 1, \tag{3.22}$$

and introduce its non-conforming counterparts by setting

$$V_{\sigma,\mathfrak{s}}^{\ell,0} := V^0(\mathcal{M}_\sigma^\ell, \boldsymbol{p}_\mathfrak{s}(\mathcal{M}_\sigma^\ell)), \qquad \overline{V}_{\sigma,\mathfrak{s}}^{\ell,0} := \overline{V}^0(\mathcal{M}_\sigma^\ell, \boldsymbol{p}_\mathfrak{s}(\mathcal{M}_\sigma^\ell)), \qquad \ell \geq 1. \tag{3.23}$$

Remark 3.3. The fact that the conforming spaces $V_{\sigma,\mathfrak{s}}^{\ell,1}$ define proper linear spaces will follow from our construction of conforming approximations in Sections 5 and 6 ahead. In the pure Neumann case (where $\mathcal{J}_D = \emptyset$), we note that the constant function belongs to $V_{\sigma,\mathfrak{s}}^{\ell,1}$, which will lead to well-defined factor spaces $V_{\sigma,\mathfrak{s}}^{\ell,1}/\mathbb{R}$.

The *hp*-version Galerkin discretization of the variational formulation (1.4) reads as usual: find $u^\ell \in V_{\sigma,\mathfrak{s}}^{\ell,1}$ such that

$$a(u^\ell, v) = \int_\Omega f v dx \qquad \forall v \in V_{\sigma,\mathfrak{s}}^{\ell,1}\ , \tag{3.24}$$

where we implicitly use the corresponding factor spaces $V_{\sigma,\mathfrak{s}}^{\ell,1}/\mathbb{R}$ in the pure Neumann case. For every $\ell \geq 1$, the discrete variational problem (3.24) admits a unique solution $u^\ell \in V_{\sigma,\mathfrak{s}}^{\ell,1}$ which is quasi-optimal: there exists a constant $C > 0$ (only depending on Ω, the coefficient matrix $\boldsymbol{A}$ and the set $\mathcal{E}_D$) such that

$$\|u - u^\ell\|_{H^1(\Omega)} \leq C \inf_{v \in V_{\sigma,\mathfrak{s}}^{\ell,1}} \|u - v\|_{H^1(\Omega)}\ . \tag{3.25}$$

One first main result of this paper is the H^1-norm exponential convergence of *hp*-FE approximations (3.24) for problem (1.1)–(1.3) with data $f \in B_{1-\boldsymbol{b}}(\Omega; \mathcal{C}', \mathcal{E}')$ as in the regularity shifts in (2.10), (2.11) or (2.12). This follows from the quasi-optimality (3.25) and the following *approximation property* of the *hp*-version finite element spaces $V_{\sigma,\mathfrak{s}}^{\ell,1}$.

Theorem 3.4. *Let $\boldsymbol{b}$ be a weight exponent vector satisfying* (2.13)*. For parameters $\sigma \in (0,1)$, $\mathfrak{s} > 0$, consider the sequence $V_{\sigma,\mathfrak{s}}^{\ell,1}$ of H^1-conforming hp-version finite element spaces in* (3.22)*. Then there exist quasi-interpolation projectors $\Pi_{\sigma,\mathfrak{s}}^{\ell,1} : V \to V_{\sigma,\mathfrak{s}}^{\ell,1}$ such that for functions $u \in V$ with $u \in B_{-1-\boldsymbol{b}}(\Omega;\emptyset,\emptyset) \cap H^{1+\theta}(\Omega)$ for some $\theta \in (0,1)$ there holds*

$$\|u - \Pi_{\sigma,\mathfrak{s}}^{\ell,1} u\|_{H^1(\Omega)} \leq C \exp\left(-b\ell\right)\ , \tag{3.26}$$

with constants $b, C > 0$ independent of ℓ, but depending on the parameters σ, $\mathfrak{s}$, the macro-mesh $\mathcal{M}^0$ with its associated patch maps, the minimum weight exponent in (2.13)*, the exponent θ, and on u through the analytic regularity constant C_u in Definition 2.1.*

In particular, if the variational solution $u \in V$ of problem (1.1)–(1.3) *belongs to $B_{-1-\boldsymbol{b}}(\Omega;\emptyset,\emptyset) \cap H^{1+\theta}(\Omega)$ for some $\theta \in (0,1)$, cf.* (2.10), (2.11), (2.12) *and Remark 2.4, then the conforming finite element approximations $u^\ell \in V^{\ell,1}_{\sigma,\mathfrak{s}}$ in* (3.24) *converge exponentially:*

$$\|u - u^\ell\|_{H^1(\Omega)} \leq C \exp\left(-b\sqrt[5]{N}\right) , \tag{3.27}$$

where the constants $b, C > 0$ are independent of $N = \dim(V^{\ell,1}_{\sigma,\mathfrak{s}})$, the number of degrees of freedom of the hp-FE discretization.

Remark 3.5. The projectors $\Pi^{\ell,1}_{\sigma,\mathfrak{s}}$ in (3.26) constructed ahead are well-defined on the space $V \subseteq H^1(\Omega)$. This is in contrast to the projectors constructed in [18] for homogeneous Dirichlet boundary conditions. They require H^2-regularity in each coordinate direction in the interior of Ω, and are set to zero on elements abutting at corners and edges of Ω.

Remark 3.6. The global hp-version projectors $\Pi^{\ell,1}_{\sigma,\mathfrak{s}}$ in (3.26) are assembled from *hp-patch projectors* $\Pi^{\ell,1,\mathfrak{p}}_{\sigma,\mathfrak{s}}$. We write formally, with restrictions to patches $\mathfrak{p} \in [1,...,\mathfrak{P}]$ implied in $\Pi^{\ell,1,\mathfrak{p}}_{\sigma,\mathfrak{s}}$,

$$\Pi^{\ell,1}_{\sigma,\mathfrak{s}} = \sum\nolimits_{\mathfrak{p}=1}^{\mathfrak{P}} \Pi^{\ell,1,\mathfrak{p}}_{\sigma,\mathfrak{s}} , \tag{3.28}$$

where inter-patch continuity follows from Assumption 3.1. The hp-patch projectors $\Pi^{\ell,1,\mathfrak{p}}_{\sigma,\mathfrak{s}}$ in (3.28), in turn, are obtained from *four families* $\{\widetilde{\Pi}^{\ell,1,\mathfrak{t}}_{\sigma,\mathfrak{s}}\}_{\ell\geq 1}$ *of hp-reference patch projectors* on the geometric reference mesh patches $\widetilde{\mathcal{M}}^{\ell,\mathfrak{t}}_\sigma$ of type $\mathfrak{t} \in \{\boldsymbol{c}, \boldsymbol{e}, \boldsymbol{ce}, \mathrm{int}\}$ which are transported to the patches $Q_\mathfrak{p} \subset \Omega$ via the patch maps $G_\mathfrak{p}$. While no liftings are necessary for interior patches (i.e., for $\mathfrak{t} = \mathrm{int}$), for patches of type $\mathfrak{t} \in \{\boldsymbol{c}, \boldsymbol{e}, \boldsymbol{ce}\}$, our construction yields jump liftings with stability bounds in the $H^1(Q_\mathfrak{p})$-norm which grow algebraically in $|\boldsymbol{p}|$.

Furthermore, the exponential consistency in $H^1(\widetilde{Q})$ of $\widetilde{\Pi}^{\ell,1,\mathfrak{t}}_{\sigma,\mathfrak{s}}$ on the reference patch $\widetilde{Q}$ can be readily verified for solutions $u \in V$ of (1.1)–(1.3) whose pullbacks from the mesh patch $Q_\mathfrak{p}$ to $\widetilde{Q}$ satisfy the *analytic patch regularity*

$$\widetilde{u}_\mathfrak{p} := u|_{Q_\mathfrak{p}} \circ G_\mathfrak{p} \in B_\mathfrak{t}(\widetilde{Q}), \;\; 1 \leq \mathfrak{p} \leq \mathfrak{P}, \;\; \mathfrak{t} \in \{\boldsymbol{c}, \boldsymbol{e}, \boldsymbol{ce}, \mathrm{int}\} , \tag{3.29}$$

where $B_\mathfrak{t}(\widetilde{Q})$ is an *analytic regularity reference class on $\widetilde{Q}$* with weighting towards corners or edges of $\widetilde{Q}$ depending on the refinement type $\mathfrak{t} \in \{\boldsymbol{c}, \boldsymbol{e}, \boldsymbol{ce}, \mathrm{int}\}$; see also [18, Section 4.4] for analytic reference classes $A_\mathfrak{t}(\widetilde{O})$ in the pure Dirichlet case. For $\mathfrak{t} \in \{\boldsymbol{c}, \boldsymbol{ce}\}$, we additionally require in (3.29) that $\widetilde{u}_\mathfrak{p} \in H^{1+\theta}(\widetilde{Q})$; cf. Remark 2.4. *All exponential convergence rate estimates in the present paper apply verbatim to any solution $u \in H^1(\Omega)$ which, in local patch coordinates, exhibit the above analytic patch regularity* (3.29).

Remark 3.7. The results of Theorem 3.4 are valid in particular for the *isotropic* finite element spaces

$$V^1(\mathcal{M}^\ell_\sigma, p_\ell) := \big\{\, v \in V \,:\, v|_K \in \mathbb{Q}_{p_\ell}(K),\; K \in \mathcal{M}^\ell_\sigma \,\big\}, \qquad \ell \geq 1, \tag{3.30}$$

with uniform polynomial degree $p_\ell \geq 1$. For these spaces, the minimum rules in Section 3.2.2 are trivially valid. The exponential convergence bounds (3.26) and (3.27) follow in this case as well, provided that $p_\ell = \max\{1, \lfloor \mathfrak{s}\ell \rfloor\}$, albeit with a generally smaller constant b.

Remark 3.8. The bounds (3.26) and (3.27) hold true in the pure Neumann case. This follows readily from Remark 3.3 and since $\Pi^{\ell,1}_{\sigma,\mathfrak{s}}$ reproduces constant functions.

Remark 3.9. The exponential convergence results in this paper apply verbatim to conforming *hp*-FEMs for second-order and possibly vector-valued elliptic problems which allow for analytic regularity shifts in the function classes in Definition 2.1. In particular, they are valid for stress-strain formulations of the equations of linear elasticity (with constant material parameters); [5, Section 7].

3.4. **Outline of the proof.** The proof of Theorem 3.4 follows along the lines of [18, Section 3.4], but is significantly more involved due to the appearance of the non-homogeneously weighted Sobolev spaces and the anisotropic and variable polynomial degree distributions. In this section, we outline the key steps. From now on we will frequently use the short-hand notation "$\lesssim_p$" for inequalities which hold up to *algebraic losses* in $|\boldsymbol{p}|$:

$$x \lesssim_p y \quad \Leftrightarrow \quad x \lesssim |\boldsymbol{p}|^a\, y \quad \text{for some } a \in \mathbb{N}. \tag{3.31}$$

3.4.1. *Base projectors with partial conformity.* We first introduce (non-conforming) base projectors with partial conformity and exponential convergence estimates.

To discuss the conformity properties, let $\mathcal{M} = \mathcal{M}^\ell_\sigma$ be a geometric mesh. For a set $\mathcal{F}' \subset \mathcal{F}_{ID}(\mathcal{M})$ of faces, we define

$$\mathrm{jmp}_{\mathcal{F}'}[u]^2 := \sum_{F\in\mathcal{F}'} \mathtt{h}_F^{-1} \|[\![u]\!]\|^2_{L^2(F)}. \tag{3.32}$$

Then, to avoid the need for jump liftings over edge-perpendicular faces between highly anisotropic elements, we construct base projectors which are conforming across certain sets $\mathcal{F}^\perp_{ID}(\mathcal{M}) \subset \mathcal{F}_{ID}(\mathcal{M})$ of edge-perpendicular faces, and generally non-conforming edge-parallel faces $F \in \mathcal{F}^\parallel_{ID}(\mathcal{M}) := \mathcal{F}_{ID}(\mathcal{M}) \setminus F^\perp_{ID}(\mathcal{M})$, which can be characterized by the property that

$$F \subseteq F' \in \mathcal{F}(K): \quad \mathtt{h}_F \simeq h^\perp_{K,F'} \simeq h^\perp_K \text{ uniformly in } \ell. \tag{3.33}$$

If we write K in the form (3.3), then (possibly after mapping) a face F satisfying (3.33) can be assumed to be of the form

$$F = (0, h^\perp_K) \times (0, h^\parallel_K) \text{ uniformly in } \ell\,. \tag{3.34}$$

Note that faces with (3.33), (3.34) appear (i) between isotropic elements and (ii) in edge-parallel direction between anisotropic elements in edge or corner-edge patches. In the following, we shall also split $\mathcal{F}^\parallel_{ID}(\mathcal{M})$ into interior and Dirichlet boundary faces, i.e., $\mathcal{F}^\parallel_{ID}(\mathcal{M}) = \mathcal{F}^\parallel_I(\mathcal{M}) \,\dot\cup\, F^\parallel_D(\mathcal{M})$.

To state exponential convergence estimates in broken norms, we split the errors into edge-perpendicular and edge-parallel contribution as in [24], except for the (isotropic) corner elements. For $\boldsymbol{c} \in \mathcal{C}$, we set $\mathfrak{T}^\ell_{\boldsymbol{c}} := \{\, K \in \mathcal{M}^\ell_\sigma \,:\, \overline{K} \cap \boldsymbol{c} \neq \emptyset \,\}$ and define

$$\mathfrak{T}^\ell_{\mathcal{C}} := \bigcup_{\boldsymbol{c}\in\mathcal{C}} \mathfrak{T}^\ell_{\boldsymbol{c}}, \qquad \mathcal{M}^\ell_{\sigma,\mathcal{C}} := \mathcal{M}^\ell_\sigma \setminus \mathfrak{T}^\ell_{\mathcal{C}}\,. \tag{3.35}$$

Here, we will always assume that the initial patch mesh $\mathcal{M}^0$ is sufficiently fine so that $\mathfrak{T}^\ell_{\boldsymbol{c}}$ and $\mathfrak{T}^\ell_{\boldsymbol{c}'}$ are disjoint for $\boldsymbol{c} \neq \boldsymbol{c}'$. For sets $\mathcal{M}' \subseteq \mathcal{M}^\ell_\sigma$ of axiparallel elements, we introduce the broken H^1-norms:

$$\Upsilon^\perp_{\mathcal{M}'}[u]^2 := \sum_{K\in\mathcal{M}'} N^\perp_K[u]^2, \qquad \Upsilon^\parallel_{\mathcal{M}'}[u]^2 := \sum_{K\in\mathcal{M}'} N^\parallel_K[u]^2, \tag{3.36}$$

with elemental norms defined by

$$\begin{aligned} N^\perp_K[u]^2 &:= (h^\perp_K)^{-2}\|u\|^2_{L^2(K)} + \|\nabla u\|^2_{L^2(K)},\\ N^\parallel_K[u]^2 &:= (h^\parallel_K)^{-2}\|u\|^2_{L^2(K)} + \|\nabla u\|^2_{L^2(K)}. \end{aligned} \tag{3.37}$$

Evidently, we have

$$N^\parallel_K[u]^2 \lesssim N^\perp_K[u]^2, \qquad K\in\mathcal{M}', \tag{3.38}$$

whereas $N^\perp_K[u] \simeq N^\parallel_K[u]$ for isotropic elements K.

Proposition 3.10. *For all parameters $\sigma \in (0,1)$, $\mathfrak{s} > 0$ there are tensor projectors*

$$\pi^\ell_{\sigma,\mathfrak{s}} = \pi^{\ell,\perp}_{\sigma,\mathfrak{s}} \otimes \pi^{\ell,\parallel}_{\sigma,\mathfrak{s}} : H^1(\Omega) \to V^{0,\ell}_{\sigma,\mathfrak{s}}, \tag{3.39}$$

which are conforming over sets $\mathcal{F}^\perp_{ID}(\mathcal{M}^\ell_\sigma) \subset \mathcal{F}_{ID}(\mathcal{M}^\ell_\sigma)$ of edge-perpendicular faces and non-conforming over the complement sets $\mathcal{F}^\parallel_{ID}(\mathcal{M}^\ell_\sigma) = \mathcal{F}^\parallel_I(\mathcal{M}^\ell_\sigma) \,\dot\cup\, \mathcal{F}^\parallel_D(\mathcal{M}^\ell_\sigma)$ of edge-parallel faces F satisfying (3.33), (3.34).

Moreover, for functions u with $u \in B_{-1-\boldsymbol{b}}(\Omega;\emptyset,\emptyset)\cap H^{1+\theta}(\Omega)$ for some $\theta\in(0,1)$ as in Theorem 3.4 and for the error terms given by

$$\eta^\ell_{\sigma,\mathfrak{s}} := u - \pi^\ell_{\sigma,\mathfrak{s}}u, \qquad \eta^{\ell,\perp}_{\sigma,\mathfrak{s}} := u - \pi^{\ell,\perp}_{\sigma,\mathfrak{s}}u, \qquad \eta^{\ell,\parallel}_{\sigma,\mathfrak{s}} := u - \pi^{\ell,\parallel}_{\sigma,\mathfrak{s}}u, \tag{3.40}$$

we have the H^1-norm bound

$$\Upsilon^\parallel_{\mathcal{M}^\ell_\sigma}[\eta^\ell_{\sigma,\mathfrak{s}}]^2 + \Upsilon^\perp_{\mathcal{M}^\ell_{\sigma,\mathcal{C}}}[\eta^{\ell,\perp}_{\sigma,\mathfrak{s}}]^2 + \Upsilon^\parallel_{\mathcal{M}^\ell_{\sigma,\mathcal{C}}}[\eta^{\ell,\parallel}_{\sigma,\mathfrak{s}}]^2 \le C\exp\big(-2b\sqrt[5]{N}\big), \tag{3.41}$$

as well as the jump bound

$$\mathrm{jmp}_{\mathcal{F}^\parallel_{ID}(\mathcal{M}^\ell_\sigma)}[\eta^\ell_{\sigma,\mathfrak{s}}]^2 \le C\exp\big(-2b\sqrt[5]{N}\big), \tag{3.42}$$

with constants $b, C > 0$ independent of $N = \dim(V^{\ell,0}_{\sigma,\mathfrak{s}})$, but depending σ and $\mathfrak{s}$.

We will show the estimate (3.41) for a more general class of quasi-interpolation tensor projectors on $H^1(\Omega)$ in Section 4, see Theorem 4.3, with most parts of the proof relegated to Appendix A. The jump bound in (3.42) will be established for the specifically chosen projectors in (3.39) under smoothness requirements which are slightly stronger than $u \in H^1(\Omega)$; in particular, $u \in B_{-1-\boldsymbol{b}}(\Omega;\emptyset,\emptyset)$ is sufficient.

3.4.2. *Discontinuous hp-version base spaces.* To exploit the approximation properties for the non-conforming base projectors $\pi^\ell_{\sigma,\mathfrak{s}}u$ in Proposition 3.10 for the minimum rule finite element spaces $\overline{V}^{\ell,0}_{\sigma,\mathfrak{s}}$ in (3.23), we introduce discontinuous *hp-base spaces* as follows. For $K \in \mathcal{M}^\ell_\sigma$ axiparallel, we introduce the subsets $\mathcal{E}^\perp(K)$ and $\mathcal{E}^\parallel(K)$ of elemental edges of $\mathcal{E}(K)$, respectively $\mathcal{F}^\perp(K)$ and $\mathcal{F}^\parallel(K)$ of elemental faces of $\mathcal{F}(K)$, which are perpendicular and parallel to the nearest singular edge. For $K \in \mathcal{F}^\parallel(K)$, we write $\boldsymbol{p}_{K,F} = (p^\perp_K, p^\parallel_K)$ to distinguish the perpendicular and parallel components $\boldsymbol{p}_{K,F}$.

Lemma 3.11. *Let $\boldsymbol{p}_{\mathfrak{s}}(\mathcal{M}_\sigma^\ell)$ be a $\mathfrak{s}$-linear degree distribution on $\mathcal{M}_\sigma^\ell$. For $K \in \mathcal{M}_\sigma^\ell$, let the face and edge degrees $\overline{p}_{K,E}$ and $\overline{\boldsymbol{p}}_{K,F}$ be defined in* (3.13) *and* (3.14)*, respectively. Then there exists $\mu \in (0,1]$ depending only on $\mathfrak{s} > 0$ such that*

$$\forall E \in \mathcal{E}^\perp(K): \quad \mu p_K^\perp \le \overline{p}_{K,E} \le p_K^\perp, \tag{3.43}$$

$$\forall E \in \mathcal{E}^\parallel(K): \quad \mu p_K^\parallel \le \overline{p}_{K,E} \le p_K^\parallel, \tag{3.44}$$

$$\forall K \in \mathcal{F}^\perp(K): \quad \mu p_K^\perp \le \overline{p}_{K,F}^1 \le p_K^\perp, \quad \mu p_K^\perp \le \overline{p}_{K,F}^2 \le p_K^\perp, \tag{3.45}$$

$$\forall K \in \mathcal{F}^\parallel(K): \quad \mu p_K^\perp \le \overline{p}_{K,F}^\perp \le p_K^\perp, \quad \mu p_K^\parallel \le \overline{p}_{K,F}^\parallel \le p_K^\parallel. \tag{3.46}$$

Proof. These properties follow from the construction of the $\mathfrak{s}$-linear degree distributions and their properties of bounded variation; cf. [22, Section 3.2 and Remark 3.9]. □

On $K \in \mathcal{M}_\sigma^\ell$ we then introduce the *base degree vector* $\check{\boldsymbol{p}}_K = (\check{p}_K^\perp, \check{p}_K^\parallel)$ as

$$\begin{aligned} \check{p}_K^\perp &:= \min\big\{ \min_{E\in\mathcal{E}^\perp(K)} \overline{p}_{K,E}, \min_{F\in\mathcal{F}^\perp(K)} p_{K,F}^1, \min_{F\in\mathcal{F}^\perp(K)} p_{K,F}^2 \big\}, \\ \check{p}_K^\parallel &:= \min\big\{ \min_{E\in\mathcal{E}^\parallel(K)} \overline{p}_{K,E}, \min_{F\in\mathcal{F}^\parallel(K)} \overline{p}_{K,F}^\parallel \big\}. \end{aligned} \tag{3.47}$$

Consequently, we have

$$\mathbb{Q}_{\check{\boldsymbol{p}}_K}(K) \subseteq \mathbb{S}_{\overline{\boldsymbol{p}}_K}(K), \qquad K \in \mathcal{M}_\sigma^\ell. \tag{3.48}$$

From Lemma 3.11, we further have $\mu p_K^\perp \le \check{p}_K^\perp$ and $\mu p_K^\parallel \le \check{p}_K^\parallel$. As a consequence, the base degree vectors $\{\check{\boldsymbol{p}}_K\}_{K\in\mathcal{M}_\sigma^\ell}$ give rise to a $\check{\mathfrak{s}}$-linear polynomial degree distribution $\boldsymbol{p}_{\check{\mathfrak{s}}}(\mathcal{M}_\sigma^\ell)$, for a *base slope parameter* $\check{\mathfrak{s}}$ with $0 < \check{\mathfrak{s}} \le \mathfrak{s}$ and *only depending on* $\mathfrak{s}$. Hence, the *discontinuous hp-base spaces* $V_{\sigma,\check{\mathfrak{s}}}^{\ell,0}$ thus constructed satisfy

$$V_{\sigma,\check{\mathfrak{s}}}^{\ell,0} \subseteq \overline{V}_{\sigma,\mathfrak{s}}^{\ell,0}. \tag{3.49}$$

We point out that for the uniform and isotropic spaces in (3.30), the construction of discontinuous *hp*-base spaces is not necessary and can be omitted.

3.4.3. *Averaging over regular vertices, edges and faces.* We denote by $\overline{V}_{\sigma,\mathfrak{s}}^{\ell,0,\perp}$ the subspace of functions in $\overline{V}_{\sigma,\mathfrak{s}}^{\ell,0}$ which are conforming over $\mathcal{F}_{ID}^\perp(\mathcal{M}_\sigma^\ell) \subset \mathcal{F}_{ID}(\mathcal{M}_\sigma^\ell)$ and possibly non-conforming over $\mathcal{F}_{ID}^\parallel(\mathcal{M}_\sigma^\ell)$. We then adopt the approach of [28] to assign to $v \in \overline{V}_{\sigma,\mathfrak{s}}^{\ell,0,\perp}$ vertex, edge and face values which are obtained by *averaging* over *regularly matching* vertices, edges and faces.

Theorem 3.12. *There are linear averaging operators $\mathcal{A}_{\sigma,\mathfrak{s}}^\ell : \overline{V}_{\sigma,\mathfrak{s}}^{\ell,0,\perp} \to \overline{V}_{\sigma,\mathfrak{s}}^{\ell,0,\perp}$ such that the following holds: (i) $\mathcal{A}_{\sigma,\mathfrak{s}}^\ell(v)$ is continuous over regular faces in the interior of each mesh patch; (ii) $\mathcal{A}_{\sigma,\mathfrak{s}}^\ell(v)$ vanishes on all Dirichlet boundary faces; (iii) $\mathcal{A}_{\sigma,\mathfrak{s}}^\ell(v)$ is continuous across adjacent mesh patches; (iv) $\mathcal{A}_{\sigma,\mathfrak{s}}^\ell(v) = v$ for $v \in V_{\sigma,\mathfrak{s}}^{\ell,1}$; (v) we have the stability bound*

$$\Upsilon_{\mathcal{M}_\sigma^\ell}^\perp [v - \mathcal{A}_{\sigma,\mathfrak{s}}^\ell(v)]^2 + \mathrm{jmp}_{\mathcal{F}_I^\parallel(\mathcal{M}_\sigma^\ell)}[\mathcal{A}_{\sigma,\mathfrak{s}}^\ell(v)]^2 \lesssim_p \mathrm{jmp}_{\mathcal{F}_{ID}^\parallel(\mathcal{M}_\sigma^\ell)}[v]^2, \tag{3.50}$$

for all $v \in \overline{V}_{\sigma,\mathfrak{s}}^{\ell,0,\perp}$.

Remark 3.13. The construction of $\mathcal{A}^\ell_{\sigma,\mathfrak{s}}(v)$ in Theorem 3.12 is carried out on each element $K \in \mathcal{M}^\ell_\sigma$ separately, by adding averaged values associated with elemental vertices $\boldsymbol{N} \in \mathcal{N}(K)$, elemental faces $E \in \mathcal{E}(K)$ and elemental faces $F \in \mathcal{F}(K)$. As a consequence, $\mathcal{A}^\ell_{\sigma,\mathfrak{s}}$ can (in principle) be obtained from corresponding reference averaging operators on $\widetilde{Q}$ as in Remark 3.6, with inter-patch continuity being ensured by Assumption 3.1.

Theorem 3.12 will be established in Section 5.

3.4.4. *Polynomial jump liftings.* The averaged approximations $\mathcal{A}^\ell_{\sigma,\mathfrak{s}}(v)$ in Theorem 3.12 are non-conforming over *irregular faces in the interior of mesh patches*. Our proof then proceeds as in [18] by introducing suitable polynomially stable jump liftings on $\mathcal{M}^\ell_\sigma$ which preserve stability bounds as in (3.50). This leads to the following result.

Theorem 3.14. *Let $\mathcal{A}^\ell_{\sigma,\mathfrak{s}}$ be the averaging operator from Theorem 3.12. Then there exist linear operators $\mathcal{L}^\ell_{\sigma,\mathfrak{s}} : \mathrm{range}(\mathcal{A}^\ell_{\sigma,\mathfrak{s}}) \to V^{\ell,1}_{\sigma,\mathfrak{s}}$ such that the following holds: (i) $\mathcal{L}^\ell_{\sigma,\mathfrak{s}}(v) = v$ for $v \in V^{\ell,1}_{\sigma,\mathfrak{s}}$; (ii) we have the stability bound*

$$\Upsilon^\perp_{\mathcal{M}^\ell_\sigma}[v - \mathcal{L}^\ell_{\sigma,\mathfrak{s}}(v)] \lesssim_p \mathrm{jmp}_{\mathcal{F}^\parallel_I(\mathcal{M}^\ell_\sigma)}[v]^2, \tag{3.51}$$

for all $v \in \mathrm{range}(\mathcal{A}^\ell_{\sigma,\mathfrak{s}}) \subset \overline{V}^{\ell,0,\perp}_{\sigma,\mathfrak{s}}$.

Remark 3.15. Since functions in $v \in \mathrm{range}(\mathcal{A}^\ell_{\sigma,\mathfrak{s}})$ have non-vanishing jumps only over irregular faces in the interior of mesh patches, upon mapping it is sufficient to construct $\mathcal{L}^\ell_{\sigma,\mathfrak{s}}$ on the reference mesh patches $\widetilde{\mathcal{M}}^{\ell,\mathfrak{t}}_\sigma$ of type $\mathfrak{t} \in \{\boldsymbol{c}, \boldsymbol{e}, \boldsymbol{ce}, \mathrm{int}\}$; inter-patch continuity will again follow from Assumption 3.1; cf. [18]. This observation along with Remark 3.15 allows us to assemble $\Pi^{\ell,1}_{\sigma,\mathfrak{s}}$ from reference patch projectors as discussed in Remark 3.6.

The proof of Theorem 3.14 will be detailed in Section 6.

Remark 3.16. The bounds (3.50) and (3.51) involve relatively large algebraic losses in the polynomial order $|\boldsymbol{p}|$. As in [18], this is due to the use of polynomial trace liftings which are linear in one or more directions and can possibly be improved by employing polynomial liftings of higher order.

3.4.5. *Proof of Theorem 3.4.* To prove (3.26), consider $u \in V$. Let $\pi^\ell_{\sigma,\check{\mathfrak{s}}} u \in V^{\ell,0}_{\sigma,\check{\mathfrak{s}}}$ be the base projection of u defined in (3.39) into the hp-base space $V^{\ell,0}_{\sigma,\check{\mathfrak{s}}}$ constructed in Section 3.4.2, for the base slope parameter $\check{\mathfrak{s}} > 0$. By Proposition 3.10 and the inclusion (3.49), we have $\pi^\ell_{\sigma,\check{\mathfrak{s}}} u \in \overline{V}^{\ell,0,\perp}_{\sigma,\mathfrak{s}}$. In addition, the broken H^1-norms of the interpolation errors $\eta^{\ell,\perp}_{\sigma,\check{\mathfrak{s}}}$ and $\eta^{\ell,\parallel}_{\sigma,\check{\mathfrak{s}}}$ in (3.40) converge exponentially for u as in Proposition 3.10, albeit with respect to the base slope $\check{\mathfrak{s}}$. We then define

$$\Pi^{\ell,1}_{\sigma,\mathfrak{s}}(u) := \big(\mathcal{L}^\ell_{\sigma,\mathfrak{s}} \circ \mathcal{A}^\ell_{\sigma,\mathfrak{s}} \circ \pi^\ell_{\sigma,\check{\mathfrak{s}}}\big)(u) \in V^{\ell,1}_{\sigma,\mathfrak{s}}, \tag{3.52}$$

with the operators $\mathcal{A}^\ell_{\sigma,\mathfrak{s}}$ and $\mathcal{L}^\ell_{\sigma,\mathfrak{s}}$ from Theorems 3.12 and 3.14. Clearly, the quasi-interpolation operator $\Pi^{\ell,1}_{\sigma,\mathfrak{s}}$ is well-defined. It is linear and can readily be seen to be idempotent on a subspace on $V^{\ell,1}_{\sigma,\mathfrak{s}}$.

We now set $v = \pi^\ell_{\sigma,\check{\mathfrak{s}}} u$, $v^{\mathrm{f}} := \mathcal{A}^\ell_{\sigma,\mathfrak{s}}(v)$, and $v^{\mathrm{c}} := \mathcal{L}^\ell_{\sigma,\mathfrak{s}}(v)$. With the triangle inequality and property (3.38), we obtain

$$\|u - \Pi^{\ell,1}_{\sigma,\mathfrak{s}} u\|^2_{H^1(\Omega)} \lesssim \Upsilon^{\|}_{\mathcal{M}^\ell_\sigma}[u-v]^2 + \Upsilon^{\perp}_{\mathcal{M}^\ell_\sigma}[v-v^{\mathrm{f}}]^2 + \Upsilon^{\perp}_{\mathcal{M}^\ell_\sigma}[v^{\mathrm{f}}-v^{\mathrm{c}}]^2.$$

The bounds (3.50) and (3.51) imply

$$\Upsilon^{\perp}_{\mathcal{M}^\ell_\sigma}[v-v^{\mathrm{f}}]^2 + \Upsilon^{\perp}_{\mathcal{M}^\ell_\sigma}[v^{\mathrm{f}}-v^{\mathrm{c}}]^2 \lesssim_p \mathrm{jmp}_{\mathcal{F}^{\|}_{ID}(\mathcal{M}^\ell_\sigma)}[v]^2.$$

With the error terms (3.40) for the base projector $v = \pi^\ell_{\sigma,\check{\mathfrak{s}}} u$ (noting that $[\![u]\!]_F = 0$), we conclude that

$$\|u - \Pi^{\ell,1}_{\sigma,\mathfrak{s}} u\|^2_{H^1(\Omega)} \lesssim_p \Upsilon^{\|}_{\mathcal{M}^\ell_\sigma}[\eta^\ell_{\sigma,\check{\mathfrak{s}}}]^2 + \mathrm{jmp}_{\mathcal{F}^{\|}_{ID}(\mathcal{M}^\ell_\sigma)}[\eta^\ell_{\sigma,\check{\mathfrak{s}}}]^2.$$

Referring to (3.41), (3.42) in Proposition 3.10 yields (3.26) for u piecewise analytic as in Theorem 3.4.

4. Non-conforming Base Projectors

We introduce non-conforming and tensorized *hp*-base projectors, prove exponential convergence estimates in broken Sobolev norms, and establish Proposition 3.10.

4.1. **Tensor projectors.** We introduce a class of anisotropic tensor projectors on the reference cube $\widehat{K}$.

To this end, let $\widehat{I} = (-1,1)$ be the reference interval. For $p \geq 0$, we denote by $\widehat{\pi}_{p,0}$ the univariate L^2-projection onto $\mathbb{P}_p(\widehat{I})$. For $p \geq 1$, we further introduce the univariate H^1-projector $\widehat{\pi}_{p,1} : H^1(\widehat{I}) \to \mathbb{P}_p(\widehat{I})$ by

$$(\widehat{\pi}_{p,1}\widehat{u})(\xi) := \widehat{u}(-1) + \int_{-1}^{\xi} (\widehat{\pi}_{p-1,0}\widehat{u}')(\eta)d\eta; \tag{4.1}$$

cf. [25, Theorem 3.14]. The projector satisfies $(\widehat{\pi}_{p,1}\widehat{u})' = \widehat{\pi}_{p-1,0}(\widehat{u}')$ and

$$(\widehat{\pi}_{p,1}\widehat{u})(\pm 1) = \widehat{u}(\pm 1). \tag{4.2}$$

Some *hp*-version approximation properties of $\widehat{\pi}_{p,0}$ and $\widehat{\pi}_{p,1}$ are collected in Section A.1.1.

We next consider next the reference cube $\widehat{K} = \widehat{I}^3$ with $\widehat{I} = (-1,1)$. In analogy to (3.3), we write $\widehat{K} = \widehat{K}^\perp \times \widehat{K}^\| = \widehat{I}^2 \times \widehat{I}$. Let $\boldsymbol{p} = (p^\perp, p^\|)$ be an anisotropic polynomial degree vector, and $r \in \{0,1\}$ a conformity index in edge-parallel direction. For a function $\widehat{u} : \widehat{K} \to \mathbb{R}$, we define the tensor projector $\widehat{\pi}_{\boldsymbol{p},r}\widehat{v}$ into $\mathbb{Q}_{\boldsymbol{p}}(\widehat{K}) = \mathbb{Q}_{p^\perp}(\widehat{K}^\perp) \otimes \mathbb{P}_{p^\|}(\widehat{K}^\|)$ by

$$\widehat{\pi}_{\boldsymbol{p},r}\widehat{u} := \left(\widehat{\pi}^{(1)}_{p^\perp,0} \otimes \widehat{\pi}^{(2)}_{p^\perp,0} \otimes \widehat{\pi}^{(3)}_{p^\|,r}\right)\widehat{u} = \left(\widehat{\pi}^{\perp}_{p^\perp,0} \otimes \widehat{\pi}^{\|}_{p^\|,r}\right)\widehat{u}, \tag{4.3}$$

where the univariate projectors $\widehat{\pi}^{(i)}_{p,r}$ act in directions $\widehat{x}_1$, $\widehat{x}_2$, and $\widehat{x}_3$, respectively, and where we write $\widehat{\pi}^{\perp}_{p^\perp,0}$ and $\widehat{\pi}^{\|}_{p^\|,r}$ to denote the projectors in edge-perpendicular and in edge-parallel direction, respectively. The projector $\widehat{\pi}_{\boldsymbol{p},0}$ is the (tensor-product) L^2-projector which is well-defined for $\widehat{u} \in L^2(\widehat{K})$, whereas $\widehat{\pi}_{\boldsymbol{p},1}$ is an anisotropic projector which is well-defined for $\widehat{u} \in L^2(\widehat{K}^\perp) \otimes H^1(\widehat{K}^\|)$ and nodally exact in edge-parallel direction; cf. property (4.2). Note that $H^1(\widehat{K}) \subset L^2(\widehat{K}^\perp) \otimes H^1(\widehat{K}^\|)$. In Section A.1.2 we derive approximation properties for $\widehat{\pi}_{\boldsymbol{p},r}$ in (4.3), with the aid of tensor-product arguments and consistency bounds for the univariate projectors $\widehat{\pi}_{p,0}$ and $\widehat{\pi}_{p,1}$.

4.2. **Exponential convergence in broken norms.** We next establish exponential convergence bounds in broken norms for families of tensor projectors obtained from (4.3).

4.2.1. *Families of projectors.* Let $\mathcal{M} = \mathcal{M}_\sigma^\ell$ be a geometric mesh and let $\boldsymbol{p}_{\mathfrak{s}}(\mathcal{M}) = \{\boldsymbol{p}_K\}_{K\in\mathcal{M}}$ denote a σ-linear polynomial degree distribution on $\mathcal{M}$. To each element $K \in \mathcal{M}$, we further assign an *elemental conformity index* $r_K \in \{0,1\}$. We then consider the tensor projectors $\pi : H^1(\Omega) \to V^{\ell,0}_{\sigma,\mathfrak{s}}$ given by

$$\pi u|_K := \pi_{\boldsymbol{p}_K,r_K}(u|_K), \qquad K \in \mathcal{M}, \tag{4.4}$$

where the elemental projectors $\pi_{\boldsymbol{p}_K,r_K} : H^1(K) \to \mathbb{Q}_{\boldsymbol{p}_K}(K)$ are defined by

$$\pi_{\boldsymbol{p}_K,r_K}(u|_K) := (\widehat{\pi}_{\boldsymbol{p}_K,r_K}(u|_K \circ\ \Phi_K)) \circ \Phi_K^{-1}, \tag{4.5}$$

with $\widehat{\pi}_{\boldsymbol{p}_K,r_K}$ defined in (4.3) and $\Phi_K : \widehat{K} \to K$ the element mapping. As the projectors $\pi_{\boldsymbol{p}_K,r_K}$ tensorize into $\pi_{\boldsymbol{p}_K,r_K} = \pi^\perp_{p^\perp_K,0} \otimes \pi^\parallel_{p^\parallel_K,r_K}$ on $K = K^\perp \times K^\parallel$ and L^2-projections are used in perpendicular direction, we write

$$\pi u|_K = \pi_0^\perp \otimes \pi^\parallel u|_K. \tag{4.6}$$

For $u \in H^1(\Omega)$, we consider the error terms

$$\eta = u - \pi u, \qquad \eta_0^\perp = u - \pi_0^\perp u, \qquad \eta^\parallel = u - \pi^\parallel u, \tag{4.7}$$

and note that

$$\eta = (u - \pi_0^\perp u) + \pi_0^\perp(u - \pi^\parallel u) = \eta_0^\perp + \pi_0^\perp \eta^\parallel. \tag{4.8}$$

In the notation in (4.4)–(4.8), we generally omit the dependence on r_K in edge-parallel direction. However, if $r_K = r \in \{0,1\}$ for all $K \in \mathcal{M}_\sigma^\ell$, we write $\pi_r = \pi_0^\perp \otimes \pi_r^\parallel$ for the projectors resulting in (4.4), as well as η_r, $\eta_r^\parallel$ for the errors in (4.7). In particular, $\pi_0 = \pi_0^\perp \otimes \pi_0^\parallel : L^2(\Omega) \to V^{\ell,0}_{\sigma,\mathfrak{s}}$ is the usual L^2-projection. A specific choice of conformity indices r_K leading to $\pi^\ell_{\sigma,\mathfrak{s}}$ in Proposition 3.10 will be introduced in Section 4.3 below.

4.2.2. *Error bounds.* We show that the full errors η can be bounded in terms of the errors $\eta^\perp$ and $\eta^\parallel$ in edge-perpendicular and in edge-parallel directions, in appropriate norms. We first establish the following stability result.

Lemma 4.1. *Let $K = K^\perp \times K^\parallel \in \mathcal{M}_\sigma^\ell$ be of the form* (3.3) *and $p_K^\perp \geq 1$. Then*

$$\|\mathsf{D}_\perp(\pi^\perp_{p^\perp_K,0}u)\|^2_{L^2(K^\perp)} \lesssim (p_K^\perp)^4 \|\mathsf{D}_\perp u\|^2_{L^2(K^\perp)}, \qquad u \in H^1(K^\perp). \tag{4.9}$$

Furthermore, for the element errors in (4.7) *and any $r_K \in \{0,1\}$, we have*

$$\begin{aligned} \|\eta\|^2_{L^2(K)} &\lesssim \|\eta_0^\perp\|^2_{L^2(K)} + \|\eta^\parallel\|^2_{L^2(K)}, \\ \|\mathsf{D}_\perp\eta\|^2_{L^2(K)} &\lesssim \|\mathsf{D}_\perp\eta_0^\perp\|^2_{L^2(K)} + (p_K^\perp)^4\|\mathsf{D}_\perp\eta^\parallel\|^2_{L^2(K)}, \\ \|\mathsf{D}_\parallel\eta\|^2_{L^2(K)} &\lesssim \|\mathsf{D}_\parallel\eta_0^\perp\|^2_{L^2(K)} + \|\mathsf{D}_\parallel\eta^\parallel\|^2_{L^2(K)}. \end{aligned} \tag{4.10}$$

Proof. Since both sides of the inequalities in (4.9) and (4.10) scale in the same way, it is sufficient to prove the results for the reference element $\widehat{K} = \widehat{K}^\perp \times \widehat{K}^\parallel$.

We prove (4.9) on $\widehat{K}^\perp$. To do so, note that

$$\widehat{\mathsf{D}}_\perp(\widehat{\pi}^\perp_{p^\perp_K,0}\widehat{u}) = \widehat{\mathsf{D}}_\perp(\widehat{\pi}^\perp_{p^\perp_K,0}\widehat{u} - \widehat{\pi}^\perp_{0,0}\widehat{u}) = \widehat{\mathsf{D}}_\perp(\widehat{\pi}^\perp_{p^\perp_K,0}(\widehat{u} - \widehat{\pi}^\perp_{0,0}\widehat{u})). \tag{4.11}$$

The inverse inequalities in [25, Theorem 3.91], the L^2-stability of $\widehat{\pi}^{\perp}_{p_K^{\perp},0}$ and standard approximation properties for $\widehat{\pi}^{\perp}_{0,0}$ yield

$$\begin{aligned}\|\widehat{\mathsf{D}}_{\perp}(\widehat{\pi}^{\perp}_{p_K^{\perp},0}\widehat{u})\|^2_{L^2(\widehat{K}^{\perp})} &\lesssim (p_K^{\perp})^4\|\widehat{\pi}^{\perp}_{p_K^{\perp},0}(\widehat{u}-\widehat{\pi}^{\perp}_{0,0}\widehat{u})\|^2_{L^2(\widehat{K}^{\perp})}\\ &\lesssim (p_K^{\perp})^4\|\widehat{u}-\widehat{\pi}^{\perp}_{0,0}\widehat{u}\|^2_{L^2(\widehat{K}^{\perp})} \lesssim (p_K^{\perp})^4\|\widehat{\mathsf{D}}_{\perp}\widehat{u}\|^2_{L^2(\widehat{K}^{\perp})}.\end{aligned}$$

This yields (4.9).

Then, the L^2-norm bound in (4.10) follows from the splitting (4.8) with the aid of the triangle inequality and the L^2-stability of the L^2-projection $\widehat{\pi}^{\perp}_{p_K^{\perp},0}$. The second estimate in (4.10) is a consequence of (4.8), the triangle inequality and the p-dependent stability bound (4.9) in perpendicular direction. The third estimate in (4.10) is again obtained from (4.8), by employing the commutativity of $\mathsf{D}_{\|}$ and $\widehat{\pi}^{\perp}_{p_K^{\perp},0}$, as well as the L^2-stability of $\widehat{\pi}^{\perp}_{p_K^{\perp},0}$. □

In addition to the broken H^1-norms in (3.36), we introduce

$$\|u\|^2_{L^2(\mathcal{M}')} := \sum_{K\in\mathcal{M}'}\|u\|^2_{L^2(K)}, \qquad \mathcal{M}'\subseteq\mathcal{M}^{\ell}_{\sigma}. \tag{4.12}$$

The next lemma ensures the stable splitting of the errors into edge-perpendicular and edge-parallel contributions.

Lemma 4.2. *Let $u\in H^1(\Omega)$ and let $\pi u=\pi_0^{\perp}\otimes\pi^{\|}u$ be the base interpolant in* (4.4) *for any conformity indices $r_K\in\{0,1\}$. For the error terms in* (4.7)*, we have*

$$\Upsilon^{\|}_{\mathcal{M}^{\ell}_{\sigma}}[\eta]^2 \lesssim_p \Upsilon^{\perp}_{\mathcal{M}^{\ell}_{\sigma,\mathcal{C}}}[\eta_0^{\perp}]^2+\Upsilon^{\|}_{\mathcal{M}^{\ell}_{\sigma,\mathcal{C}}}[\eta^{\|}]^2+\Upsilon^{\|}_{\mathfrak{T}^{\ell}_{\mathcal{C}}}[\eta]^2. \tag{4.13}$$

Moreover, let $u\in L^2(\Omega)$ and let $\pi_0 u=\pi_0^{\perp}\otimes\pi_0^{\|}u$ be the L^2-projection obtained in (4.4) *by taking $r_K=0$ for all $K\in\mathcal{M}^{\ell}_{\sigma}$. Then we have*

$$\|\eta_0\|^2_{L^2(\mathcal{M}^{\ell}_{\sigma})}\lesssim\|\eta_0^{\perp}\|^2_{L^2(\mathcal{M}^{\ell}_{\sigma,\mathcal{C}})}+\|\eta_0^{\|}\|^2_{L^2(\mathcal{M}^{\ell}_{\sigma,\mathcal{C}})}+\|\eta_0\|^2_{L^2(\mathfrak{T}^{\ell}_{\mathcal{C}})}. \tag{4.14}$$

Proof. These bounds follow from Lemma 4.1 and the inequality (3.38). □

4.2.3. *Exponential convergence.* We now state exponential convergence results in broken norms. Note that the results do not provide jump estimates as in (3.42).

Theorem 4.3. *Let $\boldsymbol{b}$ be a weight exponent vector satisfying* (2.13)*. For parameters $\sigma\in(0,1)$ and $\mathfrak{s}>0$, consider the sequence $V^{\ell,0}_{\sigma,\mathfrak{s}}$ of discontinuous finite element spaces* (3.23) *with elemental polynomial degrees $p_K^{\perp}\geq 1$, $p_K^{\|}\geq 1$.*

Let $u\in B_{-1-\boldsymbol{b}}(\Omega;\emptyset,\emptyset)\cap H^{1+\theta}(\Omega)$ for some $\theta\in(0,1)$, cf. Remark 2.4, and let $\pi u=\pi_0^{\perp}\otimes\pi^{\|}u: H^1(\Omega)\to V^{\ell,0}_{\sigma,\mathfrak{s}}$ be the non-conforming family of tensor projectors introduced in (4.4)*, for any elemental conformity indices $r_K\in\{0,1\}$. For the errors η, $\eta_0^{\perp}$ and $\eta^{\|}$ in* (4.7)*, we have*

$$\Upsilon^{\|}_{\mathcal{M}^{\ell}_{\sigma}}[\eta]^2+\Upsilon^{\perp}_{\mathcal{M}^{\ell}_{\sigma,\mathcal{C}}}[\eta_0^{\perp}]^2+\Upsilon^{\|}_{\mathcal{M}^{\ell}_{\sigma,\mathcal{C}}}[\eta^{\|}]^2\leq C\exp\left(-2b\sqrt[5]{N}\right), \tag{4.15}$$

with constants $b,C>0$ independent of $N=\dim(V^{\ell,0}_{\sigma,\mathfrak{s}})$.

In addition, let $u\in B_{-\boldsymbol{b}}(\Omega;\emptyset,\emptyset)\cap H^{\theta}(\Omega)$ for some $\theta\in(0,1)$, and let $\pi_0 u=\pi_0^{\perp}\otimes\pi_0^{\|}u$ be the L^2-projection obtained in (4.4) *by taking $r_K=0$ for all $K\in\mathcal{M}^{\ell}_{\sigma}$. For the errors η_0, $\eta_0^{\perp}$ and $\eta_0^{\|}$, we have*

$$\|\eta_0\|^2_{L^2(\mathcal{M}^{\ell}_{\sigma})}+\|\eta_0^{\perp}\|^2_{L^2(\mathcal{M}^{\ell}_{\sigma,\mathcal{C}})}+\|\eta_0^{\|}\|^2_{L^2(\mathcal{M}^{\ell}_{\sigma,\mathcal{C}})}\leq C\exp\left(-2b\sqrt[5]{N}\right), \tag{4.16}$$

with constants $b, C > 0$ independent of N.

Remark 4.4. For the sake of simplicity, our proof of Theorem 4.3 is based on univariate hp-approximation bounds for $\widehat{\pi}_{p,0}$ and $\widehat{\pi}_{p,1}$ in (4.1) which require $p \geq 1$; cf. (A.1) and (A.3). Alternatively, the proof of the L^2-bound (4.16) could be solely based on the L^2-norm estimates for the L^2-projection in [25, Theorem 3.11], thereby allowing elemental polynomial degrees $p_K^{\perp} \geq 0$, $p_K^{\parallel} \geq 0$ for the bound (4.16).

Remark 4.5. If $u \in H^1(\Omega)/\mathbb{R}$ in (4.15) (as is relevant in the pure Neumann problem) respectively $u \in L^2(\Omega)/\mathbb{R}$ in (4.16), the bounds (4.15) respectively (4.16) remain true over the factor space $V^{\ell,0}_{\sigma,\mathfrak{s}}/\mathbb{R}$. This follows from the fact that the elemental interpolants $\pi_{\boldsymbol{p}_K, r_K}(u|_K)$ in (4.4) reproduce functions which are constant in Ω.

Remark 4.6. The L^2-norm bound (4.16) is of independent interest in the context of mixed hp-approximations for the (Navier-)Stokes equations or for linear elasticity in mixed form under $B_{-\boldsymbol{b}}(\Omega; \emptyset, \emptyset)$-regularity assumptions on the multipliers (although corresponding regularity shifts do not seem to be available in the literature). We refer to [20, 21], where the inf-sup stability of mixed hp-discontinuous Galerkin methods is established on anisotropic geometric meshes. Based on these results, an exponential convergence proof of mixed hp-discontinuous Galerkin methods for mixed formulations with solutions in $A_{-1-\boldsymbol{b}}(\Omega)^3 \times A_{-\boldsymbol{b}}(\Omega)$ was given in [27], for the homogeneous space $A_{\boldsymbol{\beta}}(\Omega) = B_{\boldsymbol{\beta}}(\Omega; \mathcal{C}, \mathcal{E})$.

As in [24, Section 7], by superposition and due to the structure of the patch mappings, it is sufficient to provide the the proof of the exponential convergence bounds in Theorem 4.3 to a reference corner-edge configuration on $\widetilde{Q}$ as shown in Figure 1, which involves a single corner $\boldsymbol{c} \in \mathcal{C}$ and a single Neumann edge $\boldsymbol{e} \in \mathcal{E}_{\boldsymbol{c}}$ emanating from it. The case of a Dirichlet edge is analogous; cf. [24, Section 7.3]. Interior reference mesh patches can be treated similarly to [23, Section 5.2.1]), and the reference meshes $\widetilde{\mathcal{M}}^{\ell,\boldsymbol{c}}_{\sigma}$ and $\widetilde{\mathcal{M}}^{\ell,\boldsymbol{e}}_{\sigma}$ can be viewed as collections of certain elements of $\widetilde{\mathcal{M}}^{\ell,\boldsymbol{ce}}_{\sigma}$ and can be treated as particular cases thereof; cf. [24, Section 7.1]. In a reference corner-edge patch setting, the proof of the bound (4.15) follows along the lines of [23, Section 7.2], albeit with some modifications. For the sake of completeness, we review the major steps and detail the relevant modifications of [23, Section 7.2] in Appendix A. The proof of the L^2-norm bound (4.16) follows similarly and will be outlined simultaneously.

4.3. **The base projectors $\pi^{\ell}_{\sigma,\mathfrak{s}}$ with partial conformity.** By selecting specific values of the conformity indices $r_K \in \{0, 1\}$, we now introduce and analyze particular tensor product projectors of the form (4.4), which lead to the projectors $\pi^{\ell}_{\sigma,\mathfrak{s}}$ and the sets $\mathcal{F}^{\perp}_{ID}(\mathcal{M}^{\ell}_{\sigma})$, $\mathcal{F}^{\parallel}_{ID}(\mathcal{M}^{\ell}_{\sigma})$ in Proposition 3.10.

4.3.1. *Base projectors for corner, edge and interior patches.* We define reference base projectors $\widetilde{\pi}_{\mathfrak{t}}$ on each reference mesh $\widetilde{\mathcal{M}}^{\ell,\mathfrak{t}}_{\sigma}$ for $\mathfrak{t} \in \{\boldsymbol{c}, \boldsymbol{e}, \boldsymbol{ce}, \mathrm{int}\}$ with respect to the linear polynomial degree distribution $\boldsymbol{p}_{\mathfrak{s}}(\widetilde{\mathcal{M}}^{\ell,\mathfrak{t}}_{\sigma})$. Recall that the elemental polynomial degree vectors $\boldsymbol{p}_K$ are isotropic for $\mathfrak{t} \in \{\boldsymbol{c}, \mathrm{int}\}$ and generally anisotropic for $\mathfrak{t} \in \{\boldsymbol{e}, \boldsymbol{ce}\}$. For reference patches $\widetilde{\mathcal{M}}^{\ell,\mathfrak{t}}_{\sigma}$ of type $\mathfrak{t} \in \{\boldsymbol{c}, \boldsymbol{e}, \mathrm{int}\}$, we take the reference base projectors $\widetilde{\pi}_{\mathfrak{t}}$ as

$$\widetilde{\pi}_{\mathfrak{t}}(u|_K) := \begin{cases} \pi_{\boldsymbol{p}_K,0}(u|_K), & K \in \widetilde{\mathcal{M}}^{\ell,\mathfrak{t}}_{\sigma},\ \mathfrak{t} \in \{\boldsymbol{c}, \mathrm{int}\}, \\ \pi_{\boldsymbol{p}_K,1}(u|_K), & K \in \widetilde{\mathcal{M}}^{\ell,\boldsymbol{e}}_{\sigma}, \end{cases} \tag{4.17}$$

where the nodally exact univariate projectors in (4.1) are applied in edge-parallel direction.

4.3.2. *Base projectors for corner-edge patches with refinement along one edge.* We next consider the corner-edge reference mesh patch $\widetilde{\mathcal{M}}_\sigma^{\ell,\boldsymbol{ce}}$ with refinement along one edge $\boldsymbol{e}$. Following [18], we partition $\widetilde{\mathcal{M}}_\sigma^{\ell,\boldsymbol{ce}}$ as

$$\widetilde{\mathcal{M}}_\sigma^{\ell,\boldsymbol{ce}} := \widetilde{\mathcal{M}}_\sigma^{\ell,\boldsymbol{ce},\perp} \,\dot\cup\, \widetilde{\mathcal{M}}_\sigma^{\ell,\boldsymbol{ce},\parallel}\,, \qquad \ell \geq 2\,, \tag{4.18}$$

where the mesh $\widetilde{\mathcal{M}}_\sigma^{\ell,\boldsymbol{ce},\perp}$ is a corner-patch type mesh of elements which are isotropically refined into the corner $\boldsymbol{c}$. The mesh $\widetilde{\mathcal{M}}_\sigma^{\ell,\boldsymbol{ce},\parallel}$ consists of a sequence of $\ell-1$ geometrically scaled edge-patch meshes, translated along the edge $\boldsymbol{e}$:

$$\widetilde{\mathcal{M}}_\sigma^{\ell,\boldsymbol{ce},\parallel} = \bigcup_{\ell'=2}^{\ell} \widetilde{\Psi}^{\ell',\boldsymbol{ce}}(\widetilde{\mathcal{M}}_\sigma^{\ell',\boldsymbol{e}}), \qquad \ell \geq 2\,, \tag{4.19}$$

where we denote by $\widetilde{\Psi}^{\ell',\boldsymbol{ce}}$ the operation of translation with respect to the edge-parallel variable $x^\parallel$ combined with a dilation by a factor only depending on σ, ℓ, ℓ', and where the mesh $\widetilde{\mathcal{M}}_\sigma^{\ell',\boldsymbol{e}}$ is a reference edge mesh patch on $\widetilde{Q}$ with $\ell'+1$ mesh layers. In Figure 2 (left), a schematic illustration of the patch decomposition (4.18), (4.19) is provided in which the scaled edge-patch blocks are highlighted in boldface. In Figure 2 (right), we show two adjacent edge-patch meshes as in (4.19) along the edge $\boldsymbol{e}$.

A particular role will be played by the subset $\widetilde{\mathcal{D}}_\sigma^{\ell,\boldsymbol{ce}} \subset \widetilde{\mathcal{M}}_\sigma^{\ell,\boldsymbol{ce},\parallel}$ of the elements in the outermost layer of each scaled mesh-patch block. It also consists of $\ell-1$ layers:

$$\widetilde{\mathcal{D}}_\sigma^{\ell,\boldsymbol{ce}} := \bigcup_{\ell'=2}^{\ell} \widetilde{\mathcal{D}}_\sigma^{\ell',\boldsymbol{ce}}, \qquad \ell \geq 2. \tag{4.20}$$

Elements in $\widetilde{\mathcal{D}}_\sigma^{\ell,\boldsymbol{ce}}$ are referred to as *diagonal elements of* $\widetilde{\mathcal{M}}_\sigma^{\ell,\boldsymbol{ce},\parallel}$; cf. [18]. They are *isotropic* and illustrated in Figure 2. The isotropic mesh $\widetilde{\mathcal{M}}_\sigma^{\ell,\boldsymbol{ce},\perp}$ is decomposed into

$$\widetilde{\mathcal{M}}_\sigma^{\ell,\boldsymbol{ce},\perp} := \widetilde{\mathfrak{T}}_\sigma^{\ell,\boldsymbol{c}} \,\dot\cup\, \widetilde{\mathfrak{O}}_\sigma^{\ell,\boldsymbol{ce},\perp}, \tag{4.21}$$

where $\widetilde{\mathfrak{T}}_\sigma^{\ell,\boldsymbol{c}}$ is given by the eight elements nearest to $\boldsymbol{c}$, and where the remaining elements are collected in the mesh $\widetilde{\mathfrak{O}}_\sigma^{\ell,\boldsymbol{ce},\perp}$. We then choose the reference base projector on the reference corner-edge mesh as

$$\widetilde{\pi}_{\boldsymbol{ce}}(u|_K) := \begin{cases} \pi_{\boldsymbol{p}_K,0}(u|_K), & K \in \widetilde{\mathfrak{T}}_\sigma^{\ell,\boldsymbol{c}} \,\dot\cup\, \widetilde{\mathfrak{O}}_\sigma^{\ell,\boldsymbol{ce},\perp} \,\dot\cup\, \widetilde{\mathcal{D}}_\sigma^{\ell,\boldsymbol{ce}}, \\ \pi_{\boldsymbol{p}_K,1}(u|_K), & K \in \widetilde{\mathcal{M}}_\sigma^{\ell,\boldsymbol{ce},\parallel} \setminus \widetilde{\mathcal{D}}_\sigma^{\ell,\boldsymbol{ce}}, \end{cases} \tag{4.22}$$

where in the definition of $\pi_{\boldsymbol{p}_K,1}$ the nodally exact projectors in (A.1) are applied in edge-parallel direction of edge $\boldsymbol{e}$.

4.3.3. *Base projectors for corner-edge patches with refinements along two or three edges.* We next consider a corner-edge patch $\widetilde{\mathcal{M}}_\sigma^{\ell,\boldsymbol{ce}}$ with anisotropic refinement along two edges $\boldsymbol{e}_1, \boldsymbol{e}_2$ meeting at a common vertex $\boldsymbol{c}$ and isotropic refinement in perpendicular direction as illustrated in Figure 3 (left). In this case, we write

$$\widetilde{\mathcal{M}}_\sigma^{\ell,\boldsymbol{ce}} := \widetilde{\mathcal{M}}_\sigma^{\ell,\boldsymbol{ce},\perp} \,\dot\cup\, \big(\widetilde{\mathcal{M}}_\sigma^{\ell,\boldsymbol{ce}_1,\parallel} \cup \widetilde{\mathcal{M}}_\sigma^{\ell,\boldsymbol{ce}_2,\parallel}\big), \qquad \ell \geq 2, \tag{4.23}$$

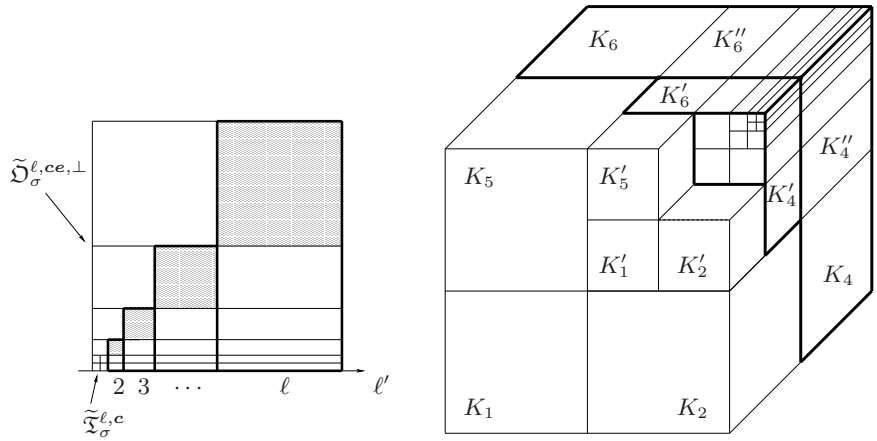

FIGURE 2. Left: Patch decomposition (4.18)–(4.21) for $\sigma = 0.5$ and $\ell = 5$. The diagonal elements are shaded. Right: The scaled edge-patch blocks $\widetilde{\Psi}^{\ell',\boldsymbol{ce}}(\widetilde{\mathcal{M}}_\sigma^{\ell',\boldsymbol{e}})$ and $\widetilde{\Psi}^{\ell'-1,\boldsymbol{ce}}(\widetilde{\mathcal{M}}_\sigma^{\ell'-1,\boldsymbol{e}})$ for $\sigma = 0.5$ and $\ell' = 5$. The diagonal elements K_4, K_6 and K_4', K_6' belong to $\widetilde{\mathcal{D}}_\sigma^{\ell',\boldsymbol{ce}}$ and $\widetilde{\mathcal{D}}_\sigma^{\ell'-1,\boldsymbol{ce}}$, respectively.

with two sequences of $\ell - 1$ scaled edge-patch meshes as in (4.19) and an isotropic corner-type mesh $\widetilde{\mathcal{M}}_\sigma^{\ell,\boldsymbol{ce},\perp}$ perpendicular to $\boldsymbol{e}_1, \boldsymbol{e}_2$. The latter mesh is again decomposed as

$$\widetilde{\mathcal{M}}_\sigma^{\ell,\boldsymbol{ce},\perp} := \widetilde{\mathfrak{T}}_\sigma^{\ell,\boldsymbol{c}} \,\dot\cup\, \widetilde{\mathfrak{O}}_\sigma^{\ell,\boldsymbol{ce},\perp}, \tag{4.24}$$

where $\widetilde{\mathfrak{T}}_\sigma^{\ell,\boldsymbol{c}}$ is the same set of corner elements as in (4.21) and $\widetilde{\mathfrak{O}}_\sigma^{\ell,\boldsymbol{ce},\perp}$ the set of all remaining elements. We denote by $\widetilde{\mathcal{D}}_\sigma^{\ell,\boldsymbol{ce}_i} \subset \widetilde{\mathcal{M}}_\sigma^{\ell,\boldsymbol{ce}_i,\parallel}$ the diagonal elements of $\widetilde{\mathcal{M}}_\sigma^{\ell,\boldsymbol{ce}_i,\parallel}$ defined as above; cf. Figure 3 (left). We then set

$$\widetilde{\pi}_{\boldsymbol{ce}}(u|_K) := \begin{cases} \pi_{\boldsymbol{p}_K,0}(u|_K), & K \in \widetilde{\mathfrak{T}}_\sigma^{\ell,\boldsymbol{c}} \,\dot\cup\, \widetilde{\mathfrak{O}}_\sigma^{\ell,\boldsymbol{ce},\perp} \,\dot\cup\, \big(\widetilde{\mathcal{D}}_\sigma^{\ell,\boldsymbol{ce}_1} \cup \widetilde{\mathcal{D}}_\sigma^{\ell,\boldsymbol{ce}_2}\big), \\ \pi_{\boldsymbol{p}_K,1}(u|_K), & K \in \widetilde{\mathcal{M}}_\sigma^{\ell,\boldsymbol{ce}_i,\parallel} \setminus \widetilde{\mathcal{D}}_\sigma^{\ell,\boldsymbol{ce}_i},\ i = 1,2, \end{cases} \tag{4.25}$$

with the understanding that the univariate nodally exact projectors in (4.1) are applied in the direction of edge $\boldsymbol{e}_i$ for $i = 1, 2$.

Remark 4.7. The diagonal elements in $\widetilde{\mathcal{D}}_\sigma^{\ell,\boldsymbol{ce}_i}$ act as isotropic *buffer zones* and allow us to unambiguously assign different directions in the submeshes $\widetilde{\mathcal{M}}_\sigma^{\ell,\boldsymbol{ce}_1,\parallel}$ and $\widetilde{\mathcal{M}}_\sigma^{\ell,\boldsymbol{ce}_2,\parallel}$.

Finally, if $\widetilde{\mathcal{M}}_\sigma^{\ell,\boldsymbol{ce}}$ is refined along three edges $\boldsymbol{e}_1, \boldsymbol{e}_2, \boldsymbol{e}_3$ meeting at a common vertex $\boldsymbol{c}$, as depicted in Figure 3 (right), we analogously write

$$\widetilde{\mathcal{M}}_\sigma^{\ell,\boldsymbol{ce}} := \widetilde{\mathfrak{T}}_\sigma^{\ell,\boldsymbol{c}} \,\dot\cup\, \big(\widetilde{\mathcal{M}}_\sigma^{\ell,\boldsymbol{ce}_1,\parallel} \cup \widetilde{\mathcal{M}}_\sigma^{\ell,\boldsymbol{ce}_2,\parallel} \cup \widetilde{\mathcal{M}}_\sigma^{\ell,\boldsymbol{ce}_3,\parallel}\big), \tag{4.26}$$

each now with three sequences of $\ell - 1$ scaled edge-patch blocks. As before, the set $\widetilde{\mathcal{D}}_\sigma^{\ell,\boldsymbol{ce}_i} \subset \widetilde{\mathcal{M}}_\sigma^{\ell,\boldsymbol{ce}_i,\parallel}$ denotes the diagonal elements of $\widetilde{\mathcal{M}}_\sigma^{\ell,\boldsymbol{ce}_i,\parallel}$. With (4.26), we define

$$\widetilde{\pi}_{\boldsymbol{ce}}(u|_K) := \begin{cases} \pi_{\boldsymbol{p}_K,0}(u|_K), & K \in \widetilde{\mathfrak{T}}_\sigma^{\ell,\boldsymbol{c}} \,\dot\cup\, \big(\cup_{i=1}^3 \widetilde{\mathcal{D}}_\sigma^{\ell,\boldsymbol{ce}_i}\big), \\ \pi_{\boldsymbol{p}_K,1}(u|_K), & K \in \widetilde{\mathcal{M}}_\sigma^{\ell,\boldsymbol{ce}_i,\parallel} \setminus \widetilde{\mathcal{D}}_\sigma^{\ell,\boldsymbol{ce}_i},\ 1 \le i \le 3, \end{cases} \tag{4.27}$$

again with the univariate nodally exact projectors applied in the direction of edge $\boldsymbol{e}_i$.

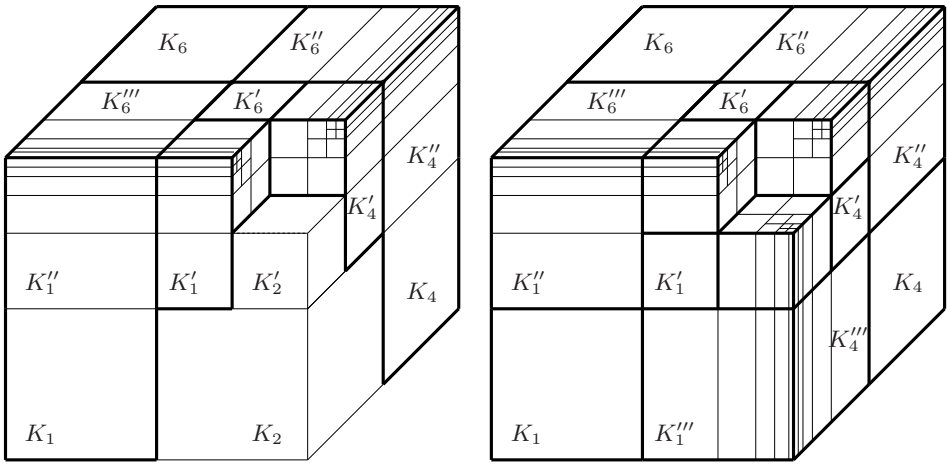

FIGURE 3. Scaled edge-patch blocks for $\sigma = 0$ and $\ell' = 5$. Left: Refinement along two edges with diagonal elements K_1, K_4, K_6 and K_1', K_4', K_6'. Right: Refinement along three edges with diagonal elements K_1, K_4, K_6 and K_1', K_4', K_6'.

4.3.4. *The base projectors* $\pi^{\ell}_{\sigma,\mathfrak{s}}$. The reference base projectors $\widehat{\pi}_{\mathfrak{t}}$ in (4.17), (4.22), as well as the variants in (4.25) and (4.27), give rise to the (non-conforming) base tensor projectors $\pi^{\ell}_{\sigma,\mathfrak{s}} = \pi^{\ell,\perp}_{\sigma,\mathfrak{s}} \otimes \pi^{\ell,\parallel}_{\sigma,\mathfrak{s}} : H^1(\Omega) \to V^{\ell,0}_{\sigma,\mathfrak{s}}$ in (3.39); cf. (4.4). Theorem 4.3 then implies the bound (3.41) of Proposition 3.10. The sets $\mathcal{F}^{\perp}_{ID}(\mathcal{M}^{\ell}_{\sigma})$, $\mathcal{F}^{\parallel}_{ID}(\mathcal{M}^{\ell}_{\sigma})$ and the jump bound (3.42) will be discussed next.

4.3.5. *Partial conformity.* We consider edge-perpendicular patch interfaces $\Gamma_{\mathfrak{p}\,\mathfrak{p}'}$ between two mesh patches $\mathcal{M}_{\mathfrak{p}}$, $\mathcal{M}_{\mathfrak{p}'}$ containing anisotropic elements along a common edge $\boldsymbol{e}$ and coinciding on the interface due to Assumption 3.1. The interface $\Gamma_{\mathfrak{p}\,\mathfrak{p}'}$ consists of $\ell + 1$ mesh layers of elements; cf. [22, Section 3.2]. The definition of $\pi^{\ell}_{\sigma,\mathfrak{s}}$ and the nodal exactness property (4.2) imply the following results.

Lemma 4.8. *There holds: (i) if $\mathcal{M}_{\mathfrak{p}}, \mathcal{M}_{\mathfrak{p}'}$ are two adjacent edge mesh patches along the same edge, then $\pi^{\ell}_{\sigma,\mathfrak{s}} u$ is continuous across all layers of the interface $\Gamma_{\mathfrak{p}\,\mathfrak{p}'}$; (ii) if $\mathcal{M}_{\mathfrak{p}}$ is an edge mesh patch and $\mathcal{M}_{\mathfrak{p}'}$ an adjacent corner-edge patch along the same edge, then $\pi^{\ell}_{\sigma,\mathfrak{s}} u$ is continuous across the inner layers of the interface $\Gamma_{\mathfrak{p}\,\mathfrak{p}'}$, but is generally discontinuous across the outermost layer of $\Gamma_{\mathfrak{p}\,\mathfrak{p}'}$.*

Remark 4.9. Conformity properties analogous to those in Lemma 4.8 hold on edge-perpendicular boundaries of elements in edge or corner-edge mesh patches which are situated on a Dirichlet boundary face $\Gamma_{\boldsymbol{\iota}}$ for $\boldsymbol{\iota} \in \mathcal{J}_D$. On the corresponding elemental boundaries, the projection $\pi^{\ell}_{\sigma,\mathfrak{s}} u$ satisfies homogeneous Dirichlet boundary conditions.

Next, we analyze the continuity within $\widetilde{\mathcal{M}}^{\ell,\boldsymbol{ce},\parallel}_{\sigma} = \cup_{\ell'=2}^{\ell} \widetilde{\Psi}^{\ell',\boldsymbol{ce}}(\widetilde{\mathcal{M}}^{\ell',\boldsymbol{e}}_{\sigma})$ in (4.19) and as appearing in the representations (4.18), (4.23) and (4.26). The analog of Lemma 4.8 is as follows.

Lemma 4.10. *For $3 \le \ell' \le \ell$, let $\widetilde{\Psi}^{\ell'-1,\boldsymbol{ce}}(\widetilde{\mathcal{M}}_\sigma^{\ell'-1,\boldsymbol{e}})$ and $\widetilde{\Psi}^{\ell',\boldsymbol{ce}}(\widetilde{\mathcal{M}}_\sigma^{\ell',\boldsymbol{e}})$ be two adjacent edge-patch blocks along the same edge. Then $\pi^\ell_{\sigma,\mathfrak{s}}u$ is continuous across perpendicular faces on the interface between $\widetilde{\Psi}^{\ell'-1,\boldsymbol{ce}}(\widetilde{\mathcal{M}}_\sigma^{\ell'-1,\boldsymbol{e}})$ and $\widetilde{\Psi}^{\ell',\boldsymbol{ce}}(\widetilde{\mathcal{M}}_\sigma^{\ell',\boldsymbol{e}})$, except for the faces between the diagonal elements in $\widetilde{\mathcal{D}}_\sigma^{\ell'-1,\boldsymbol{ce}}$ and the corresponding elements in $\widetilde{\Psi}^{\ell',\boldsymbol{ce}}(\widetilde{\mathcal{M}}_\sigma^{\ell',\boldsymbol{e}})$.*

As an illustration of Lemma 4.10, we note that $\pi^\ell_{\sigma,\mathfrak{s}}u$ is generally non-conforming across the isotropic faces $F_{K_4',K_4''}$, $F_{K_6',K_6''}$ in Figure 2, and across the isotropic faces $F_{K_1',K_1''}$, $F_{K_4',K_4''}$, $F_{K_6',K_6''}$, $F_{K_6',K_6'''}$ in Figure 3 (left).

The conformity properties in Lemma 4.8, Remark 4.9 and Lemma 4.10 immediately allow us to identify sets $\mathcal{F}^\perp_{ID}(\mathcal{M}^\ell_\sigma)$ and $\mathcal{F}^\parallel_{ID}(\mathcal{M}^\ell_\sigma) = \mathcal{F}^\parallel_I(\mathcal{M}^\ell_\sigma) \cup \mathcal{F}^\parallel_D(\mathcal{M}^\ell_\sigma)$, over which $\pi^\ell_{\sigma,\mathfrak{s}}u$ is conforming and non-conforming, respectively. By construction, faces $F \in \mathcal{F}^\parallel_{ID}(\mathcal{M}^\ell_\sigma)$ satisfy (3.33), (3.34), as claimed in Proposition 3.10.

4.3.6. *Polynomial face jump bounds.* Next, we bound the face jumps of $\pi^\ell_{\sigma,\mathfrak{s}}u$ over the faces $F \in \mathcal{F}^\parallel_{ID}(\mathcal{M})$ for a geometric mesh $\mathcal{M} = \mathcal{M}^\ell_\sigma$. To this end, we first recall the anisotropic trace inequality from [22, Lemma 4.2] (with $t = 2$).

Lemma 4.11. *For $F \in \mathcal{F}^\parallel_{ID}(\mathcal{M})$ with $F \subseteq F' \in \mathcal{F}(K)$ and $u \in H^1(K)$, there holds*

$$\mathtt{h}_F^{-1}\|u\|^2_{L^2(F)} \lesssim (h_K^\perp)^{-2}\|u\|^2_{L^2(K)} + \|\mathsf{D}_\perp u\|^2_{L^2(K)} \lesssim N_K^\perp[u]^2. \tag{4.28}$$

Next, we establish the following variant of the jump estimate of [24, Section 5.5], which is essential for controlling jumps of $\pi^\ell_{\sigma,\mathfrak{s}}u$ over anisotropic faces of $\mathcal{M}$. Due to the appearance of H^1-projectors in edge-parallel direction, we require in this bound a local smoothness assumption which is slightly stronger than H^1-regularity.

Lemma 4.12. *Consider an* edge-parallel *face $F = F_{K_1,K_2} \in \mathcal{F}^\parallel_I(\mathcal{M})$ shared by two axiparallel elements $K_1 = K_1^\perp \times K^\parallel$ and $K_2 = K_2^\perp \times K^\parallel$ as in* (3.3)*, with $K^\parallel = (0, h^\parallel)$ in parallel direction and with $K_1^\perp$ and $K_2^\perp$ two shape-regular and possibly non-matching rectangles of diameters $h^\perp_{K_1} \simeq h^\perp_{K_2} \simeq h^\perp$ in perpendicular direction, for parameters $h^\perp \lesssim h^\parallel$. Let the elemental polynomial degrees be given by $\boldsymbol{p}_{K_i} = (p_i^\perp, p^\parallel)$. Let $u \in H^1((\overline{K}_1^\perp \cup \overline{K}_2^\perp)^\circ) \otimes H^1(K^\parallel)$ and $\pi_1 u|_{K_i} = \pi_0^\perp \otimes \pi_1^\parallel u|_{K_i} = \pi_{\boldsymbol{p}_{K_i},1}(u|_{K_i})$ for $i = 1, 2$. For the error terms $\eta_1 = u - \pi_1 u$, $\eta_0^\perp = u - \pi_0^\perp u$ and $\eta_1^\parallel = u - \pi_1^\parallel u$ as in* (4.7)*, we have the bound*

$$\mathtt{h}_F^{-1}\|[\![\pi u]\!]_F\|^2_{L^2(F)} \lesssim_p \sum_{i=1}^2 \big(\|\mathsf{D}_\perp \eta_0^\perp\|^2_{L^2(K_i)} + \|\mathsf{D}_\perp \eta_1^\parallel\|^2_{L^2(K_i)}\big). \tag{4.29}$$

Similarly, let $F = F_{K,\Gamma_\iota} \in \mathcal{F}^\parallel_D(\mathcal{M})$, $\boldsymbol{\iota} \in \mathcal{J}_D$, be a Dirichlet face of $K = K^\perp \times K^\parallel$, with $K^\parallel = (0, h^\parallel)$ and $K^\perp$ a shape-regular rectangle of diameter $h^\perp$, for $h^\perp \lesssim h^\parallel$. Let the elemental polynomial degrees be given by $\boldsymbol{p}_K = (p^\perp, p^\parallel)$. Let $u \in H^1(K^\perp) \otimes H^1(K^\parallel)$ with $u|_F = 0$ and $\pi_1 u|_K = \pi_0^\perp \otimes \pi_1^\parallel u|_K = \pi_{\boldsymbol{p}_K,1}(u|_K)$. Then we have the bound

$$\mathtt{h}_F^{-1}\|[\![\pi u]\!]_F\|^2_{L^2(F)} \lesssim_p \|\mathsf{D}_\perp \eta_0^\perp\|^2_{L^2(K)} + \|\mathsf{D}_\perp \eta_1^\parallel\|^2_{L^2(K)}. \tag{4.30}$$

Proof. Note that the setting is such that property (3.33) is fulfilled. On element K_i, $i = 1, 2$, we have

$$\eta_0^\perp - \pi_0^\perp \eta_0^\perp = (u - \pi_0^\perp u) - \pi_0^\perp(u - \pi_0^\perp u) = u - \pi_0^\perp u = \eta_0^\perp. \tag{4.31}$$

Then, we note that $\pi_1^{\parallel} u|_{K_i} \in H^1(K_i^{\perp}) \otimes \mathbb{P}_{p^{\parallel}}(K^{\parallel}) \subset H^1(K)$ for $i = 1, 2$ and $\big(\pi_1^{\parallel} u|_{K_1}\big)|_F = \big(\pi_1^{\parallel} u|_{K_2}\big)|_F$ in $L^2(F)$. With the latter identity and since $\pi_0^{\perp}$ and $\pi_1^{\parallel}$ commute, we conclude that

$$\begin{aligned}\|[\![\pi u]\!]_F\|^2_{L^2(F)} &= \|\pi_1 u|_{K_1} - \pi_1 u|_{K_2}\|^2_{L^2(F)} \\ &\lesssim \sum_{i=1}^{2} \|\pi_0^{\perp} \otimes \pi_1^{\parallel} u|_{K_i} - \pi_1^{\parallel} u|_{K_i}\|^2_{L^2(F)} = \sum_{i=1}^{2} \|\pi_1^{\parallel} \eta_0^{\perp}|_{K_i}\|^2_{L^2(F)}.\end{aligned}$$

We then consider element K_i for $i = 1, 2$. With the trace inequality (4.28), we have

$$\mathtt{h}_F^{-1} \|\pi_1^{\parallel} \eta_0^{\perp}|_{K_i}\|^2_{L^2(F)} \lesssim (h_{K_i}^{\perp})^{-2} \|\pi_1^{\parallel} \eta_0^{\perp}\|^2_{L^2(K_i)} + \|\mathsf{D}_{\perp}(\pi_1^{\parallel} \eta_0^{\perp})\|^2_{L^2(K_i)}.$$

Property (4.31) and standard h-version approximation results for $\pi_0^{\perp}$ in perpendicular direction yield

$$\|\pi_1^{\parallel} \eta_0^{\perp}\|^2_{L^2(K_i)} = \|(\pi_1^{\parallel} \eta_0^{\perp}) - \pi_0^{\perp}(\pi_1^{\parallel} \eta_0^{\perp})\|^2_{L^2(K_i)} \lesssim (h_{K_i}^{\perp})^2 \|\mathsf{D}_{\perp}(\pi_1^{\parallel} \eta_0^{\perp})\|^2_{L^2(K_i)}.$$

Therefore,

$$\begin{aligned}\mathtt{h}_F^{-1} \|\pi_1^{\parallel} \eta_0^{\perp}|_{K_i}\|^2_{L^2(F)} &\lesssim \|\mathsf{D}_{\perp}(\pi_1^{\parallel} \eta_0^{\perp})\|^2_{L^2(K_i)} \\ &\lesssim \|\mathsf{D}_{\perp}((\pi_1^{\parallel} - \pi_0^{\parallel})\eta_0^{\perp})\|^2_{L^2(K_i)} + \|\mathsf{D}_{\perp}(\pi_0^{\parallel} \eta_0^{\perp})\|^2_{L^2(K_i)}. \qquad (4.32)\end{aligned}$$

We next bound the two terms in (4.32). We write the first term as

$$\begin{aligned}(\pi_1^{\parallel} - \pi_0^{\parallel})\eta_0^{\perp} &= (\pi_1^{\parallel} - \pi_0^{\parallel})u - \pi_0^{\perp}(\pi_1^{\parallel} - \pi_0^{\parallel})u \\ &= \pi_0^{\parallel}(\pi_1^{\parallel} u - u) - \pi_0^{\perp}\big(\pi_0^{\parallel}(\pi_1^{\parallel} u - u)\big).\end{aligned}$$

With the stability bound (4.9) for $\pi_0^{\perp}$ in edge-perpendicular direction, we find that

$$\|\mathsf{D}_{\perp}\big((\pi_1^{\parallel} - \pi_0^{\parallel})\eta_0^{\perp}\big)\|^2_{L^2(K_i)} \lesssim (p_i^{\perp})^4 \|\mathsf{D}_{\perp}\big(\pi_0^{\parallel}(\pi_1^{\parallel} u - u)\big)\|^2_{L^2(K_i)}.$$

Then, since $\mathsf{D}_{\perp}^{\boldsymbol{\alpha}^{\perp}}$ and $\pi^{\parallel}_{p^{\parallel},0}$ commute, the L^2-stability of the L^2-projection $\pi_0^{\parallel}$ implies

$$\|\mathsf{D}_{\perp}\big((\pi_1^{\parallel} - \pi_0^{\parallel})\eta_0^{\perp}\big)\|^2_{L^2(K_i)} \lesssim (p_i^{\perp})^4 \|\mathsf{D}_{\perp}\eta_1^{\parallel}\|^2_{L^2(K_i)}.$$

To estimate the second term in (4.32), we again invoke the L^2-stability of $\pi_0^{\parallel}$ as before to obtain

$$\|\mathsf{D}_{\perp}(\pi_0^{\parallel} \eta_0^{\perp})\|^2_{L^2(K_1)} \lesssim \|\mathsf{D}_{\perp}\eta_0^{\perp}\|^2_{L^2(K_1)}.$$

Combining these arguments yields (4.29).

The proof of (4.30) for a Dirichlet boundary face F is obtained by proceeding analogously, noting that $\big(\pi_1 u|_K\big)|_F = 0$ in $L^2(F)$. □

Lemma 4.13. *Under the assumptions in Proposition 3.10, let $\pi^{\ell}_{\sigma,\mathfrak{s}} u$ be the hp-base projectors introduced in Section 4.3.4. With the error terms in* (3.40)*, we have the bound*

$$\mathrm{jmp}_{\mathcal{F}^{\parallel}_{ID}(\mathcal{M}^{\ell}_{\sigma})}[\eta^{\ell}_{\sigma,\mathfrak{s}}]^2 \lesssim_p \Upsilon^{\perp}_{\mathcal{M}^{\ell}_{\sigma,\mathcal{C}}}[\eta^{\ell,\perp}_{\sigma,\mathfrak{s}}]^2 + \Upsilon^{\parallel}_{\mathcal{M}^{\ell}_{\sigma,\mathcal{C}}}[\eta^{\ell,\parallel}_{\sigma,\mathfrak{s}}]^2 + \Upsilon^{\parallel}_{\mathfrak{T}^{\ell}_{\mathcal{C}}}[\eta^{\ell}_{\sigma,\mathfrak{s}}]^2. \qquad (4.33)$$

Proof. Anisotropic faces F in $\mathcal{F}^{\parallel}_{ID}(\mathcal{M}^{\ell)}_{\sigma})$ arise in mapped edge patches $\widetilde{\mathcal{M}}^{\ell,\boldsymbol{ce}}_{\sigma}$ and in mapped submeshes $\widetilde{\mathcal{M}}^{\ell,\boldsymbol{ce},\parallel}_{\sigma} \setminus \widetilde{\mathcal{D}}^{\ell,\boldsymbol{ce}}_{\sigma}$; see (4.19), (4.20). For faces F in the interior of these subsets or on Dirichlet boundaries away from corners, the jumps of $\pi^{\ell}_{\sigma,\mathfrak{s}} u$ can be bounded by the estimates in Lemma 4.12, upon noting that the same elemental polynomial degrees $p^{\parallel}_K$ are employed in edge-parallel directions and that, for $u \in$

$B_{-1-\boldsymbol{b}}(\Omega;\emptyset,\emptyset)$, the smoothness assumptions in Lemma 4.12 are satisfied, also for Dirichlet boundary faces away from corners. The remaining faces in $\mathcal{F}^{\shortparallel}_{ID}(\mathcal{M}^\ell_\sigma)$ are isotropic and the jumps over them can by bounded by isotropic versions of the trace inequality (4.28), along with the stability bounds in Lemma 4.1. □

Lemma 4.13 along with estimate (3.41) then establishes the bound (3.42) for $\mathrm{jmp}_{\mathcal{F}^{\shortparallel}_{ID}(\mathcal{M}^\ell_\sigma)}[\eta^\ell_{\sigma,\mathfrak{s}}]$, which completes the proof of Proposition 3.10.

5. Averaging Operators

We prove Theorem 3.12 and construct the averaging operators $\mathcal{A}^\ell_{\sigma,\mathfrak{s}}$ over the geometric mesh $\mathcal{M}=\mathcal{M}^\ell_\sigma$. Throughout this section, let $v\in\overline{V}^{\ell,0,\perp}_{\sigma,\mathfrak{s}}$ be fixed.

5.1. **Sets of adjacent elements.** Let $K\in\mathcal{M}$. For $\boldsymbol{N}\in\mathcal{N}(K)$, $E\in\mathcal{E}(K)$ and $F\in\mathcal{F}(K)$, we introduce the following sets of elements which *regularly* share $\boldsymbol{N}$, E and F, respectively:

$$\Delta_{K,\boldsymbol{N}} := \{\, K'\in\mathcal{M} \,:\, \boldsymbol{N}\in\mathcal{N}(K')\,\}, \tag{5.1}$$

$$\Delta_{K,E} := \{\, K'\in\mathcal{M} \,:\, E\in\mathcal{E}(K')\,\}, \tag{5.2}$$

$$\Delta_{K,F} := \{\, K'\in\mathcal{M} \,:\, F\in\mathcal{F}(K')\,\}. \tag{5.3}$$

Clearly, we have $K\in\Delta_{K,\boldsymbol{N}}$, $K\in\Delta_{K,E}\subseteq\delta_{K,E}$ and $K\in\Delta_{K,F}\subseteq\delta_{K,F}$, with $\delta_{K,E}$ and $\delta_{K,F}$ introduced in (3.11) and (3.12), respectively. Then, $\mathrm{card}(\Delta_{K,\boldsymbol{N}})\geq 1$, $\mathrm{card}(\Delta_{K,E})\geq 1$, and $\mathrm{card}(\Delta_{K,F})\in\{1,2\}$. It can be seen that

$$\boldsymbol{N}\in\mathcal{N}(E):\ \Delta_{K,E}\subseteq\Delta_{K,\boldsymbol{N}} \qquad\text{and}\qquad E\in\mathcal{E}(F):\ \Delta_{K,F}\subseteq\Delta_{K,E}. \tag{5.4}$$

Moreover, the sets defined in (5.1)–(5.3) have the property that

$$\Delta_{K,\boldsymbol{N}}=\Delta_{K',\boldsymbol{N}}, \qquad K'\in\Delta_{K,\boldsymbol{N}}, \tag{5.5}$$

$$\Delta_{K,E}=\Delta_{K',E}, \qquad K'\in\Delta_{K,E}, \tag{5.6}$$

$$\Delta_{K,F}=\Delta_{K',F}, \qquad K'\in\Delta_{K,F}. \tag{5.7}$$

For $\boldsymbol{N}\in\mathcal{N}(\mathcal{M})\setminus\mathcal{N}_D(\mathcal{M})$ respectively $\boldsymbol{N}\in\mathcal{N}_D(\mathcal{M})$, we require the sets

$$\begin{aligned}
\mathcal{F}^{\shortparallel}_I(\Delta_{K,\boldsymbol{N}}) &:= \{\, F=F_{K,K'}\in\mathcal{F}^{\shortparallel}_I(\mathcal{M}) \,:\, K'\in\Delta_{K,\boldsymbol{N}}\setminus\{K\}\,\},\\
\mathcal{F}^{\shortparallel}_D(\Delta_{K,\boldsymbol{N}}) &:= \{F=F_{K',\Gamma_\iota}\in\mathcal{F}^{\shortparallel}_D(\mathcal{M}) \,:\, K'\in\Delta_{K,\boldsymbol{N}} \text{ and } \boldsymbol{\iota}\in\mathcal{J}_D\,\}.
\end{aligned} \tag{5.8}$$

Similarly, for $\mathcal{E}\in\mathcal{E}(\mathcal{M})\setminus\mathcal{E}_D(\mathcal{M})$ respectively $E\in\mathcal{E}_D(\mathcal{M})$, we set

$$\begin{aligned}
\mathcal{F}^{\shortparallel}_I(\Delta_{K,E}) &:= \{\, F=F_{K,K'}\in\mathcal{F}^{\shortparallel}_I(\mathcal{M}) \,:\, K'\in\Delta_{K,E}\setminus\{K\}\,\},\\
\mathcal{F}^{\shortparallel}_D(\Delta_{K,E}) &:= \{F=F_{K',\Gamma_\iota}\in\mathcal{F}^{\shortparallel}_D(\mathcal{M}) \,:\, K'\in\Delta_{K,E} \text{ and } \boldsymbol{\iota}\in\mathcal{J}_D\,\}.
\end{aligned} \tag{5.9}$$

We further define

$$\mathcal{F}^{\shortparallel}_{ID}(\Delta_{K,\boldsymbol{N}}) := \mathcal{F}^{\shortparallel}_I(\Delta_{K,\boldsymbol{N}})\cup\mathcal{F}^{\shortparallel}_D(\Delta_{K,\boldsymbol{N}}), \tag{5.10}$$

$$\mathcal{F}^{\shortparallel}_{ID}(\Delta_{K,E}) := \mathcal{F}^{\shortparallel}_I(\Delta_{K,E})\cup\mathcal{F}^{\shortparallel}_D(\Delta_{K,E}). \tag{5.11}$$

Notice that any of these sets could be empty.

5.2. **Averaging over $\Delta_{K,\boldsymbol{N}}$.** We construct an approximation $v^{\mathrm{n}} \in \overline{V}^{\ell,0}_{\sigma,\mathfrak{s}}$ by modifying the base projection v at possibly all elemental vertices.

For $K \in \mathcal{M}$ and $\boldsymbol{N} \in \mathcal{N}(K)$, we define the *averaged vertex value* $A_{K,\boldsymbol{N}}(v)$ by averaging v over all elements in $\Delta_{K,\boldsymbol{N}}$ in (5.1):

$$A_{K,\boldsymbol{N}}(v) := \begin{cases} \dfrac{1}{\operatorname{card}(\Delta_{K,\boldsymbol{N}})} \displaystyle\sum_{K' \in \Delta_{K,\boldsymbol{N}}} v|_{K'}(\boldsymbol{N}), & \text{if } \boldsymbol{N} \in \mathcal{N}(\mathcal{M}) \setminus \mathcal{N}_D(\mathcal{M}), \\ 0, & \text{if } \boldsymbol{N} \in \mathcal{N}_D(\mathcal{M}). \end{cases} \tag{5.12}$$

The averaged value $A_{K,\boldsymbol{N}}(v)$ in (5.12) is well-defined irrespective of whether $\boldsymbol{N} \in \mathcal{N}(K)$ gives rise to a regular or irregular node in $\mathcal{N}(\mathcal{M})$. With (5.5), we have

$$A_{K,\boldsymbol{N}}(v) = A_{K',\boldsymbol{N}}(v), \qquad K' \in \Delta_{K,\boldsymbol{N}}. \tag{5.13}$$

Hence, the values $A_{K,\boldsymbol{N}}$ assign a unique vertex value over the elements in $\Delta_{K,\boldsymbol{N}}$ which match regularly with the vertex $\boldsymbol{N}$.

For $K \in \mathcal{M}$ and $\boldsymbol{N} \in \mathcal{N}(K)$, we denote by $\mathcal{L}_{K,\boldsymbol{N}}(v) \in \mathbb{Q}_1(K)$ the polynomial vertex lifting with the property that, for $\boldsymbol{N}' \in \mathcal{N}(K)$,

$$\mathcal{L}_{K,\boldsymbol{N}}(v)(\boldsymbol{N}') = \begin{cases} v|_K(\boldsymbol{N}) - A_{K,\boldsymbol{N}}(v) & \boldsymbol{N}' = \boldsymbol{N}, \\ 0 & \boldsymbol{N}' \neq \boldsymbol{N}. \end{cases} \tag{5.14}$$

Lemma 5.1. *For $K \in \mathcal{M}$ and $\boldsymbol{N} \in \mathcal{N}(K)$, let the vertex lifting $\mathcal{L}_{K,\boldsymbol{N}}(v)$ be defined by* (5.14) *with the averages $A_{K,\boldsymbol{N}}(v)$ in* (5.12)*. Then there holds*

$$N_K^{\perp}[\mathcal{L}_{K,\boldsymbol{N}}(v)]^2 \lesssim |\boldsymbol{p}_K|^8 \mathrm{jmp}_{\mathcal{F}^{\parallel}_{ID}(\Delta_{K,\boldsymbol{N}})}[v]^2, \tag{5.15}$$

with $\mathcal{F}^{\parallel}_{ID}(\Delta_{K,\boldsymbol{N}})$ in (5.10)*. If $\mathcal{F}^{\parallel}_{ID}(\Delta_{K,\boldsymbol{N}}) = \emptyset$, the sum on the right-hand side is understood as zero.*

Proof. From the definition (5.12) with anisotropic scaling, we readily find that

$$\|\mathcal{L}_{K,\boldsymbol{N}}(v)\|^2_{L^2(K)} \lesssim (h_K^{\perp})^2 h_K^{\parallel} \big|v|_K(\boldsymbol{N}) - A_{K,\boldsymbol{N}}(v)\big|^2. \tag{5.16}$$

The univariate inverse estimate (see, e.g., [25, Theorem 3.91]) combined with anisotropic scaling and employing that $h_K^{\perp} \lesssim h_K^{\parallel}$ and $p_K^{\perp} \leq p_K^{\parallel}$ yields the anisotropic inverse inequality

$$\|\nabla v\|^2_{L^2(K)} \lesssim (p_K^{\parallel})^4 (h_K^{\perp})^{-2} \|v\|^2_{L^2(K)}, \qquad v \in \mathbb{Q}_{\boldsymbol{p}_K}(K)\,. \tag{5.17}$$

Therefore,

$$N_K^{\perp}[\mathcal{L}_{K,\boldsymbol{N}}(v)]^2 \lesssim |\boldsymbol{p}_K|^4 h_K^{\parallel} \big|v|_K(\boldsymbol{N}) - A_{K,\boldsymbol{N}}(v)\big|^2. \tag{5.18}$$

We proceed to estimate $|v|_K(\boldsymbol{N}) - A_{K,\boldsymbol{N}}(v)\big|$ in (5.18). We consider first the case where the elemental node $\boldsymbol{N} \in \mathcal{N}(K)$ gives rise to a node of $\mathcal{N}(\mathcal{M}) \setminus \mathcal{N}_D(\mathcal{M})$. Then, if $\operatorname{card}(\Delta_{K,\boldsymbol{N}}) \geq 2$, with (5.12), the triangle inequality, the fact that $\operatorname{card}(\Delta_{K,\boldsymbol{N}})^{-1}$ is bounded uniformly in ℓ, and the partial conformity properties of v discussed in

Section 4.3.5, we conclude that

$$\begin{aligned}\big|v|_K(\boldsymbol{N}) - A_{K,\boldsymbol{N}}(v)\big|^2 &\lesssim \frac{1}{\operatorname{card}(\Delta_{K,\boldsymbol{N}})^2} \sum_{K'\in\Delta_{K,\boldsymbol{N}}\setminus\{K\}} \big|v|_K(\boldsymbol{N}) - v|_{K'}(\boldsymbol{N})\big|^2 \\ &\lesssim \sum_{K'\in\Delta_{K,\boldsymbol{N}}\setminus\{K\}} |[\![v]\!]_{F_{K,K'}}(\boldsymbol{N})|^2 \\ &\le \sum_{K'\in\Delta_{K,\boldsymbol{N}}\setminus\{K\}} \|[\![v]\!]_{F_{K,K'}}\|^2_{L^\infty(F_{K,K'})} \\ &= \sum_{F\in\mathcal{F}_I^{\shortparallel}(\Delta_{K,\boldsymbol{N}})} \|[\![v]\!]_F\|^2_{L^\infty(F)}.\end{aligned} \tag{5.19}$$

If $\operatorname{card}(\Delta_{K,\boldsymbol{N}}) = 1$, we have $A_{K,\boldsymbol{N}}(v) = v|_K(\boldsymbol{N})$ and $\mathcal{F}_I^{\shortparallel}(\Delta_{K,\boldsymbol{N}}) = \emptyset$. As a consequence, $\mathcal{L}_{K,\boldsymbol{N}}(v) = 0$ in (5.14). Hence, inequality (5.19) above holds true trivially if the sum over $\mathcal{F}_I^{\shortparallel}(\Delta_{K,\boldsymbol{N}})$ is understood as zero.

Second, let $\boldsymbol{N} \in \mathcal{N}(K)$ give rise to a Dirichlet node in $\mathcal{N}_D(\mathcal{M})$. Consider a Dirichlet boundary face $F = F_{K',\Gamma_\iota}$ with $\boldsymbol{N} \in \overline{F}$, $K' \in \Delta_{K,\boldsymbol{N}}$ and $\boldsymbol{\iota} \in \mathcal{J}_D$. We may assume that $F \in \mathcal{F}_D^{\shortparallel}(\Delta_{K,\boldsymbol{N}})$, otherwise we have $\mathcal{L}_{K,\boldsymbol{N}}(v) = 0$ by Remark 4.9 and since $A_{K,\boldsymbol{N}}(v) = 0$ by (5.12). We thus conclude that

$$\begin{aligned}\big|v|_K(\boldsymbol{N}) - A_{K,\boldsymbol{N}}(v)\big|^2 &= |[\![v]\!]_F(\boldsymbol{N})|^2 \\ &\le \|[\![v]\!]_F\|^2_{L^\infty(F)} \le \sum_{F\in\mathcal{F}_D^{\shortparallel}(\Delta_{K,\boldsymbol{N}})} \|[\![v]\!]_F\|^2_{L^\infty(F)}.\end{aligned} \tag{5.20}$$

Combining (5.18), (5.19) and (5.20) gives

$$N_K^{\perp}[\mathcal{L}_{K,\boldsymbol{N}}(v)]^2 \lesssim |\boldsymbol{p}_K|^4 h_K^{\shortparallel} \sum_{F\in\mathcal{F}_{ID}^{\shortparallel}(\Delta_{K,\boldsymbol{N}})} \|[\![v]\!]_F\|^2_{L^\infty(F)}. \tag{5.21}$$

To bound the L^∞-norms of the jumps of v in (5.21), we recall from [25, Theorems 3.92] the following univariate inverse inequality: let $I = (a, b)$ be an interval of size $h = b - a$. Then

$$|q(a)|^2 + |q(b)|^2 \le \|q\|^2_{L^\infty(I)} \lesssim p^2 h^{-1} \|q\|^2_{L^2(I)}\,, \qquad q \in \mathbb{P}_p(I). \tag{5.22}$$

for all polynomials $q \in \mathbb{P}_p(I)$. A face $F \in \mathcal{F}_{ID}^{\shortparallel}(\Delta_{K,\boldsymbol{N}})$ can be written in the form (3.34). Applying (5.22) in the two directions on F and the definition of the face polynomial degrees $\overline{\boldsymbol{p}}_{K,F}$ in (3.14) yield

$$\|[\![v]\!]_F\|^2_{L^\infty(F)} \lesssim |\boldsymbol{p}_K|^4 (h_K^{\perp})^{-1} (h_K^{\shortparallel})^{-1} \|[\![v]\!]_F\|^2_{L^2(F)}. \tag{5.23}$$

The bound (5.15) follows from (5.21) and (5.23). □

For $K \in \mathcal{M}$, we introduce the full vertex lifting

$$\mathcal{L}_K^{\mathrm{n}}(v) := \sum_{\boldsymbol{N}\in\mathcal{N}(K)} \mathcal{L}_{K,\boldsymbol{N}}(v) \in \mathbb{Q}_1(K). \tag{5.24}$$

We further define the approximation $v^{\mathrm{n}} \in \overline{V}^{\ell,0}_{\boldsymbol{\sigma},\mathfrak{s}}$ as

$$v^{\mathrm{n}}|_K := v|_K - \mathcal{L}_K^{\mathrm{n}}(v) \in \mathbb{S}_{\overline{\boldsymbol{p}}_K}(K), \qquad K \in \mathcal{M}. \tag{5.25}$$

The function $v^{\mathrm{n}}|_K$ has assigned vertex values at all elemental vertex nodes:

$$v^{\mathrm{n}}|_K(\boldsymbol{N}) = A_{K,\boldsymbol{N}}(v), \qquad \boldsymbol{N} \in \mathcal{N}(K). \tag{5.26}$$

Note also that, in the expansion (3.15), (3.16), only the nodal part of $v^{\mathrm{n}}|_K$ differs from the nodal part of $v|_K$, while the edge, face and interior parts of $v^{\mathrm{n}}|_K$ and $v|_K$ coincide.

Proposition 5.2. *Let $v^{\mathrm{n}}|_K$ be defined in* (5.25) *for $K \in \mathcal{M}$. Then the function v^{n} is conforming over faces $F \in \mathcal{F}_{ID}(\mathcal{M}) \setminus \mathcal{F}_{ID}^{\parallel}(\mathcal{M})$ and there holds*

$$\Upsilon_{\mathcal{M}}^{\perp}[v - v^{\mathrm{n}}]^2 + \mathrm{jmp}_{\mathcal{F}_{ID}^{\parallel}(\mathcal{M})}[v^{\mathrm{n}}]^2 \lesssim |\boldsymbol{p}|^8 \, \mathrm{jmp}_{\mathcal{F}_{ID}^{\parallel}(\mathcal{M})}[v]^2. \tag{5.27}$$

Proof. As outlined in Section 4.3.5, the base interpolant v is continuous over edge-perpendicular faces $F \in \mathcal{F}_{ID}(M) \setminus \mathcal{F}_{ID}^{\parallel}(\mathcal{M})$ between anisotropic elements across which the nodally exact interpolants (A.1) are used in edge-parallel direction. Then, the definition (5.14) and property (5.13) imply that the liftings $\mathcal{L}_{K,\boldsymbol{N}}(v)$ yield conforming approximations over the same faces. Since $v^{\mathrm{n}}|_K = v|_K - \mathcal{L}_K^{\mathrm{n}}(v)$, the approximation v^{n} is continuous over these faces as well, and thus generally non-conforming over faces in $\mathcal{F}_{ID}^{\parallel}(\mathcal{M})$.

The bound for $\Upsilon_{\mathcal{M}}^{\perp}[v - v^{\mathrm{n}}]^2$ in (5.27) follows immediately by summing (5.15) over all elements $K \in \mathcal{M}$ and $\boldsymbol{N} \in \mathcal{N}(K)$. To bound the L^2-norms of the jumps of v^{n}, consider an interior face $F = F_{K,K'} \in \mathcal{F}_{ID}^{\parallel}(\mathcal{M})$. The definition (5.25), the triangle inequality and the trace inequality (4.28) yield

$$\mathtt{h}_F^{-1} \|[\![v^{\mathrm{n}}]\!]_F\|_{L^2(F)}^2 \lesssim \mathtt{h}_F^{-1} \|[\![v]\!]_F\|_{L^2(F)}^2 + N_K^{\perp}[\mathcal{L}_K^{\mathrm{n}}(v)]^2 + N_{K'}^{\perp}[\mathcal{L}_K^{\mathrm{n}}(v)]^2.$$

A corresponding bound holds for Dirichlet faces $F \in \mathcal{F}_D^{\parallel}(\mathcal{M})$. Summing these estimates over all $F \in \mathcal{F}_{ID}^{\parallel}(\mathcal{M})$ and applying (5.15) gives the desired bound for $\mathrm{jmp}_{\mathcal{F}_{ID}^{\parallel}(\mathcal{M})}[v^{\mathrm{n}}]^2$ in (5.27). □

5.3. **Averaging over $\Delta_{K,E}$.** With (3.18), the approximation $v^{\mathrm{n}} \in \overline{V}_{\sigma,\mathfrak{s}}^{\ell,0}$ from Section 5.2 satisfies

$$(v^{\mathrm{n}}|_K)|_E \in \mathbb{P}_{\overline{p}_{K,E}}(E), \qquad K \in \mathcal{M},\ E \in \mathcal{E}(K), \tag{5.28}$$

with the minimum edge degree $\overline{p}_{K,E}$ in (3.13). For $K \in \mathcal{M}$ and $E \in \mathcal{E}(K)$, we next average v^{n} over the set $\Delta_{K,E}$ in (5.2) and define:

$$A_{K,E}(v^{\mathrm{n}}) := \begin{cases} \dfrac{1}{\mathrm{card}(\Delta_{K,E})} \displaystyle\sum_{K' \in \Delta_{K,E}} \big(v^{\mathrm{n}}|_{K'}\big)|_E, & \text{if } E \in \mathcal{E}(\mathcal{M}) \setminus \mathcal{E}_D(\mathcal{M}), \\ 0, & \text{if } E \in \mathcal{E}_D(\mathcal{M}). \end{cases} \tag{5.29}$$

By (5.28), the function $A_{K,E}(v^{\mathrm{n}})$ is a polynomial in $\mathbb{P}_{\overline{p}_{K,E}}(E)$.

Lemma 5.3. *Let $K \in \mathcal{M}$ and $E \in \mathcal{E}(K)$. Then, $A_{K,E}(v^{\mathrm{n}}) = A_{K',E}(v^{\mathrm{n}})$ for $K' \in \Delta_{K,E}$. Moreover, if $\boldsymbol{N} \in \mathcal{N}(E)$ is an end point of E, we have $A_{K,E}(v^{\mathrm{n}})(\boldsymbol{N}) = v^{\mathrm{n}}|_K(\boldsymbol{N})$.*

Proof. The first assertion follows with (5.6). Furthermore, we note that with properties (5.4) and (5.13), there holds $A_{K',\boldsymbol{N}}(v) = A_{K,\boldsymbol{N}}(v)$ for $K' \in \Delta_{K,E}$. This

property in combination with definition (5.29) and property (5.26) yields

$$\begin{aligned} A_{K,E}(v^{\mathrm{n}})(\boldsymbol{N}) &= \frac{1}{\mathrm{card}(\Delta_{K,E})} \sum_{K'\in\Delta_{K,E}} v^{\mathrm{n}}|_{K'}(\boldsymbol{N}) \\ &= \frac{1}{\mathrm{card}(\Delta_{K,E})} \sum_{K'\in\Delta_{K,E}} A_{K',\boldsymbol{N}}(v) \\ &= \frac{1}{\mathrm{card}(\Delta_{K,E})} \sum_{K'\in\Delta_{K,E}} A_{K,\boldsymbol{N}}(v) = A_{K,\boldsymbol{N}}(v) = v^{\mathrm{n}}|_K(\boldsymbol{N}). \end{aligned}$$

The second assertion follows. □

For $K \in \mathcal{M}$ and $E \in \mathcal{E}(K)$, we denote by $\mathcal{L}_{K,E}(v^{\mathrm{n}}) \in \mathbb{S}_{\overline{\boldsymbol{p}}_K}(K)$ the polynomial lifting which satisfies

$$\mathcal{L}_{K,E}(v^{\mathrm{n}})|_E = (v^{\mathrm{n}}|_K)|_E - A_{K,E}(v^{\mathrm{n}}) \in \mathbb{P}_{\overline{p}_{K,E}}(E) \quad \text{on } E, \tag{5.30}$$

and which is given by linear blending functions in the two directions orthogonal to E. With Lemma 5.3, there holds

$$\mathcal{L}_{K,E}(v^{\mathrm{n}})(\boldsymbol{N}) = 0, \qquad \boldsymbol{N} \in \mathcal{N}(E). \tag{5.31}$$

The lifting $\mathcal{L}_{K,E}(v)$ vanishes on the remaining elemental edges $E' \neq E$, as well as on faces $F \in \mathcal{F}(K)$ with $E \notin \mathcal{E}(F)$.

Lemma 5.4. *For $K \in \mathcal{M}$ and $E \in \mathcal{E}(K)$, let the edge lifting $\mathcal{L}_{K,E}(v^{\mathrm{n}})$ be defined by* (5.30) *with the averages $A_{K,E}(v^{\mathrm{n}})$ in* (5.29)*. Then there holds*

$$N_K^{\perp}[\mathcal{L}_{K,E}(v^{\mathrm{n}})]^2 \lesssim |\boldsymbol{p}_K|^6 \mathrm{jmp}_{\mathcal{F}_{ID}^{\parallel}(\Delta_{K,E})}[v^{\mathrm{n}}]^2, \tag{5.32}$$

with $\mathcal{F}_{ID}^{\parallel}(\Delta_{K,E})$ in (5.11)*. If $\mathcal{F}_{ID}^{\parallel}(\Delta_{K,E}) = \emptyset$, the sum on the right-hand side is understood as zero.*

Proof. We denote by h_E the length of $E \in \mathcal{E}(K)$. Then, either $h_E \simeq h_K^{\perp}$ or $h_E \simeq h_K^{\parallel}$. From the definition of (5.30) and anisotropic scaling, we readily see that

$$\|\mathcal{L}_{K,E}(v^{\mathrm{n}})\|_{L^2(K)}^2 \lesssim \begin{cases} h_K^{\perp} h_K^{\parallel} \|v^{\mathrm{n}}|_K - A_{K,E}(v^{\mathrm{n}})\|_{L^2(E)}^2, & \text{if } h_E \simeq h_K^{\perp}, \\ (h_K^{\perp})^2 \|v^{\mathrm{n}}|_K - A_{K,E}(v^{\mathrm{n}})\|_{L^2(E)}^2, & \text{if } h_E \simeq h_K^{\parallel}. \end{cases} \tag{5.33}$$

Hence, with (5.17), we conclude that

$$\begin{aligned} &N_K^{\perp}[\mathcal{L}_{K,E}(v^{\mathrm{n}})]^2 \\ &\quad \lesssim |\boldsymbol{p}_K|^4 \begin{cases} (h_K^{\perp})^{-1} h_K^{\parallel} \|v^{\mathrm{n}}|_K - A_{K,E}(v^{\mathrm{n}})\|_{L^2(E)}^2, & \text{if } h_E \simeq h_K^{\perp}, \\ \|v^{\mathrm{n}}|_K - A_{K,E}(v^{\mathrm{n}})\|_{L^2(E)}^2, & \text{if } h_E \simeq h_K^{\perp}. \end{cases} \end{aligned} \tag{5.34}$$

We continue by bounding $\|v^{\mathrm{n}}|_K - v^{\mathrm{e}}|_K\|_{L^2(E)}$. First, we consider the case $E \in \mathcal{E}(\mathcal{M}) \setminus \mathcal{E}_D(\mathcal{M})$. If $\mathrm{card}(\Delta_{K,E}) \geq 2$, we employ the definition (5.29), the triangle inequality, and the uniform boundedness of $\mathrm{card}(\Delta_{K,E})^{-2}$, and observe that v^{n} has the same continuity properties as those of v established in Section 4.3.5; cf.

Proposition 5.2. We obtain

$$\begin{aligned}\|v^{\mathrm{n}}|_K - A_{K,E}(v^{\mathrm{n}})\|^2_{L^2(E)} &\lesssim \frac{1}{\mathrm{card}(\Delta_{K,E})^2} \sum_{K'\in\Delta_{K,E}\setminus\{K\}} \|v^{\mathrm{n}}|_K - v^{\mathrm{n}}|_{K'}\|^2_{L^2(E)} \\ &\lesssim \sum_{K'\in\Delta_{K,E}\setminus\{K\}} \|[\![v^{\mathrm{n}}]\!]_{F_{K,K'}}\|^2_{L^2(E)} \\ &\lesssim \sum_{F\in\mathcal{F}_I^{\shortparallel}(\Delta_{K,E})} \|[\![v^{\mathrm{n}}]\!]_F\|^2_{L^2(E)}.\end{aligned} \tag{5.35}$$

If $\mathrm{card}(\Delta_{K,E}) = 1$, then $\mathcal{F}_I^{\shortparallel}(\Delta_{K,E}) = \emptyset$ and $\mathcal{L}_{K,E}(v^{\mathrm{n}}) = 0$. In this case, the inequality (5.35) holds trivially if we understand the sum above as zero.

Second, let $E \in \mathcal{E}_D(\mathcal{M})$ be a Dirichlet boundary edge. Then, consider a Dirichlet boundary face $F = F_{K',\Gamma_\iota}$ with $E \subset \overline{F}$, $K' \in \Delta_{K,E}$ and $\boldsymbol{\iota} \in \mathcal{J}_D$. As before, we may assume $F \in \mathcal{F}_D^{\shortparallel}(\Delta_{K,E})$, otherwise $\mathcal{L}_{K,E}(v^{\mathrm{n}}) = 0$; cf. Remark 4.9, Proposition 5.2 and (5.29). We find that

$$\begin{aligned}\|v^{\mathrm{n}}|_K - A_{K,E}(v^{\mathrm{n}})\|^2_{L^2(E)} &\lesssim \|v^{\mathrm{n}}|_K\|^2_{L^2(E)} \\ &\lesssim \|[\![v^{\mathrm{n}}]\!]_F\|^2_{L^2(E)} \lesssim \sum_{F\in\mathcal{F}_D^{\shortparallel}(\Delta_{K,E})} \|[\![v^{\mathrm{n}}]\!]_F\|^2_{L^2(E)}.\end{aligned} \tag{5.36}$$

For $F \in \mathcal{F}_{ID}^{\shortparallel}(\Delta_{K,E})$ written in the form (3.34), the inequality (5.22) applied on $\overline{E} \subset \overline{F}$ in direction perpendicular to E implies

$$\|[\![v^{\mathrm{n}}]\!]_F\|^2_{L^2(E)} \lesssim \begin{cases} |\boldsymbol{p}_K|^2 (h_K^{\shortparallel})^{-1} \|[\![v^{\mathrm{n}}]\!]_F\|^2_{L^2(F)} & \text{if } h_E \simeq h_K^{\perp}, \\ |\boldsymbol{p}_K|^2 (h_K^{\perp})^{-1} \|[\![v^{\mathrm{n}}]\!]_F\|^2_{L^2(F)} & \text{if } h_E \simeq h_K^{\shortparallel}. \end{cases} \tag{5.37}$$

Therefore, combining the inequalities in(5.34), (5.35), (5.36) and (5.37) gives the desired bound (5.32). □

We define the full edge lifting

$$\mathcal{L}_K^{\mathrm{e}}(v^{\mathrm{n}}) := \sum_{E\in\mathcal{E}(K)} \mathcal{L}_{K,E}(v^{\mathrm{n}}) \in \mathbb{S}_{\overline{\boldsymbol{p}}_K}(K), \qquad K \in \mathcal{M}, \tag{5.38}$$

and introduce the approximation $v^{\mathrm{e}} \in \overline{V}^{\ell,0}_{\sigma,\mathfrak{s}}$ by

$$v^{\mathrm{e}}|_K := v^{\mathrm{n}}|_K - \mathcal{L}_K^{\mathrm{e}}(v^{\mathrm{n}}) \in \mathbb{S}_{\overline{\boldsymbol{p}}_K}(K), \qquad K \in \mathcal{M}. \tag{5.39}$$

The definition (5.39) only affects the edge parts of $v^{\mathrm{n}}|_K$ in (3.15), (3.16), while nodal, face and interior parts of $v^{\mathrm{n}}|_K$ are not modified. By construction and Lemma 5.3, there holds

$$\big(v^{\mathrm{e}}|_K\big)|_E = A_{K,E}(v^{\mathrm{n}}), \qquad E \in \mathcal{E}(K), \tag{5.40}$$

$$v^{\mathrm{e}}|_K(\boldsymbol{N}) = v^{\mathrm{n}}|_K(\boldsymbol{N}), \qquad \boldsymbol{N} \in \mathcal{N}(K). \tag{5.41}$$

The analog of Proposition 5.2 reads as follows.

Proposition 5.5. *Let $v^{\mathrm{e}}|_K$ be defined in* (5.39) *for $K \in \mathcal{M}$. Then the function v^{e} is conforming over faces $F \in \mathcal{F}_{ID}(\mathcal{M}) \setminus \mathcal{F}_{ID}^{\shortparallel}(\mathcal{M})$ and there holds*

$$\Upsilon_{\mathcal{M}}^{\perp}[v - v^{\mathrm{e}}]^2 + \mathrm{jmp}_{\mathcal{F}_{ID}^{\shortparallel}(\mathcal{M})}[v^{\mathrm{e}}]^2 \;\lesssim\; |\boldsymbol{p}|^{14}\, \mathrm{jmp}_{\mathcal{F}_{ID}^{\shortparallel}(\mathcal{M})}[v]^2. \tag{5.42}$$

Proof. By proceeding as in the proof of Proposition 5.2, the estimate (5.32) yields

$$\Upsilon^{\perp}_{\mathcal{M}}[v^{\mathrm{n}} - v^{\mathrm{e}}]^2 + \mathrm{jmp}_{\mathcal{F}^{\parallel}_{ID}(\mathcal{M})}[v^{\mathrm{e}}]^2 \lesssim |\boldsymbol{p}|^6 \, \mathrm{jmp}_{\mathcal{F}^{\parallel}_{ID}(\mathcal{M})}[v^{\mathrm{n}}]^2.$$

The triangle inequality and the bound (5.27) now yield (5.42). □

5.4. **Averaging over $\Delta_{K,F}$.** With (3.19), the approximation $v^{\mathrm{e}} \in \overline{V}^{\ell,0}_{\sigma,\mathfrak{s}}$ satisfies:

$$(v^{\mathrm{e}}|_K)|_F \in \mathbb{Q}_{\overline{\boldsymbol{p}}_{K,F}}(F), \qquad K \in \mathcal{M},\ F \in \mathcal{F}(K), \tag{5.43}$$

with the minimum face degree $\overline{\boldsymbol{p}}_{K,F}$ in (3.14). We then average v^{e} over $\Delta_{K,F}$ in (5.3):

$$A_{K,F}(v^{\mathrm{e}}) := \begin{cases} \dfrac{1}{\mathrm{card}(\Delta_{K,F})} \displaystyle\sum_{K' \in \Delta_{K,F}} (v^{\mathrm{e}}|_{K'})|_F, & \text{if } F \in \mathcal{F}_I(\mathcal{M}) \cup \mathcal{F}_N(\mathcal{M}), \\ 0, & \text{if } F \in \mathcal{F}_D(\mathcal{M}). \end{cases} \tag{5.44}$$

By (5.43), the function $A_{K,F}(v^{\mathrm{e}})$ is a polynomial in $\mathbb{Q}_{\overline{p}_{K,F}}(F)$. For $F \in \mathcal{F}_N(\mathcal{M})$, we have $\mathrm{card}(\Delta_{K,F}) = 1$ and $A_{K,F}(v^{\mathrm{e}}) = (v^{\mathrm{e}}|_K)|_F$.

Lemma 5.6. *Let $K \in \mathcal{M}$ and $F \in \mathcal{F}(K)$. Then, $A_{K,F}(v^{\mathrm{e}}) = A_{K',F}(v^{\mathrm{e}})$ for $K' \in \Delta_{K,F}$. Moreover, if $E \in \mathcal{E}(F)$ is an edge of F, we have $A_{K,F}(v^{\mathrm{e}})|_E = (v^{\mathrm{e}}|_K)|_E$.*

Proof. The first property follows with (5.7). To show the second one, consider $\boldsymbol{x} \in \overline{E} \in \mathcal{E}(K)$. With (5.4) and Lemma 5.3, there holds $A_{K',E}(v^{\mathrm{n}}) = A_{K,E}(v^{\mathrm{n}})$ for $K' \in \Delta_{K,F}$. Employing (5.44) and (5.40), (5.41) (see also Lemma 5.3) then yields

$$\begin{aligned} A_{K,F}(v^{\mathrm{e}})(\boldsymbol{x}) &= \frac{1}{\mathrm{card}(\Delta_{K,F})} \sum_{K' \in \Delta_{K,F}} v^{\mathrm{e}}|_{K'}(\boldsymbol{x}) \\ &= \frac{1}{\mathrm{card}(\Delta_{K,F})} \sum_{K' \in \Delta_{K,F}} A_{K',E}(v^{\mathrm{n}})(\boldsymbol{x}) \\ &= \frac{1}{\mathrm{card}(\Delta_{K,F})} \sum_{K' \in \Delta_{K,F}} A_{K,E}(v^{\mathrm{n}})(\boldsymbol{x}) = A_{K,E}(v^{\mathrm{n}})(\boldsymbol{x}) = v^{\mathrm{e}}|_K(\boldsymbol{x}), \end{aligned}$$

which completes the proof. □

For $K \in \mathcal{M}$ and $F \in \mathcal{F}(K)$, we denote by $\mathcal{L}_{K,F}(v^{\mathrm{e}}) \in \mathbb{S}_{\overline{\boldsymbol{p}}_K}(K)$ the polynomial lifting which is given by

$$\mathcal{L}_{K,F}(v^{\mathrm{e}})|_F := (v^{\mathrm{e}}|_K)|_F - A_{K,F}(v^{\mathrm{e}}) \in \mathbb{Q}_{\overline{\boldsymbol{p}}_{K,F}}(F) \quad \text{on } F, \tag{5.45}$$

and by a linear blending function in direction orthogonal to F. With Lemma 5.6, there holds

$$\mathcal{L}_{K,F}(v^{\mathrm{e}})|_E = 0, \qquad E \in \mathcal{E}(F). \tag{5.46}$$

Therefore, the lifting $\mathcal{L}_{K,F}(v^{\mathrm{e}})$ vanishes on all other elemental faces $F' \in \mathcal{F}(K)$ with $F' \neq F$.

Remark 5.7. If $\mathrm{card}(\Delta_{K,F}) = 1$ and $F \notin \mathcal{F}_D(\mathcal{M})$, we have $\mathcal{L}_{K,F}(v^{\mathrm{e}}) = 0$, which is a consequence of definitions (5.44) and (5.45). In particular, this holds true for Neumann boundary faces $F \in \mathcal{F}_N(\mathcal{M})$. Similarly, we have $\mathcal{L}_{K,F}(v^{\mathrm{e}}) = 0$ if v^{e} is conforming over the face F. In view of the partial continuity properties of v^{e} in Proposition 5.5, in the subsequent lemma it is therefore sufficient to focus on faces $F \in \mathcal{F}^{\parallel}_{ID}(\mathcal{M})$.

Lemma 5.8. *Let $F \in \mathcal{F}(K)$ give rise to a face in $\mathcal{F}_{ID}^{\|}(\mathcal{M})$. Let the face lifting $\mathcal{L}_{K,F}(v^{\mathrm{e}})$ be defined by* (5.45) *with the averages $A_{K,F}(v^{\mathrm{e}})$ in* (5.44)*. Then there holds*

$$N_K^{\perp}[\mathcal{L}_{K,F}(v^{\mathrm{e}})]^2 \lesssim |\boldsymbol{p}_K|^4 \mathtt{h}_F^{-1} \|[\![v^{\mathrm{e}}]\!]_F\|_{L^2(F)}^2. \tag{5.47}$$

Proof. With properties (3.33), (3.34) and anisotropic scaling combined with the inverse inequality (5.17), we see that

$$N_K^{\perp}[\mathcal{L}_{K,F}(v^{\mathrm{e}})]^2 \lesssim |\boldsymbol{p}_K|^4 (h_K^{\perp})^{-1} \|v^{\mathrm{e}}|_K - A_{K,F}(v^{\mathrm{e}})\|_{L^2(F)}^2. \tag{5.48}$$

If $F = F_{K,K'} \in \mathcal{F}_I^{\|}(\mathcal{M})$, then we obtain

$$\|v^{\mathrm{e}}|_K - A_{K,F}(v^{\mathrm{e}})\|_{L^2(F)}^2 \lesssim \|[\![v^{\mathrm{e}}]\!]_F\|_{L^2(F)}^2. \tag{5.49}$$

Furthermore, for $F \in \mathcal{F}_D^{\|}(\mathcal{M})$, we have $A_{K,F}(v^{\mathrm{e}}) = 0$ and thus

$$\|v^{\mathrm{e}}|_K - A_{K,F}(v^{\mathrm{e}})\|_{L^2(F)}^2 = \|[\![v^{\mathrm{e}}]\!]_F\|_{L^2(F)}^2. \tag{5.50}$$

The bounds (5.48), (5.49) and (5.50) imply (5.47). □

For $K \in \mathcal{M}$, we define the polynomial face jump lifting at regular faces

$$\mathcal{L}_K^{\mathrm{f}}(v^{\mathrm{e}}) := \sum_{F \in \mathcal{F}(K)} \mathcal{L}_{K,F}(v^{\mathrm{e}}) \in \mathbb{S}_{\overline{\boldsymbol{p}}_K}(K), \tag{5.51}$$

and introduce $v^{\mathrm{f}} \in \overline{V}_{\sigma,\mathfrak{s}}^{\ell,0}$ by setting

$$v^{\mathrm{f}}|_K := v^{\mathrm{e}}|_K - \mathcal{L}_K^{\mathrm{f}}(v^{\mathrm{e}}) \in \mathbb{S}_{\overline{\boldsymbol{p}}_K}(K), \qquad K \in \mathcal{M}. \tag{5.52}$$

The definition (5.52) only affects the face parts of $v^{\mathrm{e}}|_K$ in (3.15), (3.16), while the other parts of $v^{\mathrm{e}}|_K$ are left unchanged. In particular, the interior part of $v^{\mathrm{f}}|_K$ is equal to that of $v|_K$. By construction, the function v^{f} is conforming over all faces $F \in F_{ID}^{\perp}(\mathcal{M}_\sigma^\ell) \cup \mathcal{F}_D^{\|}(\mathcal{M}_\sigma^\ell)$ and over all regularly matching interior faces $F \in \mathcal{F}_I^{\|}(\mathcal{M}_\sigma^\ell)$. With Lemmas 5.3 and 5.6, there holds

$$\big(v^{\mathrm{f}}|_K\big)|_F = A_{K,F}(v^{\mathrm{e}}), \qquad F \in \mathcal{F}(K), \tag{5.53}$$

$$\big(v^{\mathrm{f}}|_K\big)|_E = (v^{\mathrm{e}}|_K)|_E, \qquad E \in \mathcal{E}(K), \tag{5.54}$$

$$v^{\mathrm{f}}|_K(\boldsymbol{N}) = v^{\mathrm{n}}|_K(\boldsymbol{N}), \qquad \boldsymbol{N} \in \mathcal{N}(K). \tag{5.55}$$

We are now ready to establish Theorem 3.12 in Section 3.4.

Proof of Theorem 3.12. Given $v \in \overline{V}_{\sigma,\mathfrak{s}}^{\ell,0,\perp}$, we define $\mathcal{A}_{\sigma,\mathfrak{s}}^{\ell}(v) := v^{\mathrm{f}}$ with $v^{\mathrm{f}} \in \overline{V}_{\sigma,\mathfrak{s}}^{\ell,0,\perp}$ as introduced above. Clearly, $\mathcal{A}_{\sigma,\mathfrak{s}}^{\ell}$ is linear. By construction, the function v^{f} is conforming over all faces $F \in F_{ID}^{\perp}(\mathcal{M}) \cup \mathcal{F}_D^{\|}(\mathcal{M})$ and over all regularly matching interior faces $F \in \mathcal{F}_I^{\|}(\mathcal{M})$. With Assumption 3.1, this implies items (i), (ii), (iii) in Theorem 3.12. In addition, if $v \in V_{\sigma,\mathfrak{s}}^{\ell,1}$, all liftings constructed in this section are zero, which implies item (iv). Similarly to the proofs of Propositions 5.2 and 5.5, it follows from (5.47) that

$$\Upsilon_{\mathcal{M}}^{\perp}[v^{\mathrm{e}} - v^{\mathrm{f}}]^2 + \mathrm{jmp}_{\mathcal{F}_I^{\|}(\mathcal{M})}[v^{\mathrm{f}}]^2 \;\lesssim\; |\boldsymbol{p}|^4 \,\mathrm{jmp}_{\mathcal{F}_{ID}^{\|}(\mathcal{M})}[v^{\mathrm{e}}]^2.$$

Hence, the triangle inequality and the bounds (5.27), (5.42) yield (3.50) in Theorem 3.12. □

6. Polynomial Jump Lifting Operators

We construct the operators $\mathcal{L}^{\ell}_{\sigma,\mathfrak{s}}$ and prove Theorem 3.14. Throughout this section, we fix $v^{\mathrm{f}} = \mathcal{A}^{\ell}_{\sigma,\mathfrak{s}}(v)$ for $v \in \overline{V}^{\ell,0,\perp}_{\sigma,\mathfrak{s}}$. While conforming across regular faces and over different mesh patches, the approximations v^{f} are generally discontinuous over irregular faces between different mesh layers in the *interior of mesh patches*. By construction of our meshes, it is sufficient to consider *three* types of irregular mesh configurations in the context of reference mesh patches.

6.1. **Anisotropic faces.** Anisotropic irregular faces arise in the generic geometric situation illustrated in Figure 4 along an edge (i.e., in direction of $x^{\|}$). The figure

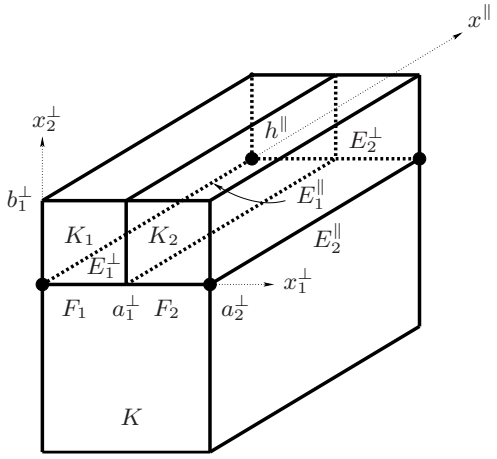

FIGURE 4. Interface between K and K_1, K_2 for $\sigma = 0.5$ and lenght $h^{\|}$. The anisotropic irregular faces F_1, F_2 and the elemental edges $E_1^{\perp}, E_1^{\|}, E_2^{\perp}, E_2^{\|}$ of K are illustrated. The highlighted nodes are regular vertex nodes.

displays the elemental face $F \in \mathcal{F}(K)$ of the outer element K, which is subdivided into *two* irregular faces $F_1 := F_{K_1,K} \in \mathcal{F}(K_1)$ and $F_2 := F_{K_2,K} \in \mathcal{F}(K_2)$, for two refined elements K_1, K_2 in the inner layer. All elements belong to the same mesh patch of the underlying geometric mesh. The elements $\{K, K_1, K_2\}$ and the faces $\{F, F_1, F_2\}$ are possibly *anisotropic*; their edge-parallel lengths are thus denoted by the generic parameter $h^{\|}$. The edge-perpendicular diameters of the elements involved are shape-regular and of size $h_K^{\perp} \simeq h_{K_i}^{\perp} \simeq h^{\perp}$ for $i = 1, 2$, with $h^{\perp} \lesssim h^{\|}$. The precise locations of the elements in edge-perpendicular direction are determined by the parameters $a_1^{\perp}, a_2^{\perp}, b_1^{\perp}, b_2^{\perp}$, whose values only depend on σ. The setting is such that the irregular faces F, F_j satisfy (3.33), (3.34). The configuration shown in Figure 4 is prototypical as it appears along edges in reference edge mesh patches $\widetilde{\mathcal{M}}^{\ell,\boldsymbol{e}}_{\sigma}$ or in the scaled edge-patch blocks $\widetilde{\mathcal{M}}^{\ell,\boldsymbol{ce},\|}_{\sigma}$ introduced in (4.18), (4.19) for reference corner-edge mesh patches $\widetilde{\mathcal{M}}^{\ell,\boldsymbol{ce}}_{\sigma}$. We note that two rotated and superimposed configurations of this type can overlap over one of the smaller elements K_1 or K_2; cf. Figure 1 and [18, Figure 2].

On the face F, we introduce the parallel elemental edges $E_1^{\|}, E_2^{\|} \in \mathcal{E}(K)$ along $x_1^{\perp} = 0$ and $x_1^{\perp} = a_2^{\perp}$; cf. Figure 4. In the reference mesh patches these edges

always appear as regular edges. With (5.4), the nodes highlighted in Figure 4 are then regular vertex nodes. We further denote by $E_1^\perp, E_2^\perp \in \mathcal{E}(K)$ the perpendicular elemental edges of K on $x^\parallel = 0$ and $x^\parallel = h^\parallel$, respectively. Accordingly, we have $\overline{E}_i^\perp = \overline{E}_{i1}^\perp \cup \overline{E}_{i2}^\perp$ for $i = 1, 2$, with $E_{ij}^\perp \in \mathcal{E}(K_j)$ irregular in $\mathcal{E}(\mathcal{M})$. Upon writing $\overline{\boldsymbol{p}}_{K,F} = (\overline{p}_{K,F}^\perp, \overline{p}_{K,F}^\parallel)$ and $\overline{\boldsymbol{p}}_{K_j,F_j} = (\overline{p}_{K_j,F_j}^\perp, \overline{p}_{K_j,F_j}^\parallel)$ as before, the definitions (3.13) and (3.14) imply

$$\overline{p}_{K,E_i^\perp} \le \overline{p}_{K_j,E_{ij}^\perp}, \qquad \overline{p}_{K,F}^\perp \le \overline{p}_{K_j,F_j}^\perp, \qquad \overline{p}_{K,F}^\parallel \le \overline{p}_{K_j,F_j}^\parallel, \qquad 1 \le i,j \le 2. \tag{6.1}$$

Hence, with properties (3.18), (3.19),

$$(v^{\mathrm{f}}|_K)|_{E_{ij}^\perp} \in \mathbb{P}_{\overline{p}_{K_j,E_{ij}^\perp}}(E_{ij}^\perp), \qquad (v^{\mathrm{f}}|_K)|_{F_j} \in \mathbb{Q}_{\overline{\boldsymbol{p}}_{K_j,F_j}}(F_j), \qquad 1 \le i,j \le 2. \tag{6.2}$$

The face approximation v^{f} is generally discontinuous across the irregular face F_j. From (6.2), it further follows that

$$\big([\![v^{\mathrm{f}}]\!]_{F_j}\big)|_{E_{ij}^\perp} \in \mathbb{P}_{\overline{p}_{K_j,E_{ij}^\perp}}(E_{ij}^\perp), \qquad [\![v^{\mathrm{f}}]\!]_{F_j} \in \mathbb{Q}_{\overline{\boldsymbol{p}}_{K_j,F_j}}(F_j). \tag{6.3}$$

We next define the jump $[\![v^{\mathrm{f}}]\!]_F$ over F piecewise as

$$\big([\![v^{\mathrm{f}}]\!]_F\big)|_{F_j} := [\![v^{\mathrm{f}}]\!]_{F_j}, \qquad j = 1, 2. \tag{6.4}$$

Lemma 6.1. *In the configuration of Figure 4, we have $[\![v^{\mathrm{f}}]\!]_F \in C^0(\overline{F})$, as well as $[\![v^{\mathrm{f}}]\!]_F = 0$ on $\overline{E}_1^\parallel$ and on $\overline{E}_2^\parallel$.*

Proof. By Theorem 3.12, the approximation v^{f} is continuous across the regular face f_{K_1,K_2}, which implies $[\![v^{\mathrm{f}}]\!]_F \in C^0(\overline{F})$. Since $E_1^\parallel$ and $E_2^\parallel$ are regular edges, the second assertion follows with (5.54), (5.55). □

To remove non-vanishing jumps of v^{f} over the perpendicular elemental edge $E_1^\perp$ of K, we introduce the polynomial edge jump lifting $\mathcal{L}_{\boldsymbol{e}}^{F,E_1^\perp}(v^{\mathrm{f}})$ by

$$\mathcal{L}_{\boldsymbol{e}}^{F,E_1^\perp}(v^{\mathrm{f}}) := \begin{cases} -[\![v^{\mathrm{f}}]\!]_F(x_1^\perp, 0, 0)(1 - x_2^\perp/b_1^\perp)(1 - x^\parallel/h^\parallel), & \text{on } K_1, K_2, \\ 0, & \text{on } K. \end{cases} \tag{6.5}$$

Due to Lemma 6.1 and (6.3), $\mathcal{L}_{\boldsymbol{e}}^{F,E_1^\perp}(v^{\mathrm{f}}) \in C^0(\overline{K}_1 \cup \overline{K}_2)$ and $\mathcal{L}_{\boldsymbol{e}}^{F,E_1^\perp}(v^{\mathrm{f}})|_{K_j} \in \mathbb{S}_{\overline{\boldsymbol{p}}_{K_j}}(K_j)$ for $j = 1, 2$. The lifting reproduces $-[\![v^{\mathrm{f}}]\!]_F$ on $E_1^\perp$ and vanishes on the planes $x_2^\perp = b_1^\perp$, $x^\parallel = h^\parallel$, as well as on the edges $E_1^\parallel$, $E_2^\parallel$. Moreover, it is zero if $E_1^\perp$ is a Dirichlet boundary edge. A corresponding lifting $\mathcal{L}_{\boldsymbol{e}}^{F,E_2^\perp}(v^{\mathrm{f}})$ can be constructed for the edge $E_2^\perp$. In the geometry of Figure 4, we then introduce the full edge lifting

$$\mathcal{L}_{\boldsymbol{e}}^{F,E}(v^{\mathrm{f}}) := \sum_{i=1}^{2} \mathcal{L}_{\boldsymbol{e}}^{F,E_i^\perp}(v^{\mathrm{f}}). \tag{6.6}$$

Lemma 6.2. *For $j = 1, 2$, there holds*

$$N_{K_j}^\perp[\mathcal{L}_{\boldsymbol{e}}^{F,E}(v^{\mathrm{f}})]^2 \lesssim |\boldsymbol{p}|^6 \mathfrak{h}_{F_j}^{-1} \|[\![v^{\mathrm{f}}]\!]_{F_j}\|_{L^2(F_j)}^2. \tag{6.7}$$

Proof. The proof follows along the lines of Lemma 5.4 by noting that $h_{E_{ij}^\perp} \simeq h_{K_j}^\perp \simeq h^\perp$ for $1 \le i, j \le 2$. Indeed, the definition (6.5) yields

$$\|\mathcal{L}_{\boldsymbol{e}}^{F,E_i^\perp}(v^{\mathrm{f}})\|_{L^2(K_j)}^2 \lesssim h^\perp h^\parallel \|[\![v^{\mathrm{f}}]\!]_{F_j}\|_{L^2(E_{ij}^\perp)}^2. \tag{6.8}$$

Then, the inequality (5.22) applied on $\overline{E}_{ij}^{\perp} \subset \overline{F}_j$ in parallel direction implies

$$\|[\![v^{\mathrm{f}}]\!]_{F_j}\|^2_{L^2(E_{ij}^{\perp})} \lesssim |\boldsymbol{p}|^2 (h^{\parallel})^{-1} \|[\![v^{\mathrm{f}}]\!]_{F_j}\|^2_{L^2(F_j)}. \tag{6.9}$$

Combining these estimates, applying the inverse estimate (5.17) and employing that $h^{\perp} \simeq \mathtt{h}_{F_j}$ give

$$N^{\perp}_{K_j}[\mathcal{L}_{\boldsymbol{e}}^{F,E_i^{\perp}}(v^{\mathrm{f}})]^2 \lesssim |\boldsymbol{p}|^6 \mathtt{h}_{F_j}^{-1} \|[\![v^{\mathrm{f}}]\!]_{F_j}\|^2_{L^2(F_j)}. \tag{6.10}$$

This implies (6.7). □

Next, we introduce the auxiliary function

$$v^{\mathrm{f},F,E} := \begin{cases} v^{\mathrm{f}} - \mathcal{L}_{\boldsymbol{e}}^{F,E}(v^{\mathrm{f}}), & \text{on } K_1, K_2, \\ v^{\mathrm{f}}, & \text{on } K. \end{cases} \tag{6.11}$$

Then, $v^{\mathrm{f},F,E} \in C^0(\overline{K}_1 \cup \overline{K}_2)$ and $v^{\mathrm{f},F,E}|_{K_j} \in \mathbb{S}_{\overline{\boldsymbol{p}}_{K_j}}(K_j)$. With (6.1) and as in Lemma 6.1, we have $[\![v^{\mathrm{f},F,E}]\!]_{F_j} \in \mathbb{Q}_{\overline{\boldsymbol{p}}_{K_j,F_j}}(F_j)$ and $[\![v^{\mathrm{f},F,E}]\!]_F \in C^0(\overline{F})$. Moreover, there holds

$$[\![v^{\mathrm{f},F,E}]\!]_F = 0 \text{ on } E_i^{\perp}, \qquad [\![v^{\mathrm{f},F,E}]\!]_F = 0 \text{ on } E_i^{\parallel}, \qquad i = 1, 2. \tag{6.12}$$

Remark 6.3. The lifting $\mathcal{L}_{\boldsymbol{e}}^{F,E}(v^{\mathrm{f}})$ does not generally vanish on $x^{\parallel} = 0$ and $x^{\parallel} = h^{\parallel}$. However, with Assumption 3.1 the constructions of corresponding liftings in adjacent elements will lead to conformity of $v^{\mathrm{f},F,E}$ across $x^{\parallel} = 0$ and $x^{\parallel} = h^{\parallel}$ in edge-perpendicular direction. This will be detailed in Section 6.3.

Following [18, Section 5.2.1], we introduce the lifting associated with the face F by

$$\mathcal{L}_{\boldsymbol{e}}^{F}(v^{\mathrm{f}}) := \begin{cases} -[\![v^{\mathrm{f},F,E}]\!]_F(x_1^{\perp}, 0, x^{\parallel})(1 - x_2^{\perp}/b_1^{\perp}), & \text{on } K_1, K_2, \\ 0, & \text{on } K, \end{cases} \tag{6.13}$$

with $v^{\mathrm{f},F,E}$ in (6.11). Clearly, $\mathcal{L}_{\boldsymbol{e}}^{F}(v^{\mathrm{f}}) \in C^0(\overline{K}_1 \cup \overline{K}_2)$, $\mathcal{L}_{\boldsymbol{e}}^{F}(v^{\mathrm{f}})|_{K_j} \in \mathbb{S}_{\overline{\boldsymbol{p}}_{K_j}}(K_j)$ for $j = 1, 2$, and $\mathcal{L}_{\boldsymbol{e}}^{F}(v^{\mathrm{f}})|_F = -[\![v^{\mathrm{f},F,E}]\!]_F$. Morever, the lifting $\mathcal{L}_{\boldsymbol{e}}^{F}(v^{\mathrm{f}})$ vanishes on the planes $x_2^{\perp} = b_1^{\perp}$, $x_1^{\perp} = 0$, $x_1^{\perp} = a_2^{\perp}$, and $x^{\parallel} = 0$, $x^{\parallel} = h^{\parallel}$.

Lemma 6.4. *For $j = 1, 2$, there holds*

$$N^{\perp}_{K_j}[\mathcal{L}_{\boldsymbol{e}}^{F}(v^{\mathrm{f}})]^2 \lesssim |\boldsymbol{p}|^{10} \mathtt{h}_{F_j}^{-1} \|[\![v^{\mathrm{f}}]\!]_{F_j}\|^2_{L^2(F_j)}. \tag{6.14}$$

Proof. As in (5.47), we have

$$N^{\perp}_{K_j}[\mathcal{L}_{\boldsymbol{e}}^{F}(v^{\mathrm{f}})]^2 \lesssim |\boldsymbol{p}|^4 \mathtt{h}_{F_j}^{-1} \|[\![v^{\mathrm{f},F,E}]\!]_{F_j}\|^2_{L^2(F_j)}. \tag{6.15}$$

Then, applying the trace inequality (4.28) yields

$$\mathtt{h}_{F_j}^{-1} \|[\![v^{\mathrm{f},F,E}]\!]_{F_j}\|^2_{L^2(F_j)} \lesssim \mathtt{h}_{F_j}^{-1} \|[\![v^{\mathrm{f}}]\!]_{F_j}\|^2_{L^2(F_j)} + N^{\perp}_{K_j}[\mathcal{L}_{\boldsymbol{e}}^{F,E}(v^{\mathrm{f}})]^2.$$

Referring to (6.7) completes the proof. □

To analyze the lifting (6.13), we introduce the piecewise polynomial function

$$v^{\mathrm{f},F} := \begin{cases} v^{\mathrm{f}} - \mathcal{L}_{\boldsymbol{e}}^{F,E}(v^{\mathrm{f}}) - \mathcal{L}_{\boldsymbol{e}}^{F}(v^{\mathrm{f}}), & \text{on } K_1, K_2, \\ v^{\mathrm{f}}, & \text{on } K, \end{cases} \tag{6.16}$$

We have $v^{\mathrm{f},F} \in C^0(\overline{K}_1 \cup \overline{K}_2)$ and $v^{\mathrm{f},F}|_{K_j} \in \mathbb{S}_{\overline{\boldsymbol{p}}_{K_j}}(K_j)$ for $j = 1, 2$.

Lemma 6.5. *The function $v^{\mathrm{f},F}$ in (6.16) is continuous across F.*

Proof. Consider $\boldsymbol{x} \in F_j$ for $j = 1, 2$. Then, with the definitions in (6.6), (6.13),

$$[\![v^{\mathrm{f},F}]\!]_{F_{K_j,K}}(\boldsymbol{x}) = v^{\mathrm{f}}|_{K_j}(\boldsymbol{x}) - v^{\mathrm{f}}|_K(\boldsymbol{x}) + \mathcal{L}_{\boldsymbol{e}}^{F,E}(v^{\mathrm{f}})|_{K_j}(\boldsymbol{x}) - [\![v^{\mathrm{f},F,E}]\!]_F(\boldsymbol{x}),$$

with $v^{\mathrm{f},F,E}$ in (6.11). Since $[\![v^{\mathrm{f},F,E}]\!]_F(\boldsymbol{x}) = [\![v^{\mathrm{f}}]\!]_{F_{K_j,K}}(\boldsymbol{x}) + \mathcal{L}_{\boldsymbol{e}}^{F,E}(v^{\mathrm{f}})|_{K_j}(\boldsymbol{x})$, it follows that $[\![v^{\mathrm{f},F}]\!]_F(\boldsymbol{x}) = [\![v^{\mathrm{f},F}]\!]_{F_{K_j,K}}(\boldsymbol{x}) = 0$. □

6.2. **Isotropic faces.** Isotropic irregular faces appear by subdivision of elemental facesa into *four* or *two* isotropic faces.

6.2.1. *Refinement of one elemental face into four faces.* First, we consider the generic configuration in Figure 5 where the elemental face $F \in \mathcal{F}(K)$ of the outer element K is subdivided into *four* irregular faces $F_j = F_{K_j,K} \in \mathcal{F}(K_j)$, $1 \le j \le 4$, with four elements K_1, K_2, K_3, K_4 in the inner layer. All elements and faces involved are in the same mesh patch and are *isotropic* of mesh size h. The faces F and F_j satisfy (3.33), (3.34). As before, the parameters a_1, a_2, b_1 and c_1, c_2 only depend on σ. We further denote by E_1, E_2, E_3, E_4 the elemental edges of K on $x_2 = 0$; cf. Figure 5. The elemental vertices of K on $x_2 = 0$ always appear as regular vertex nodes in $\mathcal{N}(\mathcal{M})$. This configuration arises in reference corner mesh

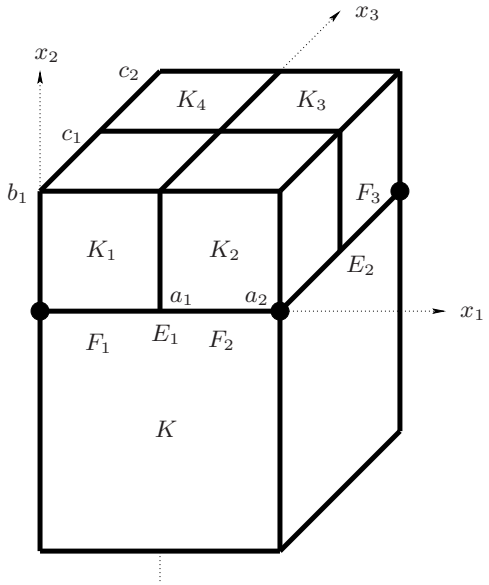

FIGURE 5. Interface between K and K_1, K_2, K_3, K_4 for $\sigma = 0.5$. The isotropic irregular faces F_1, F_2, F_3 and the elemental edges E_1, E_2 of K are indicated. The highlighted nodes are regular vertex nodes.

patches $\widetilde{\mathcal{M}}_\sigma^{\ell,\boldsymbol{c}}$ or in corner-type sub-meshes $\widetilde{\mathcal{M}}_\sigma^{\ell,\boldsymbol{ce},\perp}$ of reference corner-edge mesh patches $\widetilde{\mathcal{M}}_\sigma^{\ell,\boldsymbol{ce}}$ with refinement along one or two edges; cf. Figure 1 and [18, Figures 4, 8 and 10]. Again, two rotated and superimposed configurations of this type can overlap over two of the elements in $\{K_1, K_2, K_3, K_4\}$; cf. Figure 1 and [18, Figure 4].

From (3.14), we see that

$$\overline{p}^1_{K,F} \le \overline{p}^1_{K_j,F_j}, \qquad \overline{p}^2_{K,F} \le \overline{p}^2_{K_j,F_j}, \qquad 1 \le j \le 4. \tag{6.17}$$

Therefore, we have

$$(v^{\mathrm{f}}|_K)|_{F_j} \in \mathbb{Q}_{\overline{\boldsymbol{p}}_{K_j,F_j}}(F_j), \qquad [\![v^{\mathrm{f}}]\!]_{F_j} \in \mathbb{Q}_{\overline{\boldsymbol{p}}_{K_j,F_j}}(F_j), \qquad 1 \le j \le 4. \tag{6.18}$$

As in Section 6.1, we define the jump $[\![v^{\mathrm{f}}]\!]_F$ piecewise as

$$\big([\![v^{\mathrm{f}}]\!]_F\big)|_{F_j} := [\![v^{\mathrm{f}}]\!]_{F_j}, \qquad 1 \le j \le 4. \tag{6.19}$$

Lemma 6.6. *In the configuration of Figure 5, there holds: (i)* $[\![v^{\mathrm{f}}]\!]_F \in C^0(\overline{F})$*; (ii)* $[\![v^{\mathrm{f}}]\!]_F(\boldsymbol{N}_i) = 0$ *at the four elemental vertices* $\boldsymbol{N}_1 = (0,0,0)$*,* $\boldsymbol{N}_2 = (a_2,0,0)$*,* $\boldsymbol{N}_3 = (a_2,0,c_2)$*, and* $\boldsymbol{N}_4 = (0,0,c_2)$*.*

Proof. By Theorem 3.12, the approximation v^{f} in (5.52) is continuous over the regular faces F_{K_1,K_2}, F_{K_2,K_3}, F_{K_3,K_4} and F_{K_1,K_4}. As a consequence, we have $[\![v^{\mathrm{f}}]\!]_F \in C^0(\overline{F})$. Since the elemental vertices $\boldsymbol{N}_i \in \mathcal{N}(K)$ are regular mesh nodes, the second assertion follows from the construction of v^{f} and property (5.55). □

We introduce edge liftings associated with the elemental edges E_1, E_2, E_3, E_4 of K. We focus in detail on edge E_1 on $x_2 = 0$ and $x_3 = 0$ intersecting with F_1, F_2 and K_1, K_2. By writing $\overline{E}_1 = \overline{E}_{11} \cup \overline{E}_{12}$ with $E_{1j} \in \mathcal{E}(K_j)$, $j = 1, 2$, it follows from (3.13) that $\overline{p}_{K,E_1} \le \overline{p}_{K_j,E^{\perp}_{1j}}$. Therefore,

$$(v^{\mathrm{f}}|_K)|_{E_{1j}} \in \mathbb{P}_{\overline{p}_{K_j,E_{1j}}}(E_{1j}), \qquad \big([\![v^{\mathrm{f}}]\!]_{F_j}\big)|_{E_{1j}} \in \mathbb{P}_{\overline{p}_{K_j,E_{1j}}}(E_{1j}), \qquad j = 1, 2. \tag{6.20}$$

We then introduce the polynomial edge jump lifting associated with E_1 by

$$\mathcal{L}^{F,E_1}_{\boldsymbol{c}}(v^{\mathrm{f}}) := \begin{cases} -[\![v^{\mathrm{f}}]\!]_F(x_1,0,0)(1-x_2/b_1)(1-x_3/c_1), & \text{on } K_1, K_2, \\ 0, & \text{on } K_3, K_4. \end{cases} \tag{6.21}$$

From Lemma 6.6 and (6.18), (6.20), $\mathcal{L}^{F,E_1}_{\boldsymbol{c}}(v^{\mathrm{f}}) \in C^0(\cup_{j=1}^4 \overline{K}_j)$ and $\mathcal{L}^{F,E_1}_{\boldsymbol{c}}(v^{\mathrm{f}})|_{K_j} \in \mathbb{S}_{\overline{\boldsymbol{p}}_{K_j}}(K_j)$ for $1 \le j \le 4$. The lifting reproduces $-[\![v^{\mathrm{f}}]\!]_F$ on E_1 and vanishes on the other edges E_2, E_3, E_4; cf. Lemma 6.6. It also vanishes on $x_2 = b_1$ and $x_3 = c_1$. It vanishes identically if E_1 is a Dirichlet boundary edge. Corresponding liftings $\{\mathcal{L}^{F,E_i}_{\boldsymbol{c}}(v^{\mathrm{f}})\}_{i=2}^4$ can again be constructed for the other edges E_2, E_3, E_4. The full edge lifting is thus defined as

$$\mathcal{L}^{F,E}_{\boldsymbol{c}}(v^{\mathrm{f}}) := \sum_{i=1}^{4} \mathcal{L}^{F,E_i}_{\boldsymbol{c}}(v^{\mathrm{f}}). \tag{6.22}$$

Remark 6.7. As will be discussed in Section 6.3, the conformity of $\mathcal{L}^{F,E}_{\boldsymbol{c}}(v^{\mathrm{f}})$ across outer boundaries of $\{K_1, K_2, K_3, K_4\}$ will follow from the constructions of corresponding liftings in adjacent layers of elements; cf. Remark 6.3.

Proceeding as in Lemma 6.2 (with isotropic scaling) immediately yields the stability bound

$$N^{\perp}_{K_j}[\mathcal{L}^{F,E}_{\boldsymbol{c}}(v^{\mathrm{f}})]^2 \lesssim |\boldsymbol{p}|^6 \mathtt{h}^{-1}_{F_j} \|[\![v^{\mathrm{f}}]\!]_{F_j}\|^2_{L^2(F_j)}, \qquad 1 \le j \le 4. \tag{6.23}$$

We next consider the piecewise polynomial function

$$v^{\mathrm{f},F,E} := \begin{cases} v^{\mathrm{f}} - \mathcal{L}^{F,E}_{\boldsymbol{c}}(v^{\mathrm{f}}), & \text{on } K_1, K_2, K_3, K_4, \\ v^{\mathrm{f}}, & \text{on } K. \end{cases} \tag{6.24}$$

Then, $v^{\mathrm{f},F,E} \in C^0(\cup_{j=1}^4 \overline{K}_j)$ and $v^{\mathrm{f},F,E}|_{K_j} \in \mathbb{S}_{\overline{\boldsymbol{p}}_{K_j}}(K_j)$. With (6.17), (6.18) and similarly to Lemma 6.6, we have $[\![v^{\mathrm{f},F,E}]\!]_F \in C^0(\overline{F})$ and $[\![v^{\mathrm{f},F,E}]\!]_{F_j} \in \mathbb{Q}_{\overline{\boldsymbol{p}}_{K_j,F_j}}(F_j)$. Moreover, the analog of property (6.12) holds:

$$[\![v^{\mathrm{f},F,E}]\!]_F = 0 \text{ on } E_i, \qquad 1 \le i \le 4. \tag{6.25}$$

As in [18, Section 5.3.1], we then introduce the lifting over the face F by

$$\mathcal{L}_{\boldsymbol{c}}^F(v^{\mathrm{f}}) := \begin{cases} -[\![v^{\mathrm{f},F,E}]\!]_F(x_1,0,x_3)(1-x_2/b_1), & \text{on } K_1,K_2,K_3,K_4, \\ 0, & \text{on } K, \end{cases} \tag{6.26}$$

with $v^{\mathrm{f},F,E}$ in (6.24). Then, $\mathcal{L}_{\boldsymbol{c}}^F(v^{\mathrm{f}}) \in C^0(\cup_{j=1}^4 \overline{K}_j)$ and $\mathcal{L}_{\boldsymbol{c}}^F(v^{\mathrm{f}})|_{K_j} \in \mathbb{S}_{\overline{\boldsymbol{p}}_{K_j}}(K_j)$, $1 \le j \le 4$. By (6.25), the lifting $\mathcal{L}_{\boldsymbol{c}}^F(v^{\mathrm{f}})$ vanishes on $x_2 = b_1$ and over the sets $E_i \times (0,c_1)$, $1 \le i \le 4$. Proceeding as in the proof of (6.14) in combination with isotropic scaling, we obtain

$$N_{K_j}^{\perp}[\mathcal{L}_{\boldsymbol{c}}^F(v^{\mathrm{f}})]^2 \lesssim |\boldsymbol{p}|^{10}\mathtt{h}_{F_j}^{-1}\|[\![v^{\mathrm{f}}]\!]_{F_j}\|_{L^2(F_j)}^2, \qquad 1 \le j \le 4. \tag{6.27}$$

Analogously to (6.16), we introduce

$$v^{\mathrm{f},F} := \begin{cases} v^{\mathrm{f}} - \mathcal{L}_{\boldsymbol{c}}^{F,E}(v^{\mathrm{f}}) - \mathcal{L}_{\boldsymbol{c}}^F(v^{\mathrm{f}}), & \text{on } K_1,K_2,K_3,K_4, \\ v^{\mathrm{f}}, & \text{on } K, \end{cases} \tag{6.28}$$

We have $v^{\mathrm{f},F} \in C^0(\cup_{j=1}^4 \overline{K}_j)$ and $v^{\mathrm{f},F}|_{K_j} \in \mathbb{S}_{\overline{\boldsymbol{p}}_{K_j}}(K_j)$ for $1 \le j \le 4$.

The following variant of Lemma 6.5 holds true.

Lemma 6.8. *The approximation $v^{\mathrm{f},F}$ in* (6.28) *is continuous across F.*

6.2.2. *Refinement of two elemental faces into two faces.* Second, we consider the isotropic configuration in Figure 6. It involves an element K where *two adjacent elemental faces* $F, F' \in \mathcal{F}(K)$ are subdivided by using isotropic versions of the irregular refinement in Figure 4, thereby yielding the elements K_1, K_2 and K_1', K_2'. As in Section 6.1, we then introduce the irregular faces $F_j := F_{K_j,K} \in \mathcal{F}(K_j)$ and $F_j' := F_{K_j',K} \in \mathcal{F}(K_j')$ for $j = 1,2$. Then, $\overline{F} = \overline{F}_1 \cup \overline{F}_2$ and $\overline{F}' = \overline{F}_1' \cup \overline{F}_2'$. In Figure 6, we further illustrate the elements K_1^D, K_2^D and we consider the elemental edge $E \in \mathcal{E}(K)$ given by

$$E := \{\, (x_1,0,0) \,:\, 0 < x_1 < a_1 \,\}. \tag{6.29}$$

All elements are situated in the same mesh patch. This geometry only arises in diagonal elements of corner-edge mesh patches *with simultaneous refinement along two or three edges* $\boldsymbol{e}_i$, with K, K_1^D and K_2^D corresponding to diagonal elements; cf. Figure 3.

With (6.4) and the properties of v^{f}, we have $[\![v^{\mathrm{f}}]\!]_F = [\![v^{\mathrm{f}}]\!]_{F'}$ on $\overline{E}$. However, the edge liftings $\mathcal{L}_{\boldsymbol{e}}^{F,E}(v^{\mathrm{f}})$ over $\mathfrak{d}_{\boldsymbol{e}}^F := \{K, K_1, K_2\}$ associated with F as in (6.5) and $\mathcal{L}_{\boldsymbol{e}}^{F',E}(v^{\mathrm{f}})$ over $\mathfrak{d}_{\boldsymbol{e}}^{F'} =: \{K, K_1', K_2'\}$ associated with F' are *not necessarily* continuous across the regular faces F_{K_j,K_j^D} and F_{K_j',K_j^D} for $j = 1,2$. To correct for this, we introduce on $\{K_1^D, K_2^D\}$ the *diagonal edge lifting*

$$\mathcal{L}_D(v^{\mathrm{f}}) := -[\![v^{\mathrm{f}}]\!]_F(x_1,0,0)(1-x_2/b_1)(1-x_3/c_1), \qquad \text{on } K_1^D, K_2^D. \tag{6.30}$$

Since $[\![v^{\mathrm{f}}]\!]_F(\boldsymbol{N}) = 0$ for $\boldsymbol{N} = (0,0,0)$ and $\boldsymbol{N} = (a_1,0,0)$, see Lemma 6.1, this lifting vanishes on $\partial K_1^D \cap \{x_1 = 0\}$ and $\partial K_2^D \cap \{x_1 = a_1\}$, implying that it does not affect values ofv^{f} outside the configuration in Figure 6. We also have $\mathcal{L}_D(v^{\mathrm{f}}) \in$

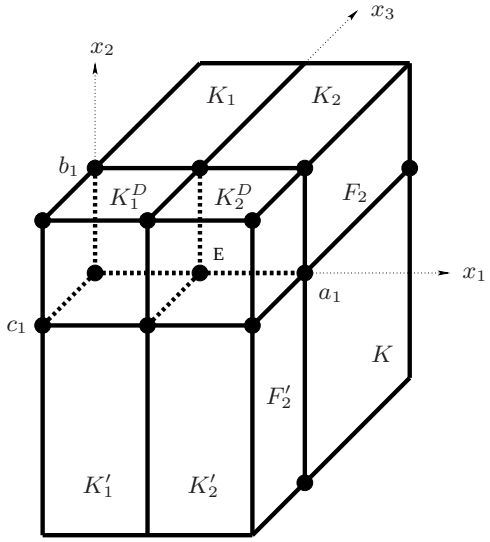

FIGURE 6. Two elemental faces $F, F' \in \mathcal{F}(K)$ are irregularly subdivided as in Figure 4. The elements $K_1, K_2, K_1', K_2', K_1^D, K_2^D$, the irregular faces F_2, F_2' and the elemental edge $E \in \mathcal{E}(K)$ are illustrated. The highlighted nodes are regular vertex nodes.

$C^0(\overline{K}_1^D, \overline{K}_2^D)$ and $\mathcal{L}_D(v^{\mathrm{f}})|_{K_j^D} \in \mathbb{S}_{\overline{\boldsymbol{p}}_{K_j^D}}(K_j^D)$ for $j = 1, 2$. As in (6.23), the following stability bound holds:

$$N_{K_j^D}^{\perp}[\mathcal{L}_D(v^{\mathrm{f}})]^2 \lesssim |\boldsymbol{p}|^6 \mathtt{h}_{F_j} \|[\![v^{\mathrm{f}}]\!]\|_{L^2(F_j)}^2, \qquad j = 1, 2. \tag{6.31}$$

Similarly to (6.11) and in the geometry of Figure 6, we then introduce the auxiliary function

$$v^{\mathrm{f},D} := \begin{cases} v^{\mathrm{f}} - \mathcal{L}_{\boldsymbol{e}}^{F,E}(v^{\mathrm{f}}), & \text{on } K_1, K_2, \\ v^{\mathrm{f}} - \mathcal{L}_{\boldsymbol{e}}^{F',E}(v^{\mathrm{f}}), & \text{on } K_1', K_2', \\ v^{\mathrm{f}} - \mathcal{L}_D(v^{\mathrm{f}}), & \text{on } K_1^D, K_2^D, \\ v^{\mathrm{f}}, & \text{on } K. \end{cases} \tag{6.32}$$

We have $v^{\mathrm{f},D}|_K \in \mathbb{S}_{\overline{\boldsymbol{p}}_K}(K)$ for $K \in \{K_1, K_2, K_1', K_2', K_1^D, K_2^D\}$. Then, since the faces F_{K_i, K_i^D} and F_{K_i', K_i^D} are regularly matching for $i = 1, 2$, the function v^{f} is conforming over these two faces due to Theorem 3.12. Moreover, from the definition of the liftings it follows that

$$v^{\mathrm{f},D} \in C^0(\overline{K}_1 \cup \overline{K}_2 \cup \overline{K}_1' \cup \overline{K}_2' \cup \overline{K}_1^D \cup \overline{K}_2^D). \tag{6.33}$$

6.3. **Superposition.** In this section, we superimpose the constructions in Sections 6.1 and 6.2. Upon mapping employing the patch maps $G_{\mathfrak{p}}$, it is sufficient to consider the geometric reference mesh patches. For $\widetilde{\mathcal{M}} \in \{\widetilde{\mathcal{M}}_\sigma^{\ell,\mathfrak{t}}\}_{\mathfrak{t} \in \{\boldsymbol{c},\boldsymbol{e},\boldsymbol{ce},\mathrm{int}\}}$, we denote by $\mathfrak{F}_{\boldsymbol{e}}(\widetilde{\mathcal{M}})$ and $\mathfrak{F}_{\boldsymbol{c}}(\widetilde{\mathcal{M}})$ the sets of all *macro-faces* F appearing as in Figures 4 and 5, respectively. We denote by $\mathfrak{d}_{\boldsymbol{e}}^F = \{K, K_1, K_2\}$ respectively $\mathfrak{d}_{\boldsymbol{c}}^F = \{K, K_1, \ldots, K_4\}$ the sets of elements associated with these configurations. The geometry in Figure 6 involves two isotropic versions of the configuration shown in

Figure 4. We then denote by $\mathfrak{D}(\widetilde{\mathcal{M}})$ the set of all pairs $D = \{K_1^D, K_2^D\}$ of elements appearing on the diagonal as in Figure 6.

Let $\mathcal{M}_\mathfrak{p} = G_\mathfrak{p}(\widetilde{\mathcal{M}})$ be a mesh patch and let $\widetilde{\mathcal{M}} \in \{\widetilde{\mathcal{M}}_\sigma^{\ell,\mathrm{t}}\}_{\mathrm{t}\in\{\boldsymbol{c},\boldsymbol{e},\boldsymbol{ce},\mathrm{int}\}}$ be the corresponding geometric reference mesh patch. The averaged approximations $v^\mathrm{f}|_{\mathcal{M}_\mathfrak{p}}$ in Theorem 3.12 restricted to the patch $\mathcal{M}_\mathfrak{p}$ can be pulled back to the reference patch $\widetilde{\mathcal{M}}$ and will be denoted by $\widetilde{v}^\mathrm{f}|_{\widetilde{\mathcal{M}}}$. We define $\widetilde{v}^\mathrm{c}|_{\widetilde{\mathcal{M}}}$ as:

$$\begin{aligned}\widetilde{v}^\mathrm{c}|_{\widetilde{\mathcal{M}}} := \widetilde{v}^\mathrm{f}|_{\widetilde{\mathcal{M}}} &- \sum_{F\in\mathfrak{F}_{\boldsymbol{e}}(\widetilde{\mathcal{M}})} \big(\mathcal{L}_{\boldsymbol{e}}^{F,E}(\widetilde{v}^\mathrm{f}) + \mathcal{L}_{\boldsymbol{e}}^{F}(\widetilde{v}^\mathrm{f})\big)\\ &- \sum_{F\in\mathfrak{F}_{\boldsymbol{c}}(\widetilde{\mathcal{M}})} \big(\mathcal{L}_{\boldsymbol{c}}^{F,E}(\widetilde{v}^\mathrm{f}) + \mathcal{L}_{\boldsymbol{c}}^{F}(\widetilde{v}^\mathrm{f})\big) - \sum_{D\in\mathfrak{D}(\widetilde{\mathcal{M}})} \mathcal{L}_D(\widetilde{v}^\mathrm{f}).\end{aligned} \tag{6.34}$$

Here, $\mathcal{L}_{\boldsymbol{e}}^{F,E}(\widetilde{v}^\mathrm{f})$ and $\mathcal{L}_{\boldsymbol{e}}^{F}(\widetilde{v}^\mathrm{f})$ are the liftings in (6.5), (6.6) and (6.13) associated with the face F and the elements in $\mathfrak{d}_{\boldsymbol{e}}^F$. The liftings $\mathcal{L}_{\boldsymbol{c}}^{F,E}(\widetilde{v}^\mathrm{f})$ and $\mathcal{L}_{\boldsymbol{c}}^{F}(\widetilde{v}^\mathrm{f})$ are given in (6.21), (6.22) and (6.26) with respect to the set $\mathfrak{d}_{\boldsymbol{c}}^F$. Finally, $\mathcal{L}_D(\widetilde{v}^\mathrm{f})$ are liftings as in (6.30) over the elements $D = \{K_1^D, K_2^D\}$ in Figure 6.

Remark 6.9. The liftings $\mathcal{L}_{\boldsymbol{e}}^{F}(\widetilde{v}^\mathrm{f})$, $\mathcal{L}_{\boldsymbol{c}}^{F}(\widetilde{v}^\mathrm{f})$ and $\mathcal{L}_D(\widetilde{v}^\mathrm{f})$ in (6.34) are locally supported and vanish at the patch interfaces of $\widetilde{\mathcal{M}}$. Hence, they are not relevant for inter-patch continuity.

For each patch $\mathcal{M}_\mathfrak{p}$, we then set $v^\mathrm{c}|_{\mathcal{M}_\mathfrak{p}} = \widetilde{v}^\mathrm{c}|_{\widetilde{\mathcal{M}}} \circ G_\mathfrak{p}^{-1}|_{Q_\mathfrak{p}}$, which gives rise to a finite element function $v^\mathrm{c} \in \overline{V}_{\sigma,\mathfrak{s}}^{\ell,0}$. The approximation v^c belongs in fact to the conforming space $V_{\sigma,\mathfrak{s}}^{\ell,1}$, as we show in two steps.

Lemma 6.10. *The approximation v^c is continuous over regular faces in the interior of each mesh patch, vanishes on all Dirichlet boundary faces, and is continuous across adjacent mesh patches.*

Proof. If $F = F_{K,K}$ is a regular interior face within a mesh patch, then v^f is conforming across F by Theorem 3.12. As definition (6.34) (and mapping) does not alter v^f on K, K', then v^c is also continuous over F. Since $\widetilde{v}^\mathrm{f}$ and the liftings in (6.34) vanish on faces corresponding to Dirichlet boundary faces, it also follows that v^c vanishes on Dirichlet boundary faces. The approximation v^f is conforming across adjacent mesh patches; see Theorem 3.12. It follows similarly from Assumption 3.1 and the properties of v^f that mapped versions of the the edge liftings $\mathcal{L}_{\boldsymbol{e}}^{F,E}(\widetilde{v}^\mathrm{f})$ and $\mathcal{L}_{\boldsymbol{c}}^{F,E}(\widetilde{v}^\mathrm{f})$ in (6.34) yield conforming approximations over the corresponding mesh layers across two matching irregular configurations of different mesh patches. With Remark 6.9, this implies inter-patch continuity. □

We next establish the inner-patch continuity of v^c over irregular faces mesh patches.

Lemma 6.11. *On each mesh patch $\mathcal{M}_\mathfrak{p}$, the approximation $v^\mathrm{c}|_{\mathcal{M}_\mathfrak{p}}$ is continuous across irregular faces within $\mathcal{M}_\mathfrak{p}$.*

Proof. Since $\mathcal{M}_\mathfrak{p} = G_\mathfrak{p}(\widetilde{\mathcal{M}})$ for $\widetilde{\mathcal{M}} \in \{\widetilde{\mathcal{M}}_\sigma^{\ell,\mathrm{t}}\}_{\mathrm{t}\in\{\boldsymbol{c},\boldsymbol{e},\boldsymbol{ce},\mathrm{int}\}}$, upon mapping it is sufficient to verify separately the continuity of $\widetilde{v}^\mathrm{c}$ in (6.34) for each reference mesh patch type.

Interior patches: For $\widetilde{\mathcal{M}} = \widetilde{\mathcal{M}}_\sigma^{\ell,\mathrm{int}}$, we have $\mathfrak{F}_{\boldsymbol{e}}(\widetilde{\mathcal{M}}) = \mathfrak{F}_{\boldsymbol{c}}(\widetilde{\mathcal{M}}) = \mathfrak{D}(\widetilde{\mathcal{M}}) = \emptyset$ in (6.34). Hence, $\widetilde{v}^\mathrm{c}|_{\widetilde{\mathcal{M}}} = \widetilde{v}^\mathrm{f}|_{\widetilde{\mathcal{M}}}$ and the inner-patch continuity follows immediately from Theorem 3.12.

Edge patches: For $\widetilde{\mathcal{M}} = \widetilde{\mathcal{M}}_\sigma^{\ell,\boldsymbol{e}}$, we have $\mathfrak{F}_{\boldsymbol{c}}(\widetilde{\mathcal{M}}) = \mathfrak{D}(\widetilde{\mathcal{M}}) = \emptyset$, and the definition (6.34) involves two rotated and overlapping versions of the anisotropic configurations in Figure 4 in each mesh layer, cf. [18, Figure 2]. This corresponds to (a slight modification of) the construction in [18, Section 5.2.1]. Let then F be an irregular face F in the patch. By the properties of the liftings $\mathcal{L}_{\boldsymbol{e}}^{F,E}(\widetilde{v}^{\mathrm{f}})$ and $\mathcal{L}_{\boldsymbol{e}}^{F}(\widetilde{v}^{\mathrm{f}})$, the jump $[\![\widetilde{v}^{\mathrm{c}}]\!]_F$ coincides with $[\![\widetilde{v}^{\mathrm{f},F}]\!]_F$, where $\widetilde{v}^{\mathrm{f},F}$ is defined in (6.16) over the elements $\mathfrak{d}_{\boldsymbol{e}}^F$ associated with F. Then Lemma 6.5 ensures the conformity across the irregular face F.

Corner patches: For $\widetilde{\mathcal{M}} = \widetilde{\mathcal{M}}_\sigma^{\ell,\boldsymbol{c}}$, we have $\mathfrak{F}_{\boldsymbol{e}}(\widetilde{\mathcal{M}}) = \mathfrak{D}(\widetilde{\mathcal{M}}) = \emptyset$ in (6.34). The definition (6.34) yields three rotated and superimposed versions of the geometry in Figure 5 in each mesh layer, exactly as in [18, Section 5.3.1 and Figure 4]. If F is an irregular face in the patch, then $[\![\widetilde{v}^{\mathrm{c}}]\!]_F$ is equal to $[\![\widetilde{v}^{\mathrm{f},F}]\!]_F$, where $\widetilde{v}^{\mathrm{f},F}$ is now defined in (6.28) in terms of liftings $\mathcal{L}_{\boldsymbol{c}}^{F,E}(\widetilde{v}^{\mathrm{f}})$ and $\mathcal{L}_{\boldsymbol{c}}^{F}(\widetilde{v}^{\mathrm{f}})$ over the elements $\mathfrak{d}_{\boldsymbol{c}}^F$ associated with F. Lemma 6.8 yields conformity across F.

Corner-edge patches with refinement along one edge: Note that $\mathfrak{D}(\widetilde{\mathcal{M}}) = \emptyset$ in (6.34). We then use the representation (4.18)–(4.21) in Figure 2. In each edge-patch block $\widetilde{\Psi}^{\ell',\boldsymbol{ce}}(\widetilde{\mathcal{M}}_\sigma^{\ell',\boldsymbol{e}})$, the definition (6.34) activates the edge-patch liftings $\mathcal{L}_{\boldsymbol{e}}^{F,E}(\widetilde{v}^{\mathrm{f}})$ and $\mathcal{L}_{\boldsymbol{e}}^{F}(\widetilde{v}^{\mathrm{f}})$ as above; thereby ensuring conformity across irregular faces F within each of these blocks due to Lemma 6.5. In edge-perpendicular direction, the isotropic mesh $\widetilde{\mathfrak{O}}_\sigma^{\ell,\boldsymbol{ce},\perp} \,\dot\cup\, \widetilde{\mathcal{D}}_\sigma^{\ell,\boldsymbol{ce}}$ consists of two sequences of $\ell-1$ irregular and overlapping configurations as in Figure 5, with the smallest configuration extending into the corner mesh $\widetilde{\mathfrak{T}}_\sigma^{\ell,\boldsymbol{c}}$; see Figure 2. The approximation $\widetilde{v}^{\mathrm{c}}$ in (6.34) then involves the corner-patch liftings $\mathcal{L}_{\boldsymbol{c}}^{F,E}(\widetilde{v}^{\mathrm{f}})$ and $\mathcal{L}_{\boldsymbol{c}}^{F}(\widetilde{v}^{\mathrm{f}})$, which enforce the continuity across irregular faces in $\widetilde{\mathfrak{O}}_\sigma^{\ell,\boldsymbol{ce},\perp} \,\dot\cup\, \widetilde{\mathcal{D}}_\sigma^{\boldsymbol{ce}}$ and from $\widetilde{\mathfrak{O}}_\sigma^{\ell,\boldsymbol{ce},\perp}$ into $\widetilde{\mathfrak{T}}_\sigma^{\ell,\boldsymbol{c}}$; cf. Lemma 6.8. The edge-jump liftings $\mathcal{L}_{\boldsymbol{e}}^{F,E}(\widetilde{v}^{\mathrm{f}})$ and $\mathcal{L}_{\boldsymbol{c}}^{F,E}(\widetilde{v}^{\mathrm{f}})$ give conforming approximations across faces of diagonal elements into the corresponding elements of $\widetilde{\mathcal{M}}_\sigma^{\ell,\boldsymbol{ce},\parallel}$ (e.g., across the regular faces $f_{K_4',K_4''}$ and $f_{K_6',K_6''}$ in Figure 2 (right)). Similarly, they yield continuous approximations from corner elements in $\widetilde{\mathfrak{T}}_\sigma^{\ell,\boldsymbol{c}}$ into elements in $\Psi^{2,\boldsymbol{ce}}(\widetilde{\mathcal{M}}_\sigma^{2,\boldsymbol{e}})$.

Corner-edge patches with refinement along two edges: We now have $\mathfrak{D}(\widetilde{\mathcal{M}}) \neq \emptyset$, as the refinements towards two edges introduces the geometric situation analyzed in Figure 6 over the diagonal elements in $\widetilde{\mathcal{D}}_\sigma^{\ell,\boldsymbol{ce}_1} \cap \widetilde{\mathcal{D}}_\sigma^{\ell,\boldsymbol{ce}_2}$ (e.g., over K_6, K_6' in Figure 3 (left)). We use the decomposition (4.23), (4.24). In the submeshes $\widetilde{\mathcal{M}}_\sigma^{\ell,\boldsymbol{ce}_1,\parallel}$ and $\widetilde{\mathcal{M}}_\sigma^{\ell,\boldsymbol{ce}_2,\parallel}$, again the liftings $\mathcal{L}_{\boldsymbol{e}}^{F,E}(\widetilde{v}^{\mathrm{f}})$ and $\mathcal{L}_{\boldsymbol{e}}^{F}(\widetilde{v}^{\mathrm{f}})$ are activated and ensure the continuity over edge-parallel anisotropic faces. Similarly, the liftings $\mathcal{L}_{\boldsymbol{c}}^{F,E}(\widetilde{v}^{\mathrm{f}})$ and $\mathcal{L}_{\boldsymbol{c}}^{F}(\widetilde{v}^{\mathrm{f}})$ yield continuity across the irregular faces in $\widetilde{\mathfrak{O}}_\sigma^{\ell,\boldsymbol{ce},\perp} \,\dot\cup\, (\widetilde{\mathcal{D}}_\sigma^{\ell,\boldsymbol{ce}_1} \cup \widetilde{\mathcal{D}}_\sigma^{\ell,\boldsymbol{ce}_2})$ in perpendicular direction and from $\widetilde{\mathfrak{O}}_\sigma^{\ell,\boldsymbol{ce},\perp}$ into the corner elements in $\widetilde{\mathfrak{T}}_\sigma^{\ell,\boldsymbol{c}}$. In addition to $\mathcal{L}_{\boldsymbol{e}}^{F,E}(\widetilde{v}^{\mathrm{f}})$, the liftings $\mathcal{L}_D(\widetilde{v}^{\mathrm{f}})$ in (6.30) are invoked in (6.34), as, e.g., from K_6 into $D = \{K_3', K_6'\}$ in Figure 3 (left). In the configuration nearest to $\boldsymbol{c}$, these liftings extend into two corner elements of $\widetilde{\mathfrak{T}}_\sigma^{\ell,\boldsymbol{c}}$. With (6.33), this procedure ensures continuity over diagonal elements along the edges. In perpendicular direction, the edge-jump liftings $\mathcal{L}_{\boldsymbol{e}}^{F,E}(\widetilde{v}^{\mathrm{f}})$ and $\mathcal{L}_{\boldsymbol{c}}^{F,E}(\widetilde{v}^{\mathrm{f}})$ give conforming approximations across faces of diagonal elements into the corresponding elements in the edge-patch blocks (e.g., across the regular faces $F_{K_1',K_1''}$ or $F_{K_4',K_4''}$ in Figure 3 (left)), as well as from $\widetilde{\mathfrak{T}}_\sigma^{\ell,\boldsymbol{c}}$ into elements in $\Psi^{2,\boldsymbol{ce}_i}(\widetilde{\mathcal{M}}_\sigma^{2,\boldsymbol{e}_i})$ for $i = 1, 2$.

Corner-edge patches with refinement along three edges: Clearly, $\mathfrak{D}(\widetilde{\mathcal{M}}) \neq \emptyset$, and with (4.26), the geometric situation in Figure 6 now appears along three edges situated on the diagonal elements in $\widetilde{\mathcal{D}}_\sigma^{\ell,\boldsymbol{ce}_1} \cap \widetilde{\mathcal{D}}_\sigma^{\ell,\boldsymbol{ce}_2}$, $\widetilde{\mathcal{D}}_\sigma^{\ell,\boldsymbol{ce}_2} \cap \widetilde{\mathcal{D}}_\sigma^{\ell,\boldsymbol{ce}_3}$, and $\widetilde{\mathcal{D}}_\sigma^{\ell,\boldsymbol{ce}_1} \cap \widetilde{\mathcal{D}}_\sigma^{\ell,\boldsymbol{ce}_3}$ (e.g., over K_1, K_1', K_4, K_4' and K_6, K_6' in Figure 3 (right)). Irregular faces as in Figure 5 are not present in this case (i.e., $\mathfrak{F}_{\boldsymbol{c}}(\widetilde{\mathcal{M}}) = \emptyset$). Hence, in (6.34) the liftings $\mathcal{L}_{\boldsymbol{e}}^{F,E}(\widetilde{v}^{\mathrm{f}})$, $\mathcal{L}_{\boldsymbol{e}}^{F}(\widetilde{v}^{\mathrm{f}})$ and $\mathcal{L}_D(\widetilde{v}^{\mathrm{f}})$ in (6.30) are activated. As before, the liftings $\mathcal{L}_D(\widetilde{v}^{\mathrm{f}})$ extend into the corner elements in $\widetilde{\mathfrak{T}}_\sigma^{\ell,\boldsymbol{c}}$ in the geometry closest to $\boldsymbol{c}$. Property (6.33) then ensures the continuity over diagonal elements and into $\widetilde{\mathfrak{T}}_\sigma^{\ell,\boldsymbol{c}}$. □

We now complete the proof of Theorem 3.14 in Section 3.4.

Proof of Theorem 3.14. We set $\mathcal{L}_{\sigma,\mathfrak{s}}^\ell(v^{\mathrm{f}}) := v^{\mathrm{c}}$. By construction, $\mathcal{L}_{\sigma,\mathfrak{s}}^\ell$ is linear and reproduces functions in $V_{\sigma,\mathfrak{s}}^{\ell,1}$. Lemmas 6.11 and 6.10 imply $v^{\mathrm{c}} \in V_{\sigma,\mathfrak{s}}^{\ell,1}$. From (6.34) and the properties of the liftings, we further find that

$$\begin{aligned}\Upsilon_{\widetilde{\mathcal{M}}}^\perp[\widetilde{v}^{\mathrm{f}} - \widetilde{v}^{\mathrm{c}}]^2 \lesssim & \sum_{F\in\mathfrak{F}_{\boldsymbol{e}}(\widetilde{\mathcal{M}})} \big(\Upsilon_{\mathfrak{d}_{\boldsymbol{e}}^F}^\perp[\mathcal{L}_{\boldsymbol{e}}^{E,F}(\widetilde{v}^{\mathrm{f}})]^2 + \Upsilon_{\mathfrak{d}_{\boldsymbol{e}}^F}^\perp[\mathcal{L}_{\boldsymbol{e}}^{F}\widetilde{v}^{\mathrm{f}})]^2\big) \\ & + \sum_{F\in\mathfrak{F}_{\boldsymbol{c}}(\widetilde{\mathcal{M}})} \big(\Upsilon_{\mathfrak{d}_{\boldsymbol{c}}^F}^\perp[\mathcal{L}_{\boldsymbol{c}}^{E,F}(\widetilde{v}^{\mathrm{f}})]^2 + \Upsilon_{\mathfrak{d}_{\boldsymbol{c}}^F}^\perp[\mathcal{L}_{\boldsymbol{c}}^{F}(\widetilde{v}^{\mathrm{f}})]^2\big) + \sum_{D\in\mathfrak{D}(\widetilde{\mathcal{M}})} \Upsilon_D^\perp[\mathcal{L}_D(\widetilde{v}^{\mathrm{f}})]^2,\end{aligned}$$

for any geometric reference mesh patch $\widetilde{\mathcal{M}}$. The stability estimates (6.7), (6.14) for $\mathcal{L}_{\boldsymbol{e}}^{E,F}(\widetilde{v}^{\mathrm{f}})$ and $\mathcal{L}_{\boldsymbol{e}}^{F}(\widetilde{v}^{\mathrm{f}})$, the estimates (6.23), (6.27) for $\mathcal{L}_{\boldsymbol{c}}^{F,E}(\widetilde{v}^{\mathrm{f}})$ and $\mathcal{L}_{\boldsymbol{c}}^{F}(\widetilde{v}^{\mathrm{f}})$, and the bound (6.31) for $\mathcal{L}_D(\widetilde{v}^{\mathrm{f}})$ yield

$$\Upsilon_{\widetilde{\mathcal{M}}}^\perp[\widetilde{v}^{\mathrm{f}} - \widetilde{v}^{\mathrm{c}}]^2 \lesssim |\boldsymbol{p}|^{10}\mathrm{jmp}_{\mathcal{F}_I^\parallel(\widetilde{\mathcal{M}})}[\widetilde{v}^{\mathrm{f}}]^2, \tag{6.35}$$

where $\mathcal{F}_I^\parallel(\widetilde{\mathcal{M}})$ denotes the interior faces on $\widetilde{\mathcal{M}}$ which satisfy (3.33), (3.34). After mapping to the physical patches and summing over all patches, this implies the bound (3.51). □

7. Conclusions

We established the H^1-norm exponential convergence rate $\exp(-b\sqrt[5]{N})$ of conforming *hp*-FEMs in axiparallel polyhedral domains $\Omega \subset \mathbb{R}^3$. The FE spaces are based on σ-geometric mesh families $\mathfrak{M}_\sigma$ of hexahedral elements containing, in general, irregular faces and edges. Geometric meshes $\mathcal{M} \in \mathfrak{M}_\sigma$ are obtained as finite unions of *four types* $\mathfrak{t} \in \{\boldsymbol{c}, \boldsymbol{e}, \boldsymbol{ce}, \mathrm{int}\}$ *of* σ*-geometric reference geometric patch meshes* $\widetilde{\mathcal{M}}_\sigma^{\ell,\mathfrak{t}}$. On the geometric reference mesh patches $\widetilde{\mathcal{M}}_\sigma^{\ell,\mathfrak{t}}$ on $\widetilde{Q}$, the *hp*-version FE spaces allow for anisotropic elemental polynomial degree distributions with $\mathfrak{s}$-linear growth in terms of the logarithmic element distance to the singularity set $\mathcal{S}$ of $\widetilde{Q}$ (for patch types $\mathfrak{t} \in \{\boldsymbol{c}, \boldsymbol{e}, \boldsymbol{ce}\}$). General subdivision ratios $0 < \sigma < 1$ and slope parameters $\mathfrak{s} > 0$ are admitted (the analysis extends in a straightforward fashion also to *directional slope parameters* $\mathfrak{s}^\parallel$ *and* $\mathfrak{s}^\perp$). Inter-patch mesh compatibility is ensured by a compatibility requirement on the patch maps, and inter-element continuity is ensured by a minimum degree rule on the local polynomial spaces.

Our principal technical contribution are the constructions of *hp*-version quasi-interpolation projectors. The projectors can be assembled from *four types of reference patch projectors* $\widetilde{\Pi}_{\sigma,\mathfrak{s}}^{\ell,1,\mathfrak{t}}$ which are well-defined on $H^1(\widetilde{Q})$ and exponentially consistent in the H^1-norm for functions $\widetilde{u}$ belonging to an analytic reference class

$B_{\mathfrak{t}}(\widetilde{Q})$, with weighting towards corners and edges of $\widetilde{Q}$ according to the patch type $\mathfrak{t} \in \{\boldsymbol{c}, \boldsymbol{e}, \boldsymbol{ce}, \mathrm{int}\}$. Analogous L^2-norm error bounds for L^2-projections for the approximation of solutions in $B_{-\boldsymbol{b}}(\Omega; \emptyset, \emptyset)$ are also obtained.

We considered the particular, second-order model elliptic problem (1.1)–(1.3) for which analytic regularity was established in [5]. The presently proved exponential convergence rate estimates are, however, independent of the particular PDE and apply to any elliptic problem which admits an analytic regularity shift in the classes $B_{-1-\boldsymbol{b}}(\Omega; \mathcal{C}', \mathcal{E}')$ in Definition 2.1. The present results extend trivially also to hp-FE spaces which enforce conformity by the maximum degree rule. The present results also imply exponential convergence bounds for hp FE spaces on *regular, geometric mesh families* consisting of shape-regular tetrahedra as well as anisotropic prisms in edge- and edge-vertex patches. They also imply exponential bounds $d_N(\mathcal{K}, \mathcal{X}) \lesssim \exp(-b\sqrt[5]{N})$ on the Kolmogoroff N-widths $d_N(\mathcal{K}, \mathcal{X})$ of the analytic classes $\mathcal{K} = B_{-1-\boldsymbol{b}}(\Omega; \emptyset, \emptyset) \cap H^{1+\theta}(\Omega)$ which are compact subsets of the Hilbert space $\mathcal{X} = H^1(\Omega)$. This bound is implied by the present results and is of interest in connection with reduced basis approximations generated by greedy algorithms in $\mathcal{X}$. We refer to [4] for theory, and to [16] for recent developments for elliptic problems.

Appendix A. Proof of Theorem 4.3

We outline the major steps of the proof of Theorem 4.3.

A.1. **Approximation results.** We first establish some auxiliary approximation results.

A.1.1. *Univariate approximation properties.* We begin by reviewing the the following consistency bound from [25, Corollary 3.15] for the H^1-projector $\widehat{\pi}_{p,1}$ in (4.1) on $\widehat{I} = (-1, 1)$.

Lemma A.1. *Let $p \geq 1$, $\widehat{u} \in H^{s+1}(\widehat{I})$ and $0 \leq s \leq p$. Then there holds*

$$\|\widehat{u} - \widehat{\pi}_{p,1}\widehat{u}\|^2_{H^1(\widehat{I})} \lesssim \Psi_{p,s}\|\widehat{u}^{(s+1)}\|^2_{L^2(\widehat{I})}. \tag{A.1}$$

Here,

$$\Psi_{q,r} := \frac{\Gamma(q+1-r)}{\Gamma(q+1+r)}, \qquad 0 \leq r \leq q, \tag{A.2}$$

where Γ is the Gamma function satisfying $\Gamma(m+1) = m!$ for any $m \in \mathbb{N}_0$.

We establish an analogous H^1-norm error bound for the L^2-projection $\widehat{\pi}_{p,0}$; see [24, Lemma 5.2]. We also refer to [25, Theorem 3.11] for optimal L^2-norm hp-version consistency estimates.

Lemma A.2. *Let $p \geq 1$, $\widehat{u} \in H^{s+1}(\widehat{I})$ and $0 \leq s \leq p$. Then there holds*

$$\|\widehat{u} - \widehat{\pi}_{p,0}\widehat{u}\|^2_{H^1(\widehat{I})} \lesssim p^4\Psi_{p,s}\|\widehat{u}^{(s+1)}\|^2_{L^2(\widehat{I})}\,. \tag{A.3}$$

Proof. We first recall from [24, Lemma 5.1] the p-dependent stability bound

$$\|(\widehat{\pi}_{p,0}\widehat{u})^{(s)}\|_{L^2(\widehat{I})} \lesssim \max\{1,p\}^{2s}\|\widehat{u}^{(s)}\|_{L^2(\widehat{I})}, \qquad p \geq 0,\ s \geq 0; \tag{A.4}$$

see also property (4.9).

Then, from the triangle inequality, the fact that $\widehat{\pi}_{p,0}$ reproduces polynomials and the estimate (A.4) for $s = 0, 1$, we conclude that, for $p \geq 1$,

$$\begin{aligned}\|\widehat{u} - \widehat{\pi}_{p,0}\widehat{u}\|_{H^1(\widehat{I})} &\leq \|\widehat{u} - \widehat{\pi}_{p,1}\widehat{u}\|_{H^1(\widehat{I})} + \|\widehat{\pi}_{p,0}(\widehat{u} - \widehat{\pi}_{p,1}\widehat{u})\|_{H^1(\widehat{I})} \\ &\lesssim p^2\|\widehat{u} - \widehat{\pi}_{p,1}\widehat{u}\|_{H^1(\widehat{I})}.\end{aligned}$$

Referring to (A.1) yields (A.4). □

A.1.2. *Approximation properties of $\widehat{\pi}_{\boldsymbol{p},r}$.* Based on the univariate results above, we now derive approximation results for the tensor projectors in (4.3). To this end, on the reference element $\widehat{K} = \widehat{I}^3$ we introduce the tensor-product space

$$H^1_{\mathrm{mix}}(\widehat{K}) := H^1_{\mathrm{mix}}(\widehat{K}^\perp) \otimes H^1(\widehat{K}^\parallel) := H^1(\widehat{I}) \otimes H^1(\widehat{I}) \otimes H^1(\widehat{I}). \tag{A.5}$$

endowed with the standard (tensor-product) norm $\|\cdot\|_{H^1_{\mathrm{mix}}(\widehat{K})}$. Note that we have the continuous embedding $H^3(\widehat{K}) \hookrightarrow H^1_{\mathrm{mix}}(\widehat{K})$.

Let $K = K^\perp \otimes K^\perp$ be an axiparallel element, $\boldsymbol{p}_K = (p_K^\perp, p_K^\parallel)$ an elemental degree vector and $r_K \in \{0, 1\}$ an elemental conformity index in edge-parallel direction. For $u : K \to \mathbb{R}$, we denote by $\widehat{u} := u \circ \Phi_K$ the pull-back to the reference element $\widehat{K}$. In this setting, the tensor projection $\widehat{\pi}_{\boldsymbol{p}_K, r_K}\widehat{u} = \widehat{\pi}^\perp_{p_K^\perp,0} \otimes \widehat{\pi}^\parallel_{p_K^\parallel, r_K}\widehat{u}$ defined in (4.3) satisfies the subsequent bounds.

Proposition A.3. *The error $\widehat{\eta}_0^\perp = \widehat{u} - \widehat{\pi}^\perp_{p_K^\perp,0}\widehat{u}$ in edge-perpendicular satisfies*

$$\|\widehat{\eta}_0^\perp\|^2_{H^1_{\mathrm{mix}}(\widehat{K})} \lesssim (p_K^\perp)^8 \Psi_{p_K^\perp, s_K^\perp} E^\perp_{s_K^\perp}(K; u), \tag{A.6}$$

for any $0 \leq s_K^\perp \leq p_K^\perp$, with

$$E^\perp_s(K; u) := \sum_{|\boldsymbol{\alpha}^\perp| = s+1}^{s+2} \sum_{\alpha^\parallel = 0,1} (h_K^\perp)^{2|\boldsymbol{\alpha}^\perp|-2} (h_K^\parallel)^{2\alpha^\parallel - 1} \|\mathsf{D}_\perp^{\boldsymbol{\alpha}^\perp} \mathsf{D}_\parallel^{\alpha^\parallel} u\|^2_{L^2(K)}\,. \tag{A.7}$$

The error $\widehat{\eta}^\parallel = \widehat{u} - \widehat{\pi}_{p_K^\parallel, r_K}\widehat{u}$ in edge-parallel direction satisfies

$$\begin{aligned}&\|\widehat{\mathsf{D}}_\perp^{\boldsymbol{\alpha}^\perp} \widehat{\mathsf{D}}_\parallel^{\alpha^\parallel} \widehat{\eta}^\parallel\|^2_{L^2(\widehat{K})} \\ &\qquad \lesssim (p_K^\parallel)^{4(1-r_K)} \Psi_{p_K^\parallel, s_K^\parallel} (h_K^\perp)^{2|\boldsymbol{\alpha}^\perp|-2} (h_K^\parallel)^{2s_K^\parallel + 1} \|\mathsf{D}_\perp^{\boldsymbol{\alpha}^\perp} \mathsf{D}_\parallel^{s_K^\parallel + 1} u\|^2_{L^2(K)},\end{aligned} \tag{A.8}$$

for any $|\boldsymbol{\alpha}^\perp| \geq 0$, $\alpha^\parallel = 0, 1$, and $0 \leq s_K^\parallel \leq p_K^\parallel$.

Proof. We have

$$\widehat{\eta}_0^\perp = \widehat{u} - \widehat{\pi}^{(1)}_{p_K^\perp,0} \otimes \widehat{\pi}^{(2)}_{p_K^\perp,0}\widehat{u} = (\widehat{u} - \widehat{\pi}^{(1)}_{p_K^\perp,0}\widehat{u}) + \widehat{\pi}^{(1)}_{p_K^\perp,0}\left(\widehat{u} - \widehat{\pi}^{(2)}_{p_K^\perp,0}\widehat{u}\right)\,.$$

Hence, by the triangle inequality and the stability property (A.4) of the univariate L^2-projector $\widehat{\pi}^{(1)}_{p_K^\perp,0}$, we find that

$$\|\widehat{\eta}_0^\perp\|^2_{H^1_{\mathrm{mix}}(\widehat{K})} \lesssim (p_K^\perp)^4 \Big(\sum_{i=1}^{2} \|\widehat{u} - \widehat{\pi}^{(i)}_{p_K^\perp,0}\widehat{u}\|^2_{H^1_{\mathrm{mix}}(\widehat{K})} \Big)\,.$$

The univariate approximation properties (A.3) in Lemma A.2 now imply

$$\|\widehat{\eta}_0^{\perp}\|^2_{H^1_{\mathrm{mix}}(\widehat{K})} \lesssim (p_K^{\perp})^8 \Psi_{p_K^{\perp},s_K^{\perp}} \Big(\sum_{0\le\alpha_2^{\perp},\alpha^{\parallel}\le 1} \|\widehat{\mathsf{D}}^{(s_K^{\perp}+1,\alpha_2^{\perp},\alpha^{\parallel})}\widehat{u}\|^2_{L^2(\widehat{K})} + \sum_{0\le\alpha_1^{\perp},\alpha^{\parallel}\le 1} \|\widehat{\mathsf{D}}^{(\alpha_1^{\perp},s_K^{\perp}+1,\alpha^{\parallel})}\widehat{u}\|^2_{L^2(\widehat{K})} \Big) ,$$

for any $0 \le s_K^{\perp} \le p_K^{\perp}$. This bound and a scaling argument as in [23, Section 5.1.4] yield the desired bound (A.6) for $\widehat{\eta}_0^{\perp}$.

The bound for $\widehat{\eta}^{\parallel}$ is an immediate consequence of the consistency bounds (A.1) ($r_K = 1$) and (A.3) ($r_K = 0$) applied in edge-parallel direction, combined again with a scaling argument as in [23, Section 5.1.4]. □

A.1.3. *Edge-parallel interpolation.* We construct univariate hp-projectors and establish exponential convergence bounds for univariate geometric refinements on the interval $\omega = (0,1)$ towards $x = 0$. These results will be used for the hp-approximations along edges $\boldsymbol{e} \in \mathcal{E}_{\boldsymbol{c}}$ towards corners $\boldsymbol{c} \in \mathcal{C}$.

In ω and for $\sigma \in (0,1)$, we introduce geometric meshes $\mathcal{T}_\sigma^\ell = \{I_j\}_{j=1}^{\ell+1}$ with elements given by $I_1 = (0, \sigma^\ell)$ and $I_j = (\sigma^{\ell+2-j}, \sigma^{\ell+1-j})$ for $2 \le j \le \ell+1$, respectively. We introduce the local mesh sizes $h_1 := \sigma^\ell$ and

$$h_j := \sigma^{\ell+1-j}(1-\sigma), \qquad 2 \le j \le \ell+1 . \tag{A.9}$$

Then, there is a constant $\kappa > 0$ solely depending on $\sigma \in (0,1)$ with

$$\kappa^{-1} h_j \le |x| \le \kappa h_j, \qquad x \in I_j,\ 2 \le j \le \ell+1 . \tag{A.10}$$

On the geometric mesh $\mathcal{T}_\sigma^\ell$, let $\boldsymbol{p}^{\parallel} = (p_1^{\parallel}, \dots, p_{\ell+1}^{\parallel})$ be an (edge-parallel) polynomial degree vector and $\boldsymbol{r} = (r_1, \dots, r_{\ell+1}) \in \{0,1\}^{\ell+1}$ a conformity index vector. As elemental polynomial degrees, we take $p_j^{\parallel} = \max\{1, \lfloor \mathfrak{s} j \rfloor\}$, for a slope parameter $\mathfrak{s} > 0$ as in Section 3.2.1. We also set $|\boldsymbol{p}^{\parallel}| = \max_{j=1}^{\ell+1} p_j^{\parallel}$. We then consider the univariate hp-version finite element spaces

$$V^r(\mathcal{T}_\sigma^\ell, \boldsymbol{p}^{\parallel}) := \Big\{ v \in H^r(\omega) \,:\, v|_{I_j} \in \mathbb{P}_{p_j^{\parallel}}(I_j),\ j = 1, \dots, \ell+1 \Big\}, \quad r = 0, 1. \tag{A.11}$$

We denote by π the projection onto the space $V^0(\mathcal{T}_\sigma^\ell, \boldsymbol{p}^{\parallel})$, defined on each interval I_j as the (scaled) univariate projector $\pi_{p_j^{\parallel}, r_j} : H^{r_j}(I_j) \to \mathbb{P}_{p_j^{\parallel}}(I_j)$ introduced in Section 4.1. If $r_j = 0$ for all $1 \le j \le \ell+1$, then $\pi : L^2(\omega) \to V^0(\mathcal{T}_\sigma^\ell, \boldsymbol{p}^{\parallel})$ is the L^2-projection. In addition, if $r_j = 1$ for all $1 \le j \le \ell+1$, then the nodal exactness property (4.2) ensures that the projector $\pi : H^1(\omega) \to V^1(\mathcal{T}_\sigma^\ell, \boldsymbol{p}^{\parallel})$ is $H^1(\omega)$-conforming.

For $u \in H^1(\omega)$, we define the approximation errors $\eta := u - \pi u$, and introduce the elemental error quantity

$$T_j[\eta]^2 := h_j^{-2} \|\eta\|^2_{L^2(I_j)} + \|\eta'\|^2_{L^2(I_j)}. \tag{A.12}$$

Lemma A.4. *For a weight exponent $\beta > 0$, let $u \in H^1(\omega)$ be such that*

$$\||x|^{-1-\beta+s} u^{(s)}\|_{L^2(\omega)} \le C_u^{s+1} \Gamma(s+1), \qquad s \ge 2. \tag{A.13}$$

Then, for any conformity indices $r_j \in \{0,1\}$, there exist $b, C > 0$ independent of $\ell \ge 1$ such that $\sum_{j=2}^{\ell+1} T_j[\eta]^2 \le C \exp(-2b\ell)$.

Proof. Fix $I_j \in \mathcal{T}_\sigma^\ell$ for $2 \le j \le \ell+1$. A straightforward scaling argument yields $T_j[\eta]^2 \simeq (h_j/2)^{-1} \|\widehat{\eta}\|^2_{H^1(\widehat{I})}$, where as usual we denote by $\widehat{\eta}$ the pull-back of $\eta|_{I_j}$ to the reference interval $\widehat{I} = (-1,1)$. The one-dimensional approximation bounds in (A.1) and (A.3) imply that

$$T_j[\eta] \lesssim |\boldsymbol{p}^\parallel|^4 \big(h_j/2\big)^{-1} \Psi_{p_j^\parallel, s_j^\parallel} \|\widehat{u}^{(s_j^\parallel+1)}\|^2_{L^2(\widehat{I})},$$

for any $1 \le s_j^\parallel \le p_j^\parallel$, where we exclude $s_j^\parallel = 0$ in (A.1), (A.3) to ensure that $s \ge 2$ in (A.13). Scaling the right-hand side above back to element I_j results in

$$T_j[\eta]^2 \lesssim |\boldsymbol{p}^\parallel|^4 \, (h_j/2)^{2s_j^\parallel} \, \Psi_{p_j^\parallel, s_j^\parallel} \|u^{(s_j^\parallel+1)}\|^2_{L^2(I_j)}. \tag{A.14}$$

Moreover, by the equivalence (A.10),

$$\|u^{(s_j^\parallel+1)}\|^2_{L^2(I_j)} \simeq h_j^{2+2\beta-2(s_j^\parallel+1)} \||x|^{-1-\beta+(s_j^\parallel+1)} u^{(s_j^\parallel+1)}\|^2_{L^2(I_j)}. \tag{A.15}$$

By combining (A.14), (A.15) with (A.13), we find that

$$\begin{aligned} T_j[\eta]^2 &\lesssim |\boldsymbol{p}^\parallel|^4 h_j^{2\beta} 2^{-2s_j^\parallel} \Psi_{p_j^\parallel, s_j^\parallel} \||x|^{-1-\beta+(s_j^\parallel+1)} u^{(s_j^\parallel+1)}\|^2_{L^2(I_j)} \\ &\lesssim |\boldsymbol{p}^\parallel|^4 h_j^{2\beta} \, (C_u/2)^{2s_j^\parallel} \, \Psi_{p_j^\parallel, s_j^\parallel} \Gamma(s_j^\parallel+2)^2 \, , \end{aligned} \tag{A.16}$$

for $1 \le s_j^\parallel \le p_j^\parallel$. An interpolation argument as in [23, Lemma 5.8] shows that the bound (A.16) holds for any real $s_j^\parallel \in [1, p_j^\parallel]$.

Next, we sum the bound (A.16) over all intervals $2 \le j \le \ell+1$. In view of (A.9), we obtain

$$\sum_{j=2}^{\ell+1} T_j[\eta]^2 \lesssim |\boldsymbol{p}^\parallel|^4 \Big(\sum_{j=2}^{\ell+1} \sigma^{2(\ell+1-j)\beta} \min_{s_j^\parallel \in [1,p_j^\parallel]} \Big[C^{2s_j^\parallel} \Psi_{p_j^\parallel, s_j^\parallel} \Gamma(s_j+2)^2 \Big] \Big) \, .$$

By [23, Lemma 5.12], the bracket on the right-hand side above is exponentially small. Adjusting the constants to absorb $|\boldsymbol{p}^\parallel|^4$ finishes the proof. □

Similarly, we obtain the following result.

Lemma A.5. *For a weight exponent $\beta > 0$, let $u \in L^2(\omega)$ be such that*

$$\||x|^{-\beta+s} u^{(s)}\|_{L^2(\omega)} \le C_u^{s+2} \Gamma(s+2), \qquad s \ge 1 \, . \tag{A.17}$$

For any conformity indices $r_j \in \{0,1\}$, there exist $b, C > 0$ independent of $\ell \ge 1$ such that $\sum_{j=2}^{\ell+1} \|\eta\|^2_{L^2(I_j)} \le C \exp(-2b\ell)$.

Proof. This follows as in Lemma A.4 or [24, Proposition 5.5]. □

A.1.4. *Estimates in two-dimensional weighted spaces.* In edge-perpendicular direction, we shall make use of estimates in two-dimensional weighted spaces analogous to the results in [11, Section 3]. To state them, let $\mathfrak{K}$ be an axiparallel and shape-regular rectangle of diameter $h_\mathfrak{K}$ which is affinely equivalent to the reference square $\widehat{\mathfrak{K}} = \widehat{I}^2$. Let $\boldsymbol{c}$ be a corner of $\mathfrak{K}$ and set $r(\boldsymbol{x}) = |\boldsymbol{x} - \boldsymbol{c}|$. For a weight exponent $\beta \in [0,1)$, we denote by $L^2_\beta(\mathfrak{K})$ the weighted L^2-space endowed with the weighted norm $\|u\|_{L^2_\beta(\mathfrak{K})} := \|r^\beta u\|_{L^2(\mathfrak{K})}$. For $m = 1, 2$, the weighted space $H^{m,m}_\beta(\mathfrak{K})$ is defined as the completion of all $C^\infty(\overline{\mathfrak{K}})$-functions with respect to the norm $\|u\|^2_{H^{m,m}_\beta(\mathfrak{K})} :=$

$\|u\|^2_{H^{m-1}(\mathfrak{K})} + |u|^2_{H^{m,m}_\beta(\mathfrak{K})}$, where $|u|^2_{H^{m,m}_\beta(\mathfrak{K})} := \sum_{|\boldsymbol{\alpha}|=m} \|r^\beta \mathsf{D}^{\boldsymbol{\alpha}} u\|^2_{L^2(\mathfrak{K})}$. We denote by $\pi^2_{p,0}$ the L^2-projection onto the tensor-product polynomial space $\mathbb{Q}_p(\mathfrak{K})$ obtained by mapping $\widehat{\pi}^2_{p,0}$ on $\widehat{\mathfrak{K}}$.

Lemma A.6. *Let $\beta \in [0,1)$ be a weight exponent. For $u \in H^{1,1}_\beta(\mathfrak{K})$ and $p \geq 0$, there holds*

$$\|u - \pi^2_{p,0} u\|^2_{L^2(\mathfrak{K})} \lesssim h_{\mathfrak{K}}^{2-2\beta} |u|^2_{H^{1,1}_\beta(\mathfrak{K})}. \tag{A.18}$$

Similarly, for $u \in H^{2,2}_\beta(\mathfrak{K})$ and $p \geq 1$, there holds

$$\|u - \pi^2_{p,0} u\|^2_{L^2(\mathfrak{K})} + h^2_{\mathfrak{K}} \|\nabla(u - \pi^2_{p,0} u)\|^2_{L^2(\mathfrak{K})} \lesssim p^4 h_{\mathfrak{K}}^{4-2\beta} |u|^2_{H^{2,2}_\beta(\mathfrak{K})}. \tag{A.19}$$

The implied constants depend on the aspect ratio of $\mathfrak{K}$.

Proof. To prove (A.18), we apply the triangle inequality and the stability of the L^2-projection $\pi^2_{p,0}$ to obtain

$$\|u - \pi^2_{p,0} u\|_{L^2(\mathfrak{K})} \lesssim \|u - \pi^2_{0,0} u\|_{L^2(\mathfrak{K})} + \|\pi^2_{p,0}(u - \pi^2_{0,0} u)\|_{L^2(\mathfrak{K})} \lesssim \|u - \pi^2_{0,0} u\|_{L^2(\mathfrak{K})}.$$

The proof of the bound (A.18) for $p = 0$ can then be found in [19, Proposition 27] or [26, Corollary A.2.11].

To show (A.19), we proceed as in [11, Section 3] and first consider the reference square $\widehat{\mathfrak{K}} = (-1,1)^2$. With the stability bound (4.9) applied on $\widehat{\mathfrak{K}}$, it follows that

$$\begin{aligned} \|\widehat{u} - \widehat{\pi}^2_{p,0} \widehat{u}\|^2_{H^1(\widehat{\mathfrak{K}})} &\lesssim \|\widehat{u} - \widehat{\pi}^2_{1,0} \widehat{u}\|^2_{H^1(\widehat{\mathfrak{K}})} + \|\widehat{\pi}^2_{p,0}(\widehat{u} - \widehat{\pi}^2_{1,0} \widehat{u})\|^2_{H^1(\widehat{\mathfrak{K}})} \\ &\lesssim p^4 \|\widehat{u} - \widehat{\pi}^2_{1,0} \widehat{u}\|^2_{H^1(\widehat{\mathfrak{K}})} \lesssim p^4 \|\widehat{u} - \widehat{\pi}^2_{1,0} \widehat{u}\|^2_{H^1(\widehat{\mathfrak{K}})}. \end{aligned}$$

Hence, up to the factor p^4 in (A.19), we need to consider the case $p = 1$. To that end, we denote by $\widehat{\mathsf{p}}^2_{1,0}$ the L^2-projection onto the linear polynomial space $\mathbb{P}_1(\widehat{\mathfrak{K}})$. For $\widehat{u} : \widehat{\mathfrak{K}} \to \mathbb{R}$, we then claim that there is a constant $\widehat{C} > 0$ independent of $\widehat{u}$ such that

$$\|\widehat{u}\|_{H^{2,2}_\beta(\widehat{\mathfrak{K}})} \leq \widehat{C} \big(|\widehat{u}|_{H^{2,2}_\beta(\widehat{\mathfrak{K}})} + \|\widehat{\mathsf{p}}^2_{1,0} \widehat{u}\|_{L^2(\widehat{\mathfrak{K}})} \big) . \tag{A.20}$$

To prove (A.20), we apply the Peetre-Tartar lemma in the spirit of [11, Lemma 3.5] and introduce the operator

$$A : H^{2,2}_\beta(\widehat{\mathfrak{K}}) \to L^2_\beta(\widehat{\mathfrak{K}})^{2\times 2} \times (\mathbb{P}_1(\widehat{\mathfrak{K}}), \|\cdot\|_{L^2(\widehat{\mathfrak{K}})}), \qquad \widehat{u} \mapsto \big(\{\widehat{\mathsf{D}}^{\boldsymbol{\alpha}} \widehat{u}\}_{|\boldsymbol{\alpha}|=2}, \widehat{\mathsf{p}}^2_{1,0} \widehat{u} \big) .$$

It is linear and bounded (by employing the L^2-stability of the projection $\widehat{\mathsf{p}}^2_{1,0}$). Moreover, A is injective. Indeed, if $A\widehat{u} = 0$, then $\widehat{\mathsf{D}}^{\boldsymbol{\alpha}} \widehat{u} = 0$ for all $|\boldsymbol{\alpha}| = 2$. Hence, $\widehat{u}$ is a linear function. The condition $\widehat{\mathsf{p}}^2_{1,0} \widehat{u} = 0$ then implies that $\widehat{u} \equiv 0$. In addition, let $T : H^{2,2}_\beta(\widehat{\mathfrak{K}}) \to H^1(\widehat{\mathfrak{K}})$ be the injection operator. By [11, Lemma 3.4], it is compact and we trivially have

$$\widehat{u} \in H^{2,2}_\beta(\widehat{\mathfrak{K}}) : \quad \|\widehat{u}\|_{H^{2,2}_\beta(\widehat{\mathfrak{K}})} \leq |\widehat{u}|^2_{H^{2,2}_\beta(\widehat{\mathfrak{K}})} + \|\widehat{\mathsf{p}}^2_{1,0} \widehat{u}\|_{L^2(\widehat{\mathfrak{K}})} + \|T\widehat{u}\|_{H^1(\widehat{\mathfrak{K}})}.$$

The inequality (A.20) then follows from [8, Lemma A.38].

We proceed by invoking (A.20) for $\widehat{u} - \widehat{\mathsf{p}}^2_{1,0} \widehat{u}$. Since $|\widehat{\mathsf{p}}^2_{1,0} \widehat{u}|_{H^{2,2}_\beta(\widehat{\mathfrak{K}})} = 0$ and $\widehat{\mathsf{p}}^2_{1,0}(\widehat{u} - \widehat{\mathsf{p}}^2_{1,0} \widehat{u}) = 0$, this results in

$$\|\widehat{u} - \widehat{\mathsf{p}}^2_{1,0} \widehat{u}\|_{H^{2,2}_\beta(\widehat{\mathfrak{K}})} \leq \widehat{C} |\widehat{u}|_{H^{2,2}_\beta(\widehat{\mathfrak{K}})}, \tag{A.21}$$

With (A.21) we then claim that

$$\|\widehat{u}-\widehat{\pi}^2_{1,0}\widehat{u}\|_{H^{2,2}_\beta(\widehat{\mathfrak{K}})} \lesssim \|\widehat{u}-\widehat{\mathsf{p}}^2_{1,0}\widehat{u}\|_{H^{2,2}_\beta(\widehat{\mathfrak{K}})} \le \widehat{C}|\widehat{u}|_{H^{2,2}_\beta(\widehat{\mathfrak{K}})}, \tag{A.22}$$

which implies the desired estimate (A.19) on the reference square $\widehat{\mathfrak{K}}$. Indeed, by the triangle inequality and since $\widehat{\pi}^2_{1,0}$ reproduces polynomials in $\mathbb{Q}_1(\widehat{\mathfrak{K}})$, we have

$$\|\widehat{u}-\widehat{\pi}^2_{1,0}\widehat{u}\|_{H^{2,2}_\beta(\widehat{\mathfrak{K}})} \lesssim \|\widehat{u}-\widehat{\mathsf{p}}^2_{1,0}\widehat{u}\|_{H^{2,2}_\beta(\widehat{\mathfrak{K}})} + \|\widehat{\pi}^2_{1,0}(\widehat{u}-\widehat{\mathsf{p}}^2_{1,0}\widehat{u})\|_{H^{2,2}_\beta(\widehat{\mathfrak{K}})}.$$

To further estimate the second term on the right-hand side above, we employ the equivalence of all norms on finite dimensional spaces and the L^2-stability of $\widehat{\pi}^2_{1,0}$. This results in

$$\begin{aligned}\|\widehat{\pi}^2_{1,0}(\widehat{u}-\widehat{\mathsf{p}}^2_{1,0}\widehat{u})\|_{H^{2,2}_\beta(\widehat{\mathfrak{K}})} &\lesssim \|\widehat{\pi}^2_{1,0}(\widehat{u}-\widehat{\mathsf{p}}^2_{1,0}\widehat{u})\|^2_{L^2(\widehat{\mathfrak{K}})}\\ &\le \|\widehat{u}-\widehat{\mathsf{p}}^2_{1,0}\widehat{u}\|_{L^2(\widehat{\mathfrak{K}})} \le \|\widehat{u}-\widehat{\mathsf{p}}^2_{1,0}\widehat{u}\|_{H^{2,2}_\beta(\widehat{\mathfrak{K}})},\end{aligned}$$

which yields (A.22).

From (A.22), a scaling argument readily yields the desired estimates in (A.19) for a generic axiparallel and shape-regular rectangle $\mathfrak{K}$ of diameter $h_{\mathfrak{K}}$. This finishes the proof. □

A.2. **Reference corner-edge mesh.** We consider the reference corner-edge mesh patch $\widetilde{\mathcal{M}}^{\ell,\boldsymbol{ce}}_\sigma$ on $\widetilde{Q}$ for $\boldsymbol{c}\in\mathcal{C}$ and $\boldsymbol{e}\in\mathcal{E}_{\boldsymbol{c}}$; cf. Figure 1 (right). As in [24, Section 7], it is sufficient to focus on the elements in $\widetilde{\mathcal{M}}^{\ell,\boldsymbol{ce}}_\sigma$ near the corner-edge pair $\boldsymbol{c}\in\mathcal{C}$ and $\boldsymbol{e}\in\mathcal{E}_{\boldsymbol{c}}$. That is, we introduce the reference corner-edge submesh $\widetilde{\mathcal{K}}^{\ell,\boldsymbol{ce}}_\sigma\subset\widetilde{\mathcal{M}}^{\ell,\boldsymbol{ce}}_\sigma$ on $\widetilde{Q}$ given by

$$\widetilde{\mathcal{K}}^{\ell,\boldsymbol{ce}}_\sigma = \bigcup_{j=1}^{\ell+1}\bigcup_{i=1}^{j}\widetilde{\mathfrak{L}}^{ij}_{\boldsymbol{ce}}, \tag{A.23}$$

where the sets $\widetilde{\mathfrak{L}}^{ij}_{\boldsymbol{ce}}$ stand for layers of elements with identical scaling properties with respect to $\boldsymbol{c}$ and $\boldsymbol{e}$; cf. [23, Section 5.2.4]. As in the one-dimensional setting in Section A.1.3 the index j indicates the number of the geometric mesh layers in edge-parallel direction along the edge $\boldsymbol{e}$, whereas the index i indicates the number of mesh layers in direction perpendicular to $\boldsymbol{e}$. In agreement with [24, Section 7.1], we split $\widetilde{\mathcal{K}}^{\ell,\boldsymbol{ce}}_\sigma$ into interior elements away from $\boldsymbol{c}$ and $\boldsymbol{e}$, boundary layer elements along $\boldsymbol{e}$ (but away from $\boldsymbol{c}$), and corner elements abutting at $\boldsymbol{c}$. That is, we have $\widetilde{\mathcal{K}}^{\ell,\boldsymbol{ce}}_\sigma = \widetilde{\mathfrak{D}}^{\ell}_{\boldsymbol{ce}}\,\dot\cup\,\widetilde{\mathfrak{T}}^{\ell}_{\boldsymbol{e}}\,\dot\cup\,\widetilde{\mathfrak{T}}^{\ell}_{\boldsymbol{c}}$, with

$$\widetilde{\mathfrak{D}}^{\ell}_{\boldsymbol{ce}} := \bigcup_{j=2}^{\ell+1}\bigcup_{i=2}^{j}\widetilde{\mathfrak{L}}^{ij}_{\boldsymbol{ce}},\qquad \widetilde{\mathfrak{T}}^{\ell}_{\boldsymbol{e}} := \bigcup_{j=2}^{\ell+1}\widetilde{\mathfrak{L}}^{1j}_{\boldsymbol{ce}},\qquad \widetilde{\mathfrak{T}}^{\ell}_{\boldsymbol{c}} := \widetilde{\mathfrak{L}}^{11}_{\boldsymbol{ce}}. \tag{A.24}$$

Here, for $2\le i,j\le\ell+1$, interior elements $K\in\mathfrak{L}^{ij}_{\boldsymbol{ce}}$ satisfy

$$r_{\boldsymbol{e}}|_K \simeq h_K^{\perp} \simeq \sigma^{\ell+1-i},\qquad r_{\boldsymbol{c}}|_K \simeq h_K^{\parallel} \simeq \sigma^{\ell+1-j}. \tag{A.25}$$

Similarly, boundary layer elements $K\in\widetilde{\mathfrak{L}}^{1j}_{\boldsymbol{ce}}$ satisfy

$$r_{\boldsymbol{e}}|_K \lesssim h_K^{\perp} \simeq \sigma^{\ell},\qquad r_{\boldsymbol{c}}|_K \simeq h_K^{\parallel} \simeq \sigma^{\ell+1-j},\qquad 2\le j\le\ell+1. \tag{A.26}$$

Finally, a corner element in the layer $\widetilde{\mathfrak{T}}^{\ell}_{\boldsymbol{c}} = \widetilde{\mathfrak{L}}^{11}_{\boldsymbol{ce}}$ is isotropic with $r_{\boldsymbol{e}}|_K \lesssim h_K \simeq \sigma^{\ell}$, and $r_{\boldsymbol{c}}|_K \lesssim h_K \simeq \sigma^{\ell}$. The sets $\widetilde{\mathfrak{L}}^{1j}_{\boldsymbol{ce}}$ and $\widetilde{\mathfrak{L}}^{11}_{\boldsymbol{ce}}$ are in fact singletons, and $K\in\widetilde{\mathfrak{L}}^{1j}_{\boldsymbol{ce}}$

can be written as

$$K_j = K^\perp \times K_j^\parallel, \qquad 2 \le j \le \ell+1\,, \tag{A.27}$$

cf. (3.3), where $K^\perp = (0,\sigma^\ell)^2$, and the sequence $\{K_j^\parallel\}_{j=2}^{\ell+1}$ forms a one-dimensional geometric mesh $\mathcal{T}_\sigma^\ell$ along the edge $\boldsymbol{e}$ as in Section A.1.3. The $\mathfrak{s}$-linearly increasing polynomial degree distributions on $\widetilde{\mathcal{K}}_\sigma^{\ell,\boldsymbol{ce}}$ in (A.23) are given by

$$\forall\, K \in \widetilde{\mathfrak{L}}_{\boldsymbol{ce}}^{ij}: \qquad \boldsymbol{p}_K = (p_i^\perp, p_j^\parallel) \simeq (\max\{1,\lfloor \mathfrak{s} i\rfloor\}, \max\{1,\lfloor \mathfrak{s} j\rfloor\}). \tag{A.28}$$

In the sequel, we introduce the domain $\widetilde{\Omega}_{\boldsymbol{ce}}^\ell := \big(\cup_{K\in\widetilde{\mathcal{K}}_\sigma^{\ell,\boldsymbol{ce}}} \overline{K}\big)^\circ$. Analogously to (2.7) and for exponents $\boldsymbol{\beta} = \{\beta_{\boldsymbol{c}}, \beta_{\boldsymbol{e}}\}$, we introduce the *non-homogeneous reference corner-edge semi-norm on* $\widetilde{\Omega}_{\boldsymbol{ce}}^\ell$:

$$|u|^2_{\widetilde{N}^k_{\boldsymbol{\beta}}(\widetilde{\Omega}^\ell_{\boldsymbol{ce}})} := \sum_{|\boldsymbol{\alpha}|=k} \Big\| r_{\boldsymbol{c}}^{\max\{\beta_{\boldsymbol{c}}+|\boldsymbol{\alpha}|,0\}} \rho_{\boldsymbol{ce}}^{\max\{\beta_{\boldsymbol{e}}+|\boldsymbol{\alpha}^\perp|,0\}} \mathsf{D}^{\boldsymbol{\alpha}} u\Big\|^2_{L^2(\widetilde{\Omega}^\ell_{\boldsymbol{ce}})}\,, \tag{A.29}$$

for any $k \ge 0$ and where $r_{\boldsymbol{c}}$ and $r_{\boldsymbol{e}}$ are the distances to $\boldsymbol{c}$ and $\boldsymbol{e}$, respectively, and $\rho_{\boldsymbol{ce}} = r_{\boldsymbol{e}}/r_{\boldsymbol{c}}$. For $m > k_{\boldsymbol{\beta}}$ as in (2.8), the weighted spaces $\widetilde{N}^m_{\boldsymbol{\beta}}(\widetilde{\Omega}^\ell_{\boldsymbol{ce}})$ are defined as in Section 2.2 with respect to the norms $\|\cdot\|^2_{\widetilde{N}^m_{\boldsymbol{\beta}}(\widetilde{\Omega}^\ell_{\boldsymbol{ce}})} = \sum_{k=0}^m |\cdot|^2_{\widetilde{N}^k_{\boldsymbol{\beta}}(\widetilde{\Omega}^\ell_{\boldsymbol{ce}})}$. The corresponding analytic reference class $B_{\boldsymbol{\beta}}(\widetilde{\Omega}^\ell_{\boldsymbol{ce}})$ consists of all functions $u : \widetilde{\Omega}^\ell_{\boldsymbol{ce}} \to \mathbb{R}$ such that $u \in \widetilde{N}^k_{\boldsymbol{\beta}}(\widetilde{\Omega}^\ell_{\boldsymbol{ce}})$ for $k > k_{\boldsymbol{\beta}}$ and such that there is a constant $d_u > 0$ with

$$|u|_{\widetilde{N}^k_{\boldsymbol{\beta}}(\widetilde{\Omega}^\ell_{\boldsymbol{ce}})} \le d_u^{k+1}\Gamma(k+1) \qquad \forall\, k > k_{\boldsymbol{\beta}}. \tag{A.30}$$

In the following, we restrict ourselves to the classes $B_{-1-\boldsymbol{b}}(\widetilde{\Omega}^\ell_{\boldsymbol{ce}})$ and $B_{-\boldsymbol{b}}(\widetilde{\Omega}^\ell_{\boldsymbol{ce}})$ for exponents $\boldsymbol{b} = \{b_{\boldsymbol{c}}, b_{\boldsymbol{e}}\}$ in $(0,1)$ as in Remark 2.4. In the first case, we have $k_{\boldsymbol{\beta}} \in (1,2)$ and the norms on the right-hand in (A.29) are given by

$$\begin{cases} \|\mathsf{D}^{\boldsymbol{\alpha}} u\|^2_{L^2(\widetilde{\Omega}^\ell_{\boldsymbol{ce}})} & |\boldsymbol{\alpha}| = 0,1,\ |\boldsymbol{\alpha}^\perp| = 0,1, \\ \|r_{\boldsymbol{c}}^{-1-b_{\boldsymbol{c}}+|\boldsymbol{\alpha}|}\mathsf{D}^{\boldsymbol{\alpha}} u\|^2_{L^2(\widetilde{\Omega}^\ell_{\boldsymbol{ce}})} & |\boldsymbol{\alpha}| \ge 2,\ |\boldsymbol{\alpha}^\perp| = 0,1, \\ \|r_{\boldsymbol{c}}^{b_{\boldsymbol{e}}-b_{\boldsymbol{c}}+\alpha^\parallel} r_{\boldsymbol{e}}^{-1-b_{\boldsymbol{e}}+|\boldsymbol{\alpha}^\perp|}\mathsf{D}^{\boldsymbol{\alpha}} u\|^2_{L^2(\widetilde{\Omega}^\ell_{\boldsymbol{ce}})} & |\boldsymbol{\alpha}| \ge 2,\ |\boldsymbol{\alpha}^\perp| \ge 2. \end{cases} \tag{A.31}$$

Similarly, for the second analytic class $B_{-\boldsymbol{b}}(\widetilde{\Omega}^\ell_{\boldsymbol{ce}})$, we have $k_{\boldsymbol{\beta}} \in (0,1)$ and the norms on the right-hand side of (A.29) take the form

$$\begin{cases} \|u\|^2_{L^2(\widetilde{\Omega}^\ell_{\boldsymbol{ce}})} & |\boldsymbol{\alpha}| = 0,\ |\boldsymbol{\alpha}^\perp| = 0, \\ \|r_{\boldsymbol{c}}^{-b_{\boldsymbol{e}}+\alpha^\parallel}\mathsf{D}^{\boldsymbol{\alpha}} u\|^2_{L^2(\widetilde{\Omega}^\ell_{\boldsymbol{ce}})} & |\boldsymbol{\alpha}| = 1,\ |\boldsymbol{\alpha}^\perp| = 0, \\ \|r_{\boldsymbol{c}}^{b_{\boldsymbol{e}}-b_{\boldsymbol{c}}+\alpha^\parallel} r_{\boldsymbol{e}}^{-b_{\boldsymbol{e}}+|\boldsymbol{\alpha}^\perp|}\mathsf{D}^{\boldsymbol{\alpha}} u\|^2_{L^2(\widetilde{\Omega}^\ell_{\boldsymbol{ce}})} & |\boldsymbol{\alpha}| \ge 1,\ |\boldsymbol{\alpha}^\perp| \ge 1. \end{cases} \tag{A.32}$$

In the *axi-parallel* setting considered in the present paper, when functions $u \in B_{-1-\boldsymbol{b}}(\Omega;\emptyset,\emptyset)$ and $u \in B_{-\boldsymbol{b}}(\Omega;\emptyset,\emptyset)$ as in Theorem 4.3 are localized and scaled to $\widetilde{\Omega}^\ell_{\boldsymbol{ce}}$, they belong to the reference classes $B_{-1-\boldsymbol{b}}(\widetilde{\Omega}^\ell_{\boldsymbol{ce}})$ and $B_{-\boldsymbol{b}}(\widetilde{\Omega}^\ell_{\boldsymbol{ce}})$, respectively; cf. [18, Section 3.4].

With the error estimates in Lemma 4.2, we need to bound the error contributions as in (3.36), (4.12), but over the reference mesh $\widetilde{\mathcal{K}}_\sigma^{\ell,\boldsymbol{ce}} = \widetilde{\mathfrak{O}}_{\boldsymbol{ce}}^\ell \,\dot\cup\, \widetilde{\mathfrak{T}}_{\boldsymbol{e}}^\ell \,\dot\cup\, \widetilde{\mathfrak{T}}_{\boldsymbol{c}}^\ell$ in the setting above. It is then sufficient to establish the following result.

Proposition A.7. *Consider weight exponents* $b_{\boldsymbol{c}}, b_{\boldsymbol{e}} \in (0,1)$ *as in* (2.13).

Let $u \in B_{-1-\boldsymbol{b}}(\widetilde{\Omega}^\ell_{\boldsymbol{ce}}) \cap H^{1+\theta}(\widetilde{\Omega}^\ell_{\boldsymbol{ce}})$ for some $\theta \in (0,1)$, and let $\pi u = \pi_0^\perp \otimes \pi^\parallel u$ be the base interpolant (4.4) over $\widetilde{\mathcal{K}}^{\ell,\boldsymbol{ce}}_\sigma$ for any conformity indices $r_K \in \{0,1\}$. For the errors η, $\eta_0^\perp$, $\eta^\parallel$ in (4.7), we have

$$\Upsilon^\perp_{\widetilde{\mathfrak{O}}^\ell_{\boldsymbol{ce}}}[\eta_0^\perp]^2 + \Upsilon^\parallel_{\widetilde{\mathfrak{O}}^\ell_{\boldsymbol{ce}}}[\eta^\parallel]^2 + \Upsilon^\perp_{\widetilde{\mathfrak{T}}^\ell_{\boldsymbol{e}}}[\eta_0^\perp]^2 + \Upsilon^\parallel_{\widetilde{\mathfrak{T}}^\ell_{\boldsymbol{e}}}[\eta^\parallel]^2 + \Upsilon^\parallel_{\widetilde{\mathfrak{T}}^\ell_{\boldsymbol{c}}}[\eta]^2 \le C\exp(-2b\ell),$$

with $b, C > 0$ independent of ℓ.

Let $u \in B_{-\boldsymbol{b}}(\widetilde{\Omega}^\ell_{\boldsymbol{ce}}) \cap H^\theta(\widetilde{\Omega}^\ell_{\boldsymbol{ce}})$ for some $\theta \in (0,1)$, and let $\pi_0 u = \pi_0^\perp \otimes \pi_0^\parallel u$ be the L^2-projection over $\widetilde{\mathcal{K}}^{\ell,\boldsymbol{ce}}_\sigma$. For the errors η_0, $\eta_0^\perp$, $\eta_0^\parallel$ in (4.7), we have

$$\|\eta_0^\perp\|^2_{L^2(\widetilde{\mathfrak{O}}^\ell_{\boldsymbol{ce}})} + \|\eta_0^\parallel\|^2_{L^2(\widetilde{\mathfrak{O}}^\ell_{\boldsymbol{ce}})} + \|\eta_0^\perp\|^2_{L^2(\widetilde{\mathfrak{T}}^\ell_{\boldsymbol{e}})} + \|\eta_0^\parallel\|^2_{L^2(\widetilde{\mathfrak{T}}^\ell_{\boldsymbol{e}})} + \|\eta_0\|^2_{L^2(\widetilde{\mathfrak{T}}^\ell_{\boldsymbol{c}})} \le C\exp(-2b\ell),$$

with $b, C > 0$ independent of ℓ.

The desired convergence bounds in Theorem 4.3 follow now from Proposition A.7 by noting that the number of degrees of freedom N in the *hp*-spaces in (3.23) is given by $N \simeq \ell^5 + \mathcal{O}(\ell^4)$, where the implied constant solely depends on $\mathfrak{s}$ and the number of mesh patches. The remainder of this section is devoted to the proof of Proposition A.7.

A.3. **Proof of Proposition A.7.** We bound the errors in Proposition A.7 separately for the set $\widetilde{\mathfrak{O}}^\ell_{\boldsymbol{ce}}$ (Propositions A.9 and A.10), for $\widetilde{\mathfrak{T}}^\ell_{\boldsymbol{e}}$ (Propositions A.11 and A.12), and for $\widetilde{\mathfrak{T}}^\ell_{\boldsymbol{c}}$ (Proposition A.13).

A.3.1. *Convergence on $\widetilde{\mathfrak{O}}^\ell_{\boldsymbol{ce}}$.* We begin our analysis by recalling essential scaling properties; see [23, Section 5.1.4].

Lemma A.8. *Let $K = (0, h_K^\perp)^2 \times (0, h_K^\parallel)$ be of the form (3.3). Let $v : K \to \mathbb{R}$, and $\widehat{v} = v \circ \Phi_K^{-1}$. Then:*

(i) $\|v\|^2_{L^2(K)} \lesssim (h_K^\perp)^2 h_K^\parallel \|\widehat{v}\|^2_{L^2(\widehat{K})}$.

(ii) $(h_K^\parallel)^{-2}\|v\|^2_{L^2(K)} + \|\mathsf{D}_\parallel v\|^2 \lesssim (h_K^\perp)^2 (h_K^\parallel)^{-1}\big(\|\widehat{v}\|^2_{L^2(\widehat{K})} + \|\widehat{\mathsf{D}}_\parallel \widehat{v}\|^2_{L^2(\widehat{K})}\big)$.

(iii) $(h_K^\perp)^{-2}\|v\|^2_{L^2(K)} + \|\mathsf{D}_\perp v\|^2_{L^2(K)} \lesssim h_K^\parallel \big(\|\widehat{v}\|^2_{L^2(\widehat{K})} + \|\widehat{\mathsf{D}}_\perp \widehat{v}\|^2_{L^2(\widehat{K})}\big)$.

We bound $\eta_0^\perp$ over $\widetilde{\mathfrak{O}}^\ell_{\boldsymbol{ce}}$ as follows.

Proposition A.9. *Let $u \in B_{-1-\boldsymbol{b}}(\widetilde{\Omega}^\ell_{\boldsymbol{ce}})$ respectively $u \in B_{-\boldsymbol{b}}(\widetilde{\Omega}^\ell_{\boldsymbol{ce}})$. Then there are constants $b, C > 0$ independent of $\ell \ge 1$ such that $\Upsilon^\perp_{\widetilde{\mathfrak{O}}^\ell_{\boldsymbol{ce}}}[\eta_0^\perp]^2 \le C\exp(-2b\ell)$ respectively $\|\eta_0^\perp\|^2_{L^2(\widetilde{\mathfrak{O}}^\ell_{\boldsymbol{ce}})} \le C\exp(-2b\ell)$.*

Proof. Let $u \in B_{-1-\boldsymbol{b}}(\widetilde{\Omega}^\ell_{\boldsymbol{ce}})$. We consider an element $K \in \widetilde{\mathfrak{L}}^{ij}_{\boldsymbol{ce}}$ with $2 \le j \le \ell+1$ and $2 \le i \le j$, according to (A.24). With Lemma A.8 (observing that $h_K^\perp \lesssim h_K^\parallel$) and the approximation results for $\widehat{\eta}_0^\perp$ in Proposition A.3 in conjunction with (A.28), we conclude that

$$N_K^\perp[\eta_0^\perp]^2 \lesssim h_K^\parallel \|\widehat{\eta}_0^\perp\|^2_{H^1_{\mathrm{mix}}(\widehat{K})} \lesssim |\boldsymbol{p}_K|^8\, h_K^\parallel \Psi_{p_i^\perp, s_i^\perp} E^\perp_{s_i^\perp}(K;u),$$

for $1 \le s_i^\perp \le p_i^\perp$, where $E^\perp_{s_i^\perp}(K;u)$ is the expression in (A.7). Notice that here we exclude the choice $s_i^\perp = 0$ to ensure that $|\boldsymbol{\alpha}| \ge |\boldsymbol{\alpha}^\perp| \ge 2$ in $E^\perp_{s_i^\perp}(K;u)$. Thanks

to the equivalences (A.26), we insert the appropriate weights as in (A.31), (A.32), and obtain

$$\|\mathsf{D}_\perp^{\boldsymbol{\alpha}^\perp}\mathsf{D}_\parallel^{\alpha^\parallel}u\|^2_{L^2(K)} \simeq (h_K^\parallel)^{2b_{\boldsymbol{c}}-2b_{\boldsymbol{e}}-2\alpha^\parallel}(h_K^\perp)^{2+2b_{\boldsymbol{e}}-2|\boldsymbol{\alpha}^\perp|} \times \|r_{\boldsymbol{c}}^{b_{\boldsymbol{e}}-b_{\boldsymbol{c}}+\alpha^\parallel} r_{\boldsymbol{e}}^{-1-b_{\boldsymbol{e}}+|\boldsymbol{\alpha}^\perp|}\mathsf{D}_\perp^{\boldsymbol{\alpha}^\perp}\mathsf{D}_\parallel^{\alpha^\parallel}u\|^2_{L^2(K)}\,.$$

Hence,

$$N_K^\perp[\eta_0^\perp]^2 \lesssim |\boldsymbol{p}_K|^8\Psi_{p_i^\perp,s_i^\perp}(h_K^\parallel)^{2b_{\boldsymbol{c}}-2b_{\boldsymbol{e}}}(h_K^\perp)^{2b_{\boldsymbol{e}}}\sum_{k=s_i^\perp+1}^{s_i^\perp+3}|u|^2_{\widetilde{N}^k_{-1-\boldsymbol{b}}(K)}\,.$$

Since $s_i^\perp+1\geq 2$, the analytic regularity (A.30) implies the existence of $C>0$ such that

$$N_K^\perp[\eta_0^\perp]^2 \lesssim |\boldsymbol{p}_K|^8\,\Psi_{p_i^\perp,s_i^\perp}(h_K^\parallel)^{2b_{\boldsymbol{c}}-2b_{\boldsymbol{e}}}(h_K^\perp)^{2b_{\boldsymbol{e}}}C^{2s_i^\perp}\Gamma(s_i^\perp+4)^2, \tag{A.33}$$

for all $1\leq s_i^\perp\leq p_i^\perp$. Summing (A.33) over all layers in $\widetilde{\mathfrak{O}}^\ell_{\boldsymbol{ce}}$ in (A.24) in combination with (A.25) results in

$$\Upsilon^\perp_{\widetilde{\mathfrak{O}}^\ell_{\boldsymbol{ce}}}[\eta_0^\perp] \lesssim |\boldsymbol{p}|^8\sum_{j=2}^{\ell+1}\sigma^{2(b_{\boldsymbol{c}}-b_{\boldsymbol{e}})(\ell+1-j)}\Big(\sum_{i=2}^{j}\sigma^{2b_{\boldsymbol{e}}(\ell+1-i)}\Psi_{p_i^\perp,s_i^\perp}C^{2s_i^\perp}\Gamma(s_i^\perp+4)^2\Big)\,.$$

By interpolating to real parameters $s_i^\perp\in[1,p_i^\perp]$ as in [23, Lemma 5.8], this sum is of the same form as $S^\perp$ in the proof of [23, Proposition 5.17], and the assertion now follows from the arguments there and after adjusting the constants to absorb the algebraic loss in $|\boldsymbol{p}|$.

For $u\in B_{-\boldsymbol{b}}(\widetilde{\Omega}^\ell_{\boldsymbol{ce}})$, we proceed similarly and note that

$$\|\eta_0^\perp\|^2_{L^2(K)} \lesssim (h_K^\perp)^2h_K^\parallel\|\widehat{\eta}_0^\perp\|^2_{H^1_{\mathrm{mix}}(\widehat{K})} \lesssim |\boldsymbol{p}_K|^8\,(h_K^\perp)^2h_K^\parallel\Psi_{p_i^\perp,s_i^\perp}E^\perp_{s_i^\perp}(K;u),$$

for $1\leq s_i^\perp\leq p_i^\perp$. Hence, we obtain

$$\|\eta_0^\perp\|^2_{L^2(K)} \lesssim |\boldsymbol{p}_K|^8\Psi_{p_i^\perp,s_i^\perp}(h_K^\parallel)^{2b_{\boldsymbol{c}}-2b_{\boldsymbol{e}}}(h_K^\perp)^{2b_{\boldsymbol{e}}}\sum_{k=s_i^\perp+1}^{s_i^\perp+3}|u|^2_{\widetilde{N}^k_{-\boldsymbol{b}}(K)}\,.$$

The second bound follows as before. □

Next, we establish the analog of Proposition A.9 in edge-parallel direction.

Proposition A.10. *Let $u\in B_{-1-\boldsymbol{b}}(\widetilde{\Omega}^\ell_{\boldsymbol{ce}})$ respectively $u\in B_{-\boldsymbol{b}}(\widetilde{\Omega}^\ell_{\boldsymbol{ce}})$. Then there are constants $b,C>0$ independent of $\ell\geq 1$ such that $\Upsilon^\parallel_{\widetilde{\mathfrak{O}}^\ell_{\boldsymbol{ce}}}[\eta^\parallel]^2\leq C\exp(-2b\ell)$ respectively $\|\eta_0^\parallel\|^2_{L^2(\widetilde{\mathfrak{O}}^\ell_{\boldsymbol{ce}})}\leq C\exp(-2b\ell)$.*

Proof. For $u\in B_{-1-\boldsymbol{b}}(\widetilde{\Omega}^\ell_{\boldsymbol{ce}})$, we claim that

$$N_K^\parallel[\eta^\parallel]^2 \lesssim (p_K^\parallel)^4\Psi_{p_K^\parallel,s_K^\parallel}(h_K^\parallel)^{2b_{\boldsymbol{c}}}\|u\|^2_{\widetilde{N}^{s_K^\parallel+2}_{-1-\boldsymbol{b}}(K)}, \tag{A.34}$$

for any $K \in \widetilde{\mathfrak{O}}^\ell_{\boldsymbol{ce}}$ and $1 \le s^\parallel_K \le p^\parallel_K$. To prove (A.34), we start by employing Lemma A.8 and the approximation property (with $|\boldsymbol{\alpha}^\perp| = 0$) for $\widehat{\eta}^\parallel$ in Proposition A.3. It follows that

$$(h^\parallel_K)^{-2}\|\eta^\parallel\|^2_{L^2(K)} + \|\mathsf{D}_\parallel\eta^\parallel\|^2_{L^2(K)} \lesssim (h^\perp_K)^2(h^\parallel_K)^{-1}\sum_{\alpha^\parallel=0,1}\|\widehat{\mathsf{D}}^{\alpha^\parallel}_\parallel\widehat{\eta}^\parallel\|^2_{L^2(\widehat{K})}$$
$$\lesssim (p^\parallel_K)^4\Psi_{p^\parallel_K,s^\parallel_K}(h^\parallel_K)^{2s^\parallel_K}\|\mathsf{D}^{s^\parallel_K+1}_\parallel u\|^2_{L^2(K)}.$$

for any $1 \le s^\parallel_K \le p^\parallel_K$, where as before we exclude the choice $s^\parallel_K = 1$ to ensure that $|\boldsymbol{\alpha}| \ge 2$. We then insert suitable weights with the aid of (A.31) and (A.25) to obtain

$$\|\mathsf{D}^{s^\parallel_K+1}_\parallel u\|^2_{L^2(K)} \simeq (h^\parallel_K)^{2+2b_{\boldsymbol{c}}-2s^\parallel_K-2}\|r_{\boldsymbol{c}}^{-1-b_{\boldsymbol{c}}+s^\parallel_K+1}\mathsf{D}^{s^\parallel_K+1}_\parallel u\|^2_{L^2(K)}$$
$$\lesssim (h^\parallel_K)^{2b_{\boldsymbol{c}}-2s^\parallel_K}|u|^2_{\widetilde{N}^{s^\parallel_K+1}_{-1-\boldsymbol{b}}(K)}.$$

Hence,

$$(h^\parallel_K)^{-2}\|\eta^\parallel\|^2_{L^2(K)} + \|\mathsf{D}_\parallel\eta^\parallel\|^2_{L^2(K)} \lesssim (p^\parallel_K)^4\Psi_{p^\parallel_K,s^\parallel_K}(h^\parallel_K)^{2b_{\boldsymbol{c}}}|u|^2_{\widetilde{N}^{s^\parallel_K+1}_{-1-\boldsymbol{b}}(K)}.$$

By proceeding similarly, we find that, for $|\boldsymbol{\alpha}^\perp| = 1$,

$$\|\mathsf{D}^{\boldsymbol{\alpha}^\perp}_\perp\eta^\parallel\|^2_{L^2(K)} \lesssim h^\parallel_K\sum_{\alpha^\parallel=0,1}\|\widehat{\mathsf{D}}^{\boldsymbol{\alpha}^\perp}_\perp\widehat{\mathsf{D}}^{\alpha^\parallel}_\parallel\widehat{\eta}^\parallel\|^2_{L^2(\widehat{K})}$$
$$\lesssim (p^\parallel_K)^4\Psi_{p^\parallel_K,s^\parallel_K}(h^\parallel_K)^{2s^\parallel_K+2}\|\mathsf{D}^{\boldsymbol{\alpha}^\perp}_\perp\mathsf{D}^{s^\parallel_K+1}_\parallel u\|^2_{L^2(K)}$$
$$\simeq (p^\parallel_K)^4\Psi_{p^\parallel_K,s^\parallel_K}(h^\parallel_K)^{2b_{\boldsymbol{c}}}\|r_{\boldsymbol{c}}^{-b_{\boldsymbol{c}}+s^\parallel_K+1}\mathsf{D}^{\boldsymbol{\alpha}^\perp}_\perp\mathsf{D}^{s^\parallel_K+1}_\parallel u\|^2_{L^2(K)}$$
$$\simeq (p^\parallel_K)^4\Psi_{p^\parallel_K,s^\parallel_K}(h^\parallel_K)^{2b_{\boldsymbol{c}}}|u|^2_{\widetilde{N}^{s^\parallel_K+2}_{-1-\boldsymbol{b}}(K)}.$$

This establishes the bound in (A.34).

For $u \in B_{-\boldsymbol{b}}(\widetilde{\Omega}^\ell_{\boldsymbol{ce}})$, we use analogous arguments based on Lemma A.8, Proposition A.3 and (A.32). This results in

$$\|\eta^\parallel_0\|^2_{L^2(K)} \lesssim (p^\parallel_K)^4\Psi_{p^\parallel_K,s^\parallel_K}(h^\parallel_K)^{2s^\parallel_K+2}\|\mathsf{D}^{s^\parallel_K+1}_\parallel u\|^2_{L^2(K)}$$
$$\lesssim (p^\parallel_K)^4\Psi_{p^\parallel_K,s^\parallel_K}(h^\parallel_K)^{2b_{\boldsymbol{c}}}\|r_{\boldsymbol{c}}^{-b_{\boldsymbol{c}}+s^\parallel_K+1}\mathsf{D}^{s^\parallel_K+1}_\parallel u\|^2_{L^2(K)} \tag{A.35}$$
$$\lesssim (p^\parallel_K)^4\Psi_{p^\parallel_K,s^\parallel_K}(h^\parallel_K)^{2b_{\boldsymbol{c}}}|u|^2_{\widetilde{N}^{s^\parallel_K+1}_{-\boldsymbol{b}}(K)}.$$

Next, we sum the bounds in (A.34), (A.35) over all layers of $\widetilde{\mathfrak{O}}^\ell_{\boldsymbol{ce}}$. By noticing (A.25), (A.28) and the analytic regularity (A.30), we conclude that

$$u \in B_{-1-\boldsymbol{b}}(\widetilde{\Omega}^\ell_{\boldsymbol{ce}}): \quad \Upsilon^\parallel_{\widetilde{\mathfrak{O}}^\ell_{\boldsymbol{ce}}}[\eta^\parallel]^2 \lesssim |\boldsymbol{p}|^4\sum_{j=2}^{\ell+1}\sum_{i=2}^{j}\Psi_{p^\parallel_j,s^\parallel_j}\sigma^{2(\ell+1-j)b_{\boldsymbol{c}}}C^{2s^\parallel_j}\Gamma(s^\parallel_j+3)^2,$$

$$u \in B_{-\boldsymbol{b}}(\widetilde{\Omega}^\ell_{\boldsymbol{ce}}): \qquad \|\eta^\parallel_0\|^2_{L^2(\widetilde{\mathfrak{O}}^\ell_{\boldsymbol{ce}})} \lesssim |\boldsymbol{p}|^4\sum_{j=2}^{\ell+1}\sum_{i=2}^{j}\Psi_{p^\parallel_j,s^\parallel_j}\sigma^{2(\ell+1-j)b_{\boldsymbol{c}}}C^{2s^\parallel_j}\Gamma(s^\parallel_j+2)^2.$$

The terms in the sums above are independent of the inner index i. Interpolation to non-integer differentiation orders $s_j^{\|} \in [1, p_j^{\|}]$ as in [23, Lemma 5.8] and applying [23, Lemma 5.12] (and adjusting constants) completes the proof. □

A.3.2. *Convergence on* $\widetilde{\mathfrak{T}}_{\boldsymbol{e}}^{\ell}$. We start by showing exponential convergence in edge-perpendicular direction.

Proposition A.11. *Let* $u \in B_{-1-\boldsymbol{b}}(\widetilde{\Omega}_{\boldsymbol{ce}}^{\ell})$ *respectively* $u \in B_{-\boldsymbol{b}}(\widetilde{\Omega}_{\boldsymbol{ce}}^{\ell})$. *Then there are constants* $b, C > 0$ *independent of* $\ell \geq 1$ *such that* $\Upsilon^{\perp}_{\widetilde{\mathfrak{T}}_{\boldsymbol{e}}^{\ell}}[\eta_0^{\perp}]^2 \leq C\exp(-2b\ell)$ *respectively* $\|\eta_0^{\perp}\|^2_{L^2(\widetilde{\mathfrak{T}}_{\boldsymbol{e}}^{\ell})} \leq C\exp(-2b\ell)$.

Proof. Let $K = K^{\perp} \times K_j^{\|}$ for $j \geq 2$, be an element in $\widetilde{\mathfrak{T}}_{\boldsymbol{e}}^{\ell}$ of the form (A.27). We claim that

$$(h_K^{\perp})^{-2}\|\eta_0^{\perp}\|^2_{L^2(K)} + \|\mathsf{D}_{\perp}\eta_0^{\perp}\|^2_{L^2(K} \lesssim \sigma^{2\min\{b_{\boldsymbol{c}},b_{\boldsymbol{e}}\}\ell}|u|^2_{\widetilde{N}^2_{-1-\boldsymbol{b}}(K)}\,, \tag{A.36}$$

$$\|\mathsf{D}_{\|}\eta_0^{\perp}\|^2_{L^2(K)} \lesssim \sigma^{2\min\{b_{\boldsymbol{c}},b_{\boldsymbol{e}}\}\ell}|u|^2_{\widetilde{N}^3_{-1-\boldsymbol{b}}(K)}\,, \tag{A.37}$$

$$\|\eta_0^{\perp}\|^2_{L^2(K)} \lesssim \sigma^{2\min\{b_{\boldsymbol{c}},b_{\boldsymbol{e}}\}\ell}|u|^2_{\widetilde{N}^1_{-\boldsymbol{b}}(K)}. \tag{A.38}$$

To show (A.36), let $s = |\boldsymbol{\alpha}^{\perp}| = 0, 1$. From the bound (A.19) (with $\beta = 1 - b_{\boldsymbol{e}}$ and noting the $p_K^{\perp} = \max\{1, \mathfrak{s}\}$ by (A.28)), we see that

$$\begin{aligned}(h_K^{\perp})^{2(s-1)}\|\mathsf{D}_{\perp}^{\boldsymbol{\alpha}^{\perp}}\eta_0^{\perp}\|^2_{L^2(K)} &\lesssim (h_K^{\perp})^{2s-2}(h_K^{\perp})^{4-2s-2(1-b_{\boldsymbol{e}})}\|r_{\boldsymbol{e}}^{1-b_{\boldsymbol{e}}}\mathsf{D}_{\perp}^2 u\|^2_{L^2(K)},\\ &\lesssim (h_K^{\perp})^{2b_{\boldsymbol{e}}}\|r_{\boldsymbol{e}}^{1-b_{\boldsymbol{e}}}\mathsf{D}_{\perp}^2 u\|^2_{L^2(K)}.\end{aligned}$$

From (A.26) and (A.31), we further obtain

$$\begin{aligned}\|r_{\boldsymbol{e}}^{1-b_{\boldsymbol{e}}}\mathsf{D}_{\perp}^2 u\|^2_{L^2(K)} &\lesssim (h_K^{\|})^{-2(b_{\boldsymbol{e}}-b_{\boldsymbol{c}})}\|r_{\boldsymbol{c}}^{b_{\boldsymbol{e}}-b_{\boldsymbol{c}}}r_{\boldsymbol{e}}^{1-b_{\boldsymbol{e}}}\mathsf{D}_{\perp}^2 u\|^2_{L^2(K)}\\ &\lesssim (h_K^{\|})^{-2b_{\boldsymbol{e}}+2b_{\boldsymbol{c}}}|u|^2_{\widetilde{N}^2_{-1-\boldsymbol{b}}(K)}\,.\end{aligned}$$

Thus, combining these estimates and expressing the mesh sizes in terms of σ, cf. (A.26), we see that

$$\begin{aligned}(h_K^{\perp})^{2(s-1)}\|\mathsf{D}_{\perp}^{\boldsymbol{\alpha}^{\perp}}\eta_0^{\perp}\|^2_{L^2(K)} &\lesssim (h_K^{\perp})^{2b_{\boldsymbol{e}}}(h_K^{\|})^{-2b_{\boldsymbol{e}}+2b_{\boldsymbol{c}}}|u|^2_{\widetilde{N}^2_{-1-\boldsymbol{b}}(K)}\\ &\simeq \sigma^{2b_{\boldsymbol{c}}(\ell+1-j)+2b_{\boldsymbol{e}}(j-1)}|u|^2_{\widetilde{N}^2_{-1-\boldsymbol{b}}(K)}\\ &\lesssim \sigma^{2\min\{b_{\boldsymbol{c}},b_{\boldsymbol{e}}\}\ell}|u|^2_{\widetilde{N}^2_{-1-\boldsymbol{b}}(K)},\end{aligned}$$

which yields (A.36).

To prove (A.37), we proceed similarly and obtain

$$\begin{aligned}\|\mathsf{D}_{\|}\eta_0^{\perp}\|^2_{L^2(K)} &\lesssim (h_K^{\perp})^{4-2(1-b_{\boldsymbol{e}})}\|r_{\boldsymbol{e}}^{1-b_{\boldsymbol{e}}}\mathsf{D}_{\perp}^2\mathsf{D}_{\|}u\|^2_{L^2(K)}\\ &\lesssim (h_K^{\|})^{-2-2b_{\boldsymbol{e}}+2b_{\boldsymbol{c}}}(h_K^{\perp})^{2+2b_{\boldsymbol{e}}}\|r_{\boldsymbol{c}}^{b_{\boldsymbol{e}}-b_{\boldsymbol{c}}+1}r_{\boldsymbol{e}}^{1-b_{\boldsymbol{e}}}\mathsf{D}_{\perp}^2\mathsf{D}_{\|}u\|^2_{L^2(K)}\\ &\lesssim \sigma^{2b_{\boldsymbol{c}}(\ell+1-j)+2b_{\boldsymbol{e}}(j-1)}\sigma^{2(j-1)}|u|^2_{\widetilde{N}^3_{-1-\boldsymbol{b}}(K)}\\ &\lesssim \sigma^{2\min\{b_{\boldsymbol{c}},b_{\boldsymbol{e}}\}\ell}|u|^2_{\widetilde{N}^3_{-1-\boldsymbol{b}}(K)}\,.\end{aligned}$$

To obtain (A.38), we employ an analogous argument based on (A.18) (with $\beta = 1 - b_{\boldsymbol{e}}$). With (A.26) and (A.32), this results in

$$\begin{aligned}\|\eta_0^\perp\|^2_{L^2(K)} &\lesssim (h_K^\perp)^{2-2(1-b_{\boldsymbol{e}})}\|r_{\boldsymbol{e}}^{1-b_{\boldsymbol{e}}}\mathsf{D}_\perp u\|^2_{L^2(K)}\\ &\lesssim (h_K^\parallel)^{2b_{\boldsymbol{c}}-2b_{\boldsymbol{e}}}(h_K^\perp)^{2b_{\boldsymbol{e}}}\|r_{\boldsymbol{c}}^{b_{\boldsymbol{e}}-b_{\boldsymbol{c}}}r_{\boldsymbol{e}}^{1-b_{\boldsymbol{e}}}\mathsf{D}_\perp u\|^2_{L^2(K)}\\ &\lesssim \sigma^{2b_{\boldsymbol{c}}(\ell+1-j)+2b_{\boldsymbol{e}}(j-1)}|u|^2_{\widetilde{N}^1_{-\boldsymbol{b}}(\widetilde{\Omega}^\ell_{\boldsymbol{ce}})}\\ &\lesssim \sigma^{2\min\{b_{\boldsymbol{c}},b_{\boldsymbol{e}}\}\ell}|u|^2_{\widetilde{N}^1_{-\boldsymbol{b}}(\widetilde{\Omega}^\ell_{\boldsymbol{ce}})},\end{aligned}$$

which is (A.38).

The assertions now follow by summing the estimates (A.36), (A.37) and (A.38) over all elements $K \in \widetilde{\mathfrak{T}}^\ell_{\boldsymbol{e}}$ (i.e., over $2 \le j \le \ell+1$) and by suitably adjusting constants. □

A similar estimate holds for the approximation errors in direction parallel to $\boldsymbol{e}$.

Proposition A.12. *Let $u \in B_{-1-\boldsymbol{b}}(\widetilde{\Omega}^\ell_{\boldsymbol{ce}})$ respectively $u \in B_{-\boldsymbol{b}}(\widetilde{\Omega}^\ell_{\boldsymbol{ce}})$. Then there are constants $b, C > 0$ independent of $\ell \ge 1$ such that $\Upsilon^\parallel_{\widetilde{\mathfrak{T}}^\ell_{\boldsymbol{e}}}[\eta^\parallel]^2 \le C\exp(-2b\ell)$ respectively $\|\eta_0^\parallel\|^2_{L^2(\widetilde{\mathfrak{T}}^\ell_{\boldsymbol{e}})} \le C\exp(-2b\ell)$.*

Proof. For $u \in B_{-1-\boldsymbol{b}}(\widetilde{\Omega}^\ell_{\boldsymbol{ce}})$, properties (A.31), (A.30) imply $u, \mathsf{D}_\parallel u, \mathsf{D}_\perp u \in L^2(\widetilde{\Omega}^\ell_{\boldsymbol{ce}})$ and

$$\begin{aligned}\|r_{\boldsymbol{c}}^{-1-b_{\boldsymbol{c}}+\alpha^\parallel}\mathsf{D}_\parallel^{\alpha^\parallel}u\|_{L^2(\widetilde{\Omega}^\ell_{\boldsymbol{ce}})} &\le C^{\alpha^\parallel+1}\Gamma(\alpha^\parallel+1), \qquad \alpha^\parallel \ge 2,\\ \|r_{\boldsymbol{c}}^{-b_{\boldsymbol{c}}+\alpha^\parallel}\mathsf{D}_\parallel^{\alpha^\parallel}\mathsf{D}_\perp u\|_{L^2(\widetilde{\Omega}^\ell_{\boldsymbol{ce}})} &\le C^{\alpha^\parallel+2}\Gamma(\alpha^\parallel+2), \qquad \alpha^\parallel \ge 1.\end{aligned}$$

Similarly, for $u \in B_{-\boldsymbol{b}}(\widetilde{\Omega}^\ell_{\boldsymbol{ce}})$ it follows with (A.32) that $u \in L^2(\widetilde{\Omega}^\ell_{\boldsymbol{ce}})$ and

$$\|r_{\boldsymbol{c}}^{-b_{\boldsymbol{c}}+\alpha^\parallel}\mathsf{D}_\parallel^{\alpha^\parallel}u\|_{L^2(\widetilde{\Omega}^\ell_{\boldsymbol{ce}})} \le C^{\alpha^\parallel+1}\Gamma(\alpha^\parallel+1), \qquad \alpha^\parallel \ge 1.$$

In view of (A.26), (A.27), these properties correspond to the one-dimensional analytic regularity assumptions considered in (A.13) and (A.17), respectively. Moreover, due to (A.28), the polynomial degrees $p_K^\parallel$ along the edge $\boldsymbol{e}$ are $\mathfrak{s}$-linearly increasing away from the corner $\boldsymbol{c}$. Hence, Lemma A.4 respectively Lemma A.5, and the tensor-product structure of the elements readily yield the assertions. □

A.3.3. *Convergence on $\widetilde{\mathfrak{T}}^\ell_{\boldsymbol{c}}$.* It remains to show exponential convergence for the corner elements in $\widetilde{\mathfrak{T}}^\ell_{\boldsymbol{c}}$.

Proposition A.13. *Let $u \in H^{1+\theta}(\widetilde{\Omega}^\ell_{\boldsymbol{ce}})$ respectively $u \in H^\theta(\widetilde{\Omega}^\ell_{\boldsymbol{ce}})$ for some $\theta \in (0,1)$. Then there exist constants $b, C > 0$ independent of $\ell \ge 1$ such that $\Upsilon^\parallel_{\widetilde{\mathfrak{T}}^\ell_{\boldsymbol{c}}}[\eta]^2 \le C\exp(-2b\ell)$ respectively $\|\eta_0\|^2_{L^2(\widetilde{\mathfrak{T}}^\ell_{\boldsymbol{c}})} \le C\exp(-2b\ell)$.*

Proof. The element $K \in \widetilde{\mathfrak{T}}^\ell_{\boldsymbol{c}}$ is isotropic with $h_K^\perp \simeq h_K^\parallel \simeq h_K \simeq \sigma^\ell$; cf. (A.24). Standard h-version approximation properties then readily show that

$$N_K^\parallel[\eta]^2 \lesssim h_K^{2\theta}\|u\|^2_{H^{1+\theta}(K)} \quad \textit{respectively} \quad \|\eta_0\|^2_{L^2(K)} \lesssim h_K^{2\theta}\|u\|^2_{H^\theta(K)}.$$

This implies the assertions. □

References

[1] I. Babuška and B. Q. Guo. The h-p version of the finite element method for domains with curved boundaries. *SIAM J. Numer. Anal.*, 25(4):837–861, 1988.

[2] I. Babuška and B. Q. Guo. Regularity of the solution of elliptic problems with piecewise analytic data. Part I. Boundary value problems for linear elliptic equation of second order. *SIAM J. Math. Anal.*, 19:172–203, 1988.

[3] I. Babuška and B. Q. Guo. Approximation properties of the h-p version of the finite element method. *Comput. Methods Appl. Mech. Engrg.*, 133(3-4):319–346, 1996.

[4] P. Binev, A. Cohen, W. Dahmen, R. DeVore, G. Petrova, and P. Wojtaszczyk. Convergence rates for greedy algorithms in reduced basis methods. *SIAM J. Math. Anal.*, 43(3):1457–1472, 2011.

[5] M. Costabel, M. Dauge, and S. Nicaise. Analytic regularity for linear elliptic systems in polygons and polyhedra. *Math. Models Methods Appl. Sci.*, 22(8), 2012.

[6] W. Dahmen and K. Scherer. Best approximation by piecewise polynomials with variable knots and degrees. *J. Approx. Theory*, 26(1):1–13, 1979.

[7] L. Demkowicz, J. Kurtz, D. Pardo, M. Paszynski, W. Rachowicz, and A. Zdunek. *Computing with hp-Adaptive Finite Elements. Volume 2, Frontiers: Three Dimensional Elliptic and Maxwell Problems with Applications.* Chapman & Hall/CRC Applied Mathematics and Nonlinear Science Series. Chapman & Hall/CRC, November 2007.

[8] A. Ern and J.-L. Guermond. *Theory and Practice of Finite Elements*, volume 159 of *Applied Mathematical Sciences*. Springer, 2004.

[9] W. Gui and I. Babuška. The h, p and h-p versions of the finite element method in one dimension. II. The error analysis of the h- and h-p versions. *Numer. Math.*, 49(6):613–657, 1986.

[10] B. Q. Guo. The h-p version of the finite element method for solving boundary value problems in polyhedral domains. In *Boundary Value Problems and Integral Equations in Nonsmooth Domains*, volume 167 of *Lecture Notes in Pure and Appl. Math.*, pages 101–120. Dekker, New York, 1995.

[11] B. Q. Guo and I. Babuška. The hp-version of the finite element method. Part I: The basic approximation results. *Comp. Mech.*, 1:21–41, 1986.

[12] B. Q. Guo and I. Babuška. The hp-version of the finite element method. Part II: General results and applications. *Comp. Mech.*, 1:203–220, 1986.

[13] B. Q. Guo and I. Babuška. Regularity of the solutions for elliptic problems on nonsmooth domains in $\mathbb{R}^3$. I. Countably normed spaces on polyhedral domains. *Proc. Roy. Soc. Edinburgh Sect. A*, 127(1):77–126, 1997.

[14] B. Q. Guo and I. Babuška. Regularity of the solutions for elliptic problems on nonsmooth domains in $\mathbb{R}^3$. I. Countably normed spaces on polyhedral domains. *Proc. Roy. Soc. Edinburgh Sect. A*, 127(1):77–126, 1997.

[15] B. Q. Guo and I. Babuška. Regularity of the solutions for elliptic problems on nonsmooth domains in $\mathbb{R}^3$. II. Regularity in neighbourhoods of edges. *Proc. Roy. Soc. Edinburgh Sect. A*, 127(3):517–545, 1997.

[16] Y. Maday, O. Mula, A.T. Patera, and M. Yano. The generalized empirical interpolation method: stability theory on Hilbert spaces with an application to the Stokes equation. *Comput. Methods Appl. Mech. Engrg.*, 287:310–334, 2015.

[17] K. Scherer. On optimal global error bounds obtained by scaled local error estimates. *Numer. Math.*, 36:257–277, 1981.

[18] D. Schötzau and C. Schwab. Exponential convergence for hp-version and spectral finite element methods for elliptic problems in polyhedra. *Math. Models Methods Appl. Sci.*, 25(9):1617–1661, 2015.

[19] D. Schötzau and Ch. Schwab. Exponential convergence in a Galerkin least squares hp-FEM for Stokes flow. *IMA J. Numer. Anal.*, 21:53–80, 2001.

[20] D. Schötzau, Ch. Schwab, and A. Toselli. Mixed hp-DGFEM for incompressible flows. *SIAM J. Numer. Anal.*, 40:2171–2194, 2003.

[21] D. Schötzau, Ch. Schwab, and A. Toselli. Mixed hp-DGFEM for incompressible flows. II. Geometric edge meshes. *IMA J. Numer. Anal.*, 24(2):273–308, 2004.

[22] D. Schötzau, Ch. Schwab, and T. P. Wihler. hp-DGFEM for second-order elliptic problems in polyhedra. I: Stability on geometric meshes. *SIAM J. Numer. Anal.*, 51(3):1610–1633, 2013.

[23] D. Schötzau, Ch. Schwab, and T. P. Wihler. *hp*-DGFEM for second-order elliptic problems in polyhedra. II: Exponential convergence. *SIAM J. Numer. Anal.*, 51(4):2005–2035, 2013.
[24] D. Schötzau, Ch. Schwab, and T. P. Wihler. *hp*-DGFEM for second-order mixed elliptic problems in polyhedra. Technical Report 2013-39, Seminar for Applied Mathematics, ETH Zürich, 2013. In press in Math. Comp.
[25] Ch. Schwab. *p- and hp-FEM – Theory and Application to Solid and Fluid Mechanics*. Oxford University Press, Oxford, 1998.
[26] T. P. Wihler. *Discontinuous Galerkin FEM for Elliptic Problems in Polygonal Domains*. PhD thesis, Swiss Federal Institute of Technology Zurich, 2002. Diss. ETH No. 14973.
[27] T. P. Wihler and M. Wirz. Mixed *hp*-discontinuous Galerkin FEM for linear elasticity and Stokes flow in three dimensions. *Math. Models Methods Appl. Sci.*, 22(8), 2012.
[28] L. Zhu, S. Giani, P. Houston, and D. Schötzau. Energy norm a posteriori error estimation for *hp*-adaptive discontinuous Galerkin methods for elliptic problem in three dimensions. *Math. Models Methods Appl. Sci.*, 21(2):267–306, 2011.

Mathematics Department, University of British Columbia, Vancouver, BC V6T 1Z2, Canada
E-mail address: schoetzau@math.ubc.ca

Seminar for Applied Mathematics, ETH Zürich, 8092 Zürich, Switzerland
E-mail address: schwab@math.ethz.ch

Recent Research Reports

Nr.	Authors/Title

2015-42 H. Ammari and Y.T. Chow and J. Zou
Super-resolution in imaging high contrast targets from the perspective

of scattering coefficients

2015-43 Ch. Schwab and R. Stevenson
Fractional space-time variational formulations of (Navier-) Stokes equations

2015-44 S. May and M. Berger
An Explicit Implicit Scheme for Cut Cells in Embedded Boundary Meshes

2015-45 L. Jacobe de Naurois and A. Jentzen and T. Welti
Weak convergence rates for spatial spectral Galerkin approximations of semilinear stochastic wave equations with multiplicative noise

2015-46 A. Jentzen and R. Kurniawan
Weak convergence rates for Euler-type approximations of semilinear stochastic evolution equations with nonlinear diffusion coefficients

2015-47 A. Andersson and A. Jentzen and R. Kurniawan
Existence, uniqueness, and regularity for stochastic evolution equations with irregular initial values

2016-01 A. Jentzen and Th. Müller-Gronbach and L. Yaroslavtseva
On stochastic differential equations with arbitrary slow convergence rates for strong approximation

2016-02 L. Herrmann and A. Lang and Ch. Schwab
Numerical Analysis of Lognormal Diffusions on the Sphere

2016-03 W. Dahmen and G. Kutyniok and W. Lim and Ch. Schwab and G. Welper
Adaptive Anisotropic Petrov-Galerkin Methods for First Order Transport Equations